Mitochondrial toxicity of drugs

Inauguraldissertation

zur

Erlangung der Würde eines Doktors der Philosophie

vorgelegt der

Philosophisch-Naturwissenschaftlichen Fakultät

der Universität Basel

von

Katri Maria Waldhauser

aus Hyvinkää (FIN)

Basel, 2008

Genehmigt von der Philosophisch-Naturwissenschaftlichen Fakultät auf Antrag der Herren:

Prof. Dr. Dr. Stephan Krähenbühl

Prof. Dr. Jürgen Drewe

Münchenstein, den 16. Oktober 2007

Prof. Dr. H.-P. Hauri

Dekan

For my family

Acknowledgements

First of all I would like to express my gratitude to Professor Jürgen Drewe for all the interesting talks and for taking part to my exam, and to Professor Alex Odermatt for being chairman. It all begun in Finland, at the University of Helsinki, where Professor Heikki Vuorela helped me to organize an exchange semester in Switzerland to write my master's thesis. That is how I landed in the pharmacology research group of Professor Urs T. Rüegg at the School of Pharmacy in Lausanne where I was encouraged to start writing a dissertation at the University Hospital Basel in the reseach group of Professor Stephan Krähenbühl. Stephan, please accept my expression of gratitude for giving me the possibility to work on a doctoral thesis in your lab. It has been very interesting to work under the guidance of such a motivating and inspiring person as you. I also would like to thank you for your support in times when everything did not turn out as planned.

In the very first year of my thesis I was very fortunate to be guided by Dr. Michael Török. There was no question I asked that Michael could not answer! The second year of my doctoral studies was not as productive as the first year. That was when I was sometimes suffering trying to get some ideas for my work. During the third year I was tutored by Dr. Karin Brecht who I would like thank for all her help. For me, it was not only an education in the laboratory and pharmacological skills that I got in this research group. I also learnt that research is not something you can guide: No, you are being guided by your results and by the equipments that you use and by the people you discuss your problems and results with. That is a very useful experience.

I would not like to miss the opportunity to express how deeply grateful I am for the help I gained from my parents (especially my father) and from my mother-in-law in taking care of Eliel while I was busy writing this thesis or working with the last experiments in the lab. I sincerely don't know what I would have done without you.

There are so many people in the lab that I am very grateful for and that I am going to miss after finishing my Ph.D. First of all Andrea and Anja: I did not only enjoy working with you all these three years, I also found a good friend in you! Saskia, Priska, Bettina and Katerina, you were an important part of my doctoral studies. Bettinas baking skills are unforgettable and Katerinas stories amused us daily. Liliane, our chief of the lab with a big heart… Bea, our really nice labororian! Also the people in the lab 411 (Uschi, Heike, Angelika, Manisha, Birk, Philipp (thank you for all the nice chats in Finnish), Christian) and in Markgräflerhof… Thank you for your good company during these years. Finally, Marco, kiitos tuestasi ja kärsivällisyydestäsi. Ilman sinua ei olisi väitöskirjaa. Omistan tämän väitöskirjan sinulle ja meidän Elielille.

Table of contents

1. Summary

The introduction of this thesis concentrates on the cellular energy supplier and an important instrument in mediating cell death, mitochondrion. First, an overview is given to explain the biochemical properties of this organelle. Then, the role of mitochondria in cell death is discussed, followed by an article about the mitochondrial toxicity of drugs. As an example of the mitochondrial toxicity of a drug, an article about statins and their effects on L6 myocytes and rat muscle mitochondria conclude the introduction part of this thesis.

The aim of the first project was to compare hepatocellular toxicity and pharmacological activity of amiodarone (B2-O-Et-N-diethyl) and eight amiodarone derivatives, including three amiodarone metabolites (B2-O-Et-NH-ethyl, B2-O-Et-NH$_2$ and B2-O-Et-OH). In addition, five amiodarone analogues were investigated (B2-O-Et-N-dimethyl, B2-O-Et-N-dipropyl, B2-O-Acetate, B2-O-Et-propionamide and B2-O-Et). The studies were accomplished using frehly isolated rat liver mitochondria, primary rat hepatocytes and the hepatoma cell line HepG2. The hepatocellular toxicity of amiodarone and most of the derivatives was confirmed. Amiodarone and most analogues showed a dose-dependent toxicity on the respiratory chain and on β-oxidation of the mitochondria. The ROS concentration in hepatocytes increased time-dependently and apoptotic/necrotic cell populations were identified using flow cytometry and annexinV/propidiumiodide staining. The effect of the three least toxic amiodarone analogues on the hERG channel was compared to amiodarone. In conclusion, three amiodarone analogues (B2-O-Et-N-dipropyl, B2-O-Acetate and B2-O-Et) showed a lower hepatocellular toxicity profile than amiodarone and two of these analogues (B2-O-Et-N-dipropyl and B2-O-Acetate) retained hERG channel interaction capacity, suggesting that amiodarone analogues with class III antiarrhythmic activity and lower hepatic toxicity could be developed.

For the second project in this thesis, we synthesized three more amiodarone analogues (B2-O-Ethylacetate, B2-O-Et-N-pyrrolidine and B2-O-Et-N-piperidine) and, together with amiodarone and its metabolites (B2-O-Et-NH-ethyl and B2-O-Et-NH$_2$) and some derivatives from the first study (B2-O-Et-N-dipropyl, B2-O-Et-propionamide, B2-O-Acetate, B2-O-Et-OH), characterized their hepatic toxicity together with the pulmonary toxicity. The interaction with the hERG channel was determined for all the derivatives. Compared to amiodarone, which showed only a weak cytotoxicity, the desethylated metabolites, B2-O-Acetate, B2-O-Et-OH and B2-O-Et-N-pyrrolidine showed a similar or higher cytotoxicity. On the other hand, B2-O-Et-N-dipropyl, B2-O-Ethylacetate, B2-O-Et, B2-O-Et-propionamide and B2-O-Et-N-piperidine were less toxic. Cytotoxicity was associated with a drop in the mitochondrial membrane potential and therefore most probably mitochondrial in origin. Substances carrying a nitrogen in the side chain (amiodarone, B2-O-Et-NH-ethyl, B2-O-Et-NH$_2$, B2-O-Et-N-dipropyl, B2-O-Et-propionamide, B2-

O-Et-N-pyrrolidine, B2-O-Et-N-piperidine) showed a much higher affinity to the hERG channel (range 0.22-12.2µmol/L) than those without a nitrogen in this position (B2-O-Acetate, B2-O-Ethylacetate, B2-O-Et-OH) (range 74-216µmol/L). Neither cytotoxicity, nor the interaction with the hERG channel, was associated with the lipophilicity of the compounds. It was concluded, that the physicochemical properties of amiodarone and its analogues were not as important for the potassium channel interaction and cytotoxicity as the chemical structure of the compounds.

In the third project of this thesis, the relationship between an unexpected toxicity of a drug and an underlying mitochondrial defect was studied using human dermal fibroblasts. These cells were derived from patients suffering from a mitochondrial defect. Simvastatin and benzbromarone are known to cause an unexpected adverse reaction (myotoxicity or hepatotoxicity, respectively). Both dermal fibroblasts with a mitochondrial defect and fibroblasts from healthy patients were treated with different concentrations of benzbromarone and simvastatin, and the overall toxicity was evaluated after different time points. There were no differences in the toxicity pattern between the cell lines, and the toxicity assayed was relatively scarce in all experiments. It was concluded that the the test system was not suitable for these studies and that they should be repeated with other cell lines of hepatic or muscle origin.

2. Abbreviations

ADP	adenosine diphosphate
Apaf-1	apoptotic protease activating factor 1
ATP	adenosine triphosphate
CHO	chinese hamster ovary
Cpt1	carnitine palmitoyltransferase 1
DCFH-DA	2,7-dichlorofluorescin diacetate
DMSO	dimethylsulfoxide
FACS	fluorescence activated cell scanning
ETC	electron transport chain
FAO	fatty acid disorder
FAS	Fas ligand
hERG	human ether-a-go-go related gene
HMG-CoA	Hydroxymethyl glutaryl coenzyme A
HPLC	high performance liquid chromatography
IDR	Idiosyncratic drug reaction
JC-1	5,5',6,6,'-tetraethylbenzimidazolylcarbocyanidde iodide
LDH	lactate dehydrogenase
MnSOD	manganese superoxide dismutase
MOMP	mitochondrial outer membrane permeabilization
mPT	mitochondrial permeability transition
mtDNA	mitochondrial DNA
MTT	3-(4,5-dimethylthiazol-2-yl)-2,5-diphenyl tetrazolium bromide
NADH	nicotinamide adenine dinucleotide
NMR	nuclear magnetic resonance
PBS	phosphate buffered saline
P_i	phosphate
PI	propidiumiodide
$\Delta\Psi m$	mitochondrial membrane potential
RCR	respiratory control ratio
ROS	reactive oxygen species
SDS	sodium dodecyl sulphate
VLCAC	very long chain acyl-CoA dehydrogenase
VDAC	voltage-dependent anion channel

3. Introduction

3.1. The mitochondrion

3.1.1. Mitochondria as cellular organelles

Mitochondria are membrane-enclosed organelles that are found in eukaryotic cells. They differ in structure and function in different cell types [1] sharing features common for all mitochondria (Figure 1). Most cells contain hundreds of mitochondria and some of them with high energetic requirements (e.g. heart and muscle cells) even more. Mitochondria have an outer membrane and an inner membrane. Between the two membranes there is the intermembraneous space and inside the mitochondria the matrix. The outer membrane encloses the entire organelle and consists of numerous integral proteins (porins, voltage-dependent anion channels, VDAC) and phospholipids as well as enzymes taking part to the metabolism of several substances (e.g. epinephrine, tryptophan) and to the transportation of the fatty acids into the mitochondrial matrix. The inner mitochondrial membrane has an inward fold called cristae and acts as a permeability barrier for a variety of compounds. While the outer membrane is relatively permeable for solutes and small drugs, the inner membrane is tight containing cardiolipin instead of cholesterol, which is present in the outer membrane. The inner transmembrane potential ($\Delta\Psi_m$) is negative (-180mV) and is being maintained by pumping protons into the intermembraneous space. There is a so-called respiratory chain on the inner surface of the inner membrane [2, 3]. Hundreds of enzymes are located in the mitochondrial matrix, including the enzymes involved in β-oxidation of fatty acids as well as mitochondrial ribosomes, tRNA and mitochondrial DNA (mtDNA). Mitochondria provide cells with energy in form of ATP by oxidising the glycolysis products NADH and $FADH_2$ in the respiratory chain. Mitochondria store calcium taking part to the cellular calcium homeostasis. Depending on the cell type, mitochondria also play an important role in cellular proliferation, regulation of the cellular redox state, heme and steroid synthesis, glutamate-mediated neuronal injury and cell death [4].
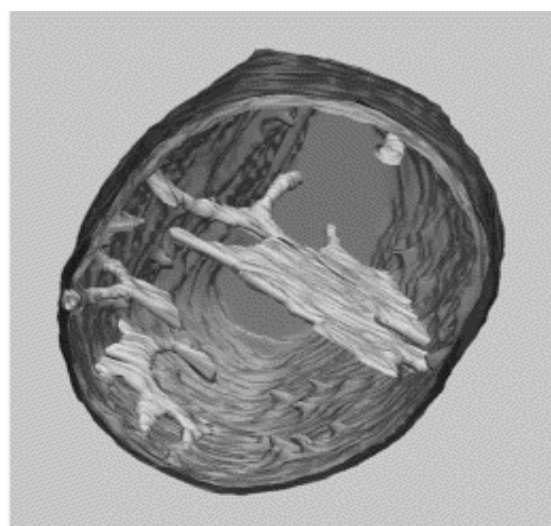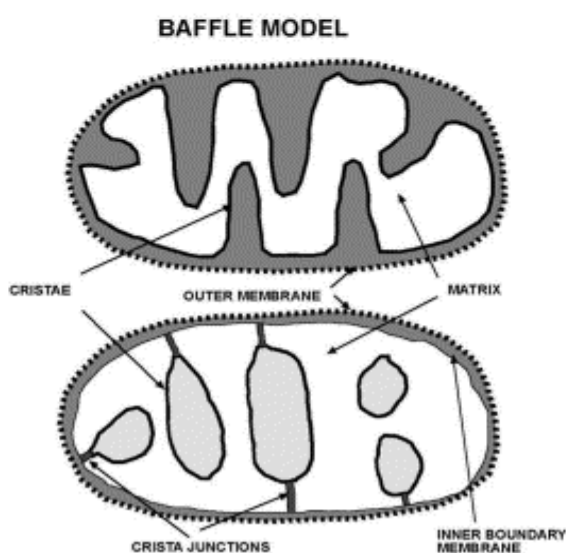
Figure 1. (A) Mitochondrion as viewed by electron tomography. The outer membrane is darker as the inner membrane that is shown in a lighter shade. (B) The Baffle model (top) was the accepted model for four decades. Recent investigations showed, though, that the inner mitochondrial membrane is composed of two or more topologically continuous but distinct domains (bottom). The inner boundary membrane is closely juxtaposed to the outer membrane around the circumference and the cristae is seen as tubular or lamellar structures connected to the inner boundary membrane by narrow tubular structures named cristae junctions or pediculi crista [4].

3.1.2. ATP production by the mitochondria

The Krebs cycle located in the mitochondrial matrix is connected to the inner mitochondrial membrane by succinate dehydrogenase. This cycle produces NADH and $FADH_2$ by oxidising acetyl-CoA. NADH and $FADH_2$ donor electrons for the electron transport chain (ETC), that consists of protein complexes [NADH:ubiquinone oxidoreductase (complex I), succinate dehydrogenase (complex II) cytocrome c reductase (complex III) and cytochrome c

oxidase (complex IV)] located in the inner mitochondrial membrane. ETC proteins transfer the electrons to oxygen (O_2). The incremental energy produced in this reaction is used to pump protons (H^+) into to the intermembraneous space. This initiates an electrochemical gradient across the inner membrane. The protons return to the matrix via the ATP synthase and are used to synthesize ATP from ADP and phosphate (P_i) [5, 6]. At certain conditions, protons may leak across the inner membrane resulting in the conversion of energy into heat. This process is called uncoupling and is mediated by a proton channel called thermogenin. The discovery of uncoupling proteins participating in thermogenesis and thermoregulation in newborns and hibernating animals has recently been gaining interest [7, 8].

3.1.3. Mitochondrial DNA

The very small, circular and double-stranded mitochondrial DNA is distinct from the nuclear DNA. It encodes for 13 specific subunits of complexes I, III, IV and V and 22 tRNAs and 2 rRNAs. The rest of the subunits of complexes I, III, IV and V and all subunits of complex II are encoded by the nuclear DNA. Thus, one finds in mitochondria distinct processes such as DNA replication and repair, transcription and protein synthesis in the matrix. All the required enzymes and factors have to be imported from the cytosol. These facts make the ETC vulnerable for the changes in the mitochondrial as well as in the nuclear genome [9].

3.2. Mitochondria and cell death

Cellular homeostasis is interfered by numerous toxicants, which can result in distraction of the structural and functional integrity of the cell. This toxicity may be followed by one or more of the three critical cellular biochemical disorders, namely ATP depletion, ROS overproduction and/or the rise of the intracellular Ca^{2+}. Since mitochondria play a pivotal role in regulating these functions, it makes them an important instrument mediating cell death, namely apoptosis or necrosis. To maintain the cellular homeostasis, each mitosis is compensated by one event of a cellular death called apoptosis. Most likely, each cell in our body is able to undergo apoptosis, and the disturbance in its regulation can cause severe malformations or illnesses. Besides apoptosis, our cells can undergo another form of cell death, necrosis, which is considered an accidental type of death. It is caused by severe and acute cell injury, and results in the death of groups of cells within a tissue [10]. Morphologically, apoptosis causes the cells to shrink and to form so called apoptotic bodies, whereas cells undergoing necrotic cell death swell (together with mitochondria), and are finally destroyed, when the cell membrane ruptures [11].

An apoptotic cell death may be induced or it is preprogrammed into the cell (e.g. during cell development) and results in the death of the individual cells. In is strictly regulated and is controlled by a family of cysteine proteases known as caspases. The surface exposure of

phosphatidylserine residues (normally on the inner membrane leaflet) allows the recognition and elimination of apoptotic cells by their healthy neighbours, before the membrane breaks up and cytosol or organelles spill into the intercellular space and trigger inflammatory reactions [12]. If apoptosis is massive or phagocytic cells are lacking, apoptosis can eventually turn into necrosis [13]. Apoptosis involves the regulated action of catabolic enzymes (proteases and nucleases), while the plasma membrane remains mostly intact [14]. It is commonly accompanied by a characteristic change of nuclear morphology (chromatin condensation, pyknosis, karyorrhexis) and of chromatin biochemistry (step-wise DNA fragmentation). In contrast to apoptosis, necrosis does not involve DNA and protein degradation [15].

Apoptotic cell death can be accomplished via two different pathways, namely the death receptor pathway or the mitochondrial pathway. Death receptors are e.g. the tumour necrosis factor receptor-1 (TNF-R1) or the Fas (also known as Apo-1 or CD95) receptor with its ligand [16, 17]. Proapoptotic and antiapoptotic members of the Bcl-2 family regulate the mitochondrial pathway leading to apoptosis. Following TNF-R1 and Fas activation in mammalian cells a balance between Bax, Bid, Bak or Bad and anti-apoptotic members of the Bcl-2 family is established. The end result of either pathway is caspase activation and the cleavage of specific cellular substrates, resulting in the morphologic and biochemical changes associated with the apoptotic phenotype [16, 17]. The mitochondrial pathway is activated by cellular events including oxidative stress or cytotoxic substances (Figure 2).
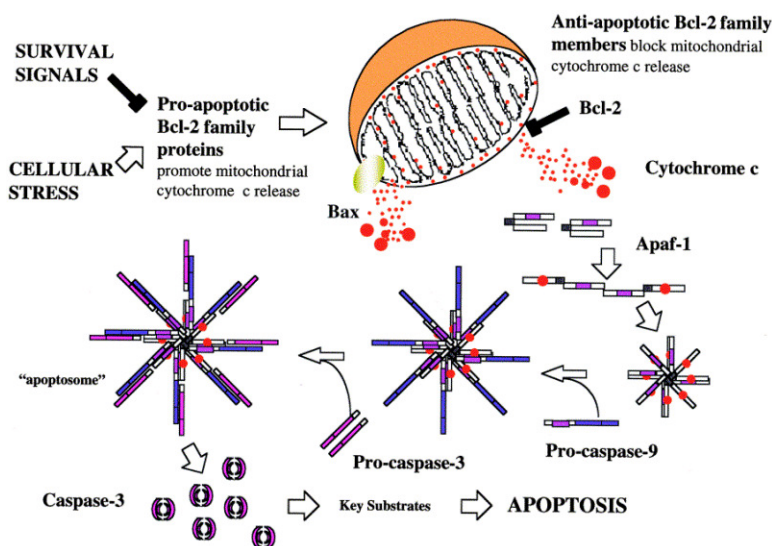
Figure 2. Mitochondrial pathway in triggering apoptosis. Pro-apoptotic Bcl-2 family members translocate from the cytosol to mitochondria by cellular stress. Cytochrome c is released, that catalyzes the oligomerization of Apaf-1 (apoptotic protease activating factor 1). Apaf-1 recruits and promotes the activation of procaspase-9. This, in turn, activates procaspase-3, leading to apoptosis [16].

There are at least three general mechanisms known to cause apoptosis or necrosis activated by mitochondria including (a) the disruption of electron transportation, oxidative phosphorylation and ATP production, (b) release of proteins triggering activation of caspase family proteases and (c) alteration of cellular reduction-oxidation (redox) potential [18].

Many toxic drugs cause either apoptosis or necrosis, depending on their dose used. What determines, whether the injured cell undergoes apoptosis or necrosis? There are suggestions, that the availability of ATP is critical in determining apoptosis, whereas the depletion of ATP leads to necrotic cell death [19]. Toxic substances may induce apoptosis at low concentrations or early after exposure whereas necrosis can occur later at higher concentrations. The induction of both forms of cell death by cytotoxic agents may involve similar metabolic disturbances and above all, mitochondrial permeability transition (mPT) [10], whereas blockers of mPT (e.g. cyclosporine) prevent both apoptosis and necrosis. Whether apoptosis or necrosis occurs, depends on the number of mitochondria affected, as illustrated in Figure 3.
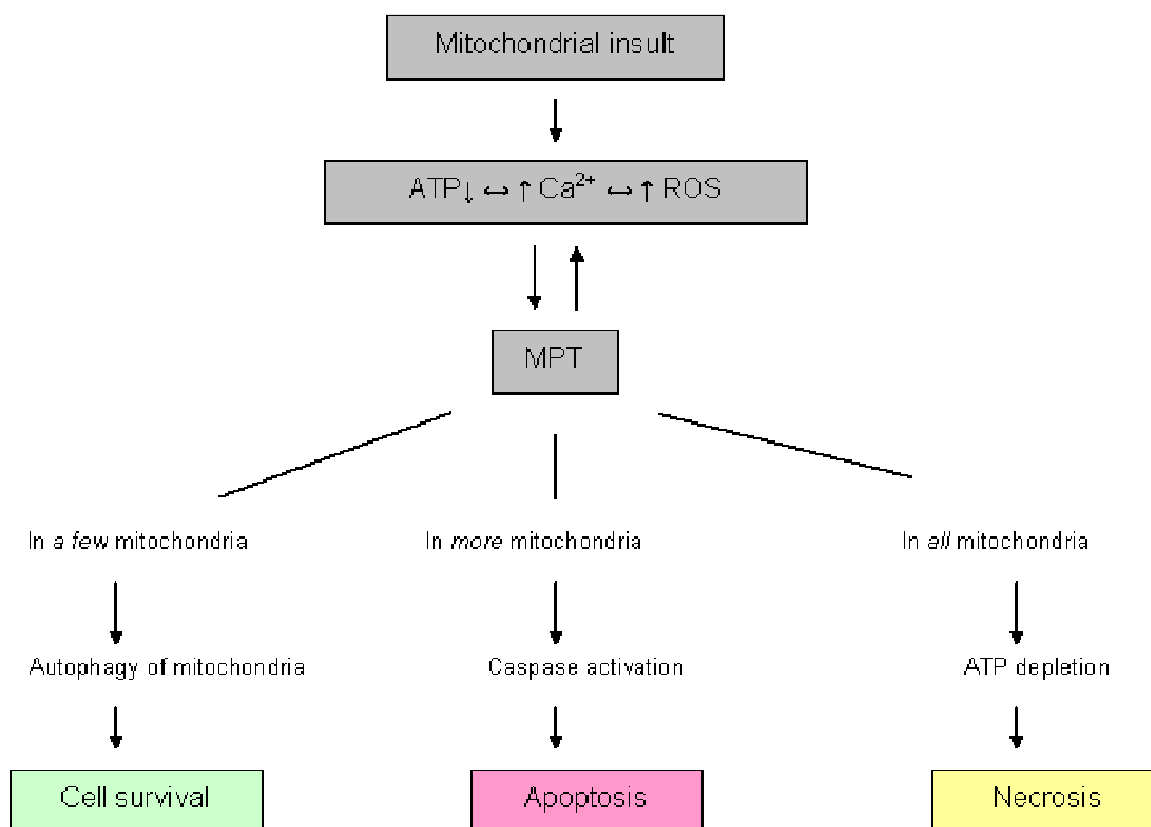
Figure 3. Cell death regulation by mitochondria. The decisive factor in triggering apoptosis or necrosis or in cell survival is the number of mitochondria involved.

3.2.1. ROS production by mitochondria

Mitochondria are the major source of reactive oxygen species (ROS), especially intracellular superoxide [20]. ROS are able to oxidize DNA leading to impaired transcription and translation with a subsequent protein deformation or absent protein formation. Furthermore, they may peroxidise membrane lipids causing membrane disruption or deformity and impair DNA repair mechanism by transforming DNA bases. A small percentage of the electrons escape from the ETC and interact with oxygen to form superoxide anions (O_2^{-}) that can react with NO or form hydroxyl radicals [18, 21, 22]. Normally, mitochondria possesses antioxidant systems preventing the oxidative imbalance in the pro-oxidant/antioxidant ratio, as an example the manganese superoxide dismutase (MnSOD), that scavenges the superoxide produced by the electron transport system in mitochondria [23]. mtDNA is extremely sensitive to oxidative damage owing to its proximity to the inner membrane, the absence of protective histones, and incomplete repair mechanisms in mitochondria [24]. Mutations in mtDNA leads to gradual increases in abnormal ETC proteins and to mitochondrial dysfunction, and the damage to part of the electron transport machinery causes more oxidant stress creating a vicious circle [9].

3.2.2. Increased mitochondrial membrane permeability

As already discussed in chapter 3.2., a loss in the integrity of the outer mitochondrial membrane can trigger the release of certain proteins mediating the cell death. There are at least two ways to provoke it, depending on the cell type: First of all, the Bcl-2 family-regulated mitochondrial outer membrane permeabilization (MOMP), and secondly, the Ca^{2+}- and/or ROS-regulated mPT. The MOMP is induced by the activation of Bax and Bak locating in the outer mitochondrial membrane. These form pores through which the death proteins can escape. In this case, the inner transmembrane potential ($\Delta\Psi m$) is retained. MOMP is lethal because it results in the release of caspase-activating molecules and caspase-independent death effectors, metabolic failure in the mitochondria, or both [25]. Cytochrome c is part of the electron transport chain and its release impaires ATP production and increases formation of ROS. Cytochrome c also acts as an initiator in the pathway leading to apoptosis, among other substances. Together with the adapter protein Apaf-1 and ATP, cytochrome c activates caspase 9 and thus induces apoptosis.

The mPT is caused by a multi-protein complex that expands both the inner and the outer membrane forming a pore that allows the exchange of ions and other molecules smaller than 1500 Da. The $\Delta\Psi m$ is not retained as a consequence of the osmotic swelling of the mitochondria, the rupturing of the outer mitochondrial membrane and the release of the death proteins. Finally, the ATP production collapses and, if enough mitochondria are affected, cell dies. There is evidence that the mPT leads to necrosis, but not to cytochrome c release and

apoptosis. However, also the signaling crosstalk between the mPT and Bcl-2 family proteins occurs indicating somekind of a role for the mPT in apoptosis [26].

3.3. Mitochondrial toxicity of drugs

Liliane Todesco, Katri Waldhauser, Stephan Krähenbühl

Clinical Pharmacology & Toxicology and Institute of Clinical Pharmacy, University of Basel, Switzerland

3.3.1. Abstract

Mitochondria are important targets of drug toxicity. A variety of drugs has been shown to affect the electron transport chain, coupling of oxidative phosphorylation, β-oxidation or other mitochondrial functions. Such damaging events may lead to the opening of a large pore across the mitochondrial membranes - the membrane permeability transition pore - eventually leading to apoptosis or necrosis of cells, depending on the cellular ATP content. Such drugs may therefore lead to organ damage, particularly in the liver, kidney, heart or skeletal muscle.

Keywords: Mitochondria, respiratory chain, β-oxidation, apoptosis, necrosis, drug toxicity

3.3.2. Introduction

During the last years, mitochondrial damage has been recognized as one of the most important causes for adverse reactions of many drugs and toxins. The fact that mitochondria represent a target of drug toxicity is not surprising, since these organelles have a central function in cellular energy production, contain multiple metabolic pathways and are key players in the initiation of apoptosis and/or necrosis of a cell [27]. The mitochondrial respiratory chain, which is an important target of drug toxicity, is illustrated in Figure 1.

As illustrated in Table 1, drugs can affect mitochondria by a variety of mechanisms. One well defined mechanism is inhibition of the electron flow across the electron transport chain (enzyme complexes I-IV, see Figure 1). The possibilities, of how these substances can impair electron flow within the electron transport chain, include direct inhibition of a protein subunit of one (or more) of the enzyme complexes or acceptance of electrons flowing across the electron transport chain instead of the natural acceptors ubiquinone or cytochrome c.

Uncoupling of oxidative phosphorylation is another well-defined mechanism for mitochondrial toxicity. Uncoupling means that the protons, shifted from the mitochondrial matrix to the space between inner and outer membrane, do not pass across the F_0F_1ATPase (complex V) back to the mitochondrial matrix, but instead go directly across the inner mitochondrial membrane. The result is production of heat, but not of energy in the form of ATP. Typical examples of this mechanism include weak acids and weak bases [27], which can be protonated in the inter-membrane space and carry protons across the inner mitochondrial membrane.

Several drugs have been shown to inhibit hepatic fatty acid metabolism, in particular mitochondrial β-oxidation of fatty acids. Such drugs can either inhibit the activation of fatty acids or decrease the activity of one of the enzymes engaged in the β-oxidation process [28]. Inhibition of mitochondrial β-oxidation is usually accompanied by the cellular accumulation of fat, which can be visualized by specific staining of histological sections.
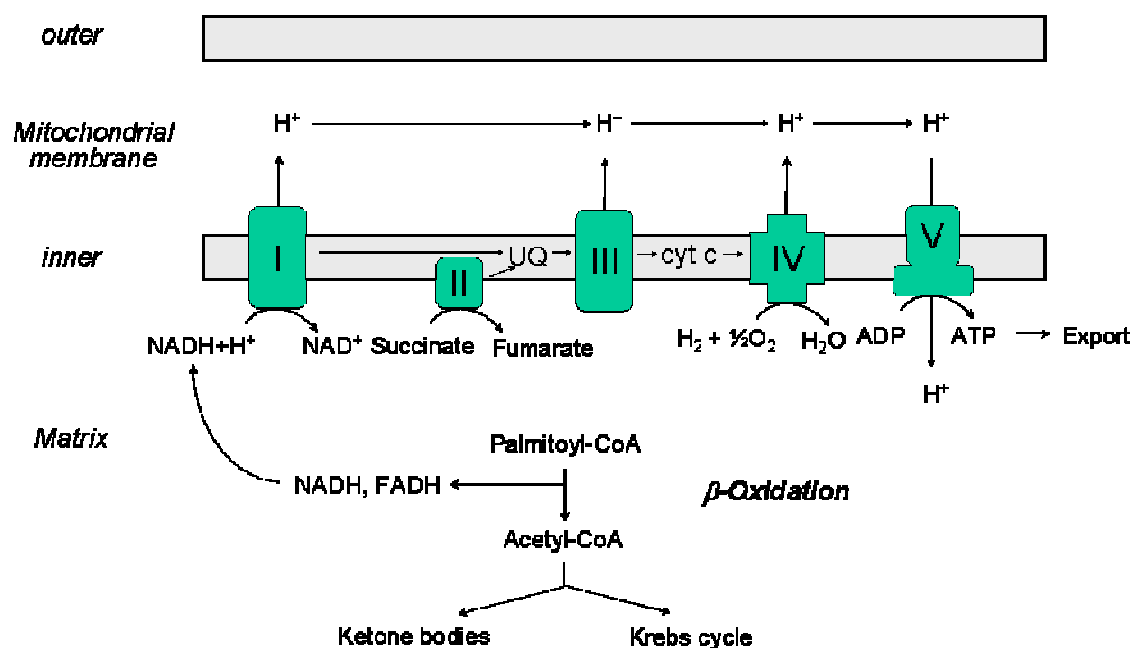
Figure 1. *Mitochondrial respiratory chain.* NADH and FADH produced by β-oxidation and other metabolic pathways within the mitochondrial matrix are metabolized by the electron transport chain consisting of the enzyme complexes I, II, III and IV. Ubiquinol (UQ) and cytochrome c (cyt c) transport electrons between complexes I or II and III, and between complexes III and IV, respectively. Complexes I, III and IV can shift protons from the mitochondrial matrix into the inter-membrane space, building up a proton gradient. This gradient is necessary to produce ATP from ADP by complex V or F_0F_1ATPase. β-Oxidation also produces acetyl-CoA which can be used for the formation of ketone bodies, or is degraded to CO_2 and H_2O by the Krebs cycle. Further explanations are given in the text.

The final mechanism is damage to the mitochondrial DNA by oxidation or by inhibition of DNA synthesis [29]. Mitochondrial DNA is more susceptible to oxidative damage than nuclear DNA due to absence of histones and efficient repair mechanisms in mitochondria, and also due to the proximity of mitochondrial DNA to the oxygen radicals producing respiratory chain. A class of drugs known to potentially impair the synthesis of mtDNA are nucleoside analogues used in the treatment of HIV or hepatitis B infections.

Opening of a mega-channel across the mitochondrial membranes (membrane permeability transition pore), leading to collapse of the membrane potential and swelling of the mitochondria, is another potential mechanism for drug toxicity. Opening of this mega-channel can lead to mitochondrial loss of cytochrome c, initiating the apoptosis cascade and eventually ending in cell death [30].

Table 1

Mitochondrial toxicity of drugs: principle mechanisms and typical examples.

- *Inhibition of the electron transport chain*
    Amiodarone, anthraline, benzbromarone, benzarone, buprenorphine, flutamide, MPP+, oxmetidine, perhexiline

- *Uncoupling of oxidative phosphorylation*
    Amiodarone, benzbromarone, benzarone, bupivacaine, buprenorphine, cerivastatin, etidocaine, tacrine

- *Mitochondrial permeability transition*
    Benzbromarone, benzarone, salicylate, valproate

- *Inhibition of mitochondrial fatty acid metabolism*
    Amiodarone, asparaginase, benzbromarone, benzarone buprenorphine, female sex hormones, NSAIDs, salicylate, tetracycline, valproate

- *Oxidation of mitochondrial DNA*
    Alcohol

- *Inhibition of mitochondrial DNA synthesis*
    Nucleoside analogues, e.g. zidovudine, fialuridine

3.3.3. Own studies in this field

Valproate hepatotoxicity

Valproate, a medium-chain branched fatty acid, is used frequently in the treatment of patients with different forms of epilepsy. Very occasionally, the intake of valproate can be associated with fulminant hepatic failure and death [31]. The most probable mechanism of valproate-associated hepatotoxicity is the production of toxic metabolites such as 4-ene-valproate, a toxin inhibiting mitochondrial β-oxidation [32] (see Figure 2 for valproate metabolism). Other mechanisms may contribute, in particular depletion of the hepatocellular free coenzyme A pool, and the formation of hepatotoxic acyl-CoAs [33]. We have investigated the CoA and carnitine metabolites in a liver from a patient with valproate-associated fulminant liver failure, and could demonstrate the expected decrease in the hepatic coenzyme A content and alterations in the hepatic carnitine pool [33].

The hallmark of liver histology in such patients is microvesicular steatosis, reflecting inhibition of mitochondrial β-oxidation [31, 33]. Since not all patients treated with valproate develop hepatotoxicity, accumulation of 4-ene-valproate alone is not enough to explain the hepatotoxicity associated with this drug. In the search for additional risk factors, we have investigated the siblings of the index patients with fulminant liver failure reported above [34]. The sister of the index patient had died from respiratory failure due to a mitochondrial disorder. In addition, her brother and mother also had clinical signs of a mitochondrial disorder, which could not be defined in more detail. Accordingly, in a muscle biopsy of the sister of the index patient, complexes I and IV of the respiratory chain showed a reduced activity, but the mitochondrial genome did not show mutations. The presence of a mitochondrial disorder, which may be sub-clinical, can therefore be regarded as a risk factor for the development of fulminant liver failure in patients treated with valproate. We are currently investigating this possibility in animal models with impaired hepatic mitochondrial β-oxidation.

In addition, treatment with valproate is associated with the formation of a variety of acylcarnitines and with a decreased carnitine plasma concentration [35]. Since we have developed a method for the determination of carnitine and acylcarnitines in plasma by LC/MS [36], we intend to study the acylcarnitines accumulating in the plasma of patients treated with valproate. Furthermore, it will be interesting to investigate the interaction between these acylcarnitines and carnitine on the level of OCTN2, the carnitine transporter responsible for proximal tubular reabsorption of carnitine [37]. We have stably expressed OCTN2 in different cell lines, and are going to use this system to study the transport of carnitine in the presence of the acylcarnitines detected in the plasma and urine of patients treated with valproate. Since our LC/MS method also allows the determination of butyrobetaine, the direct precursor of carnitine, we will be able to study the effect of valproate on renal clearance of butyrobetaine.
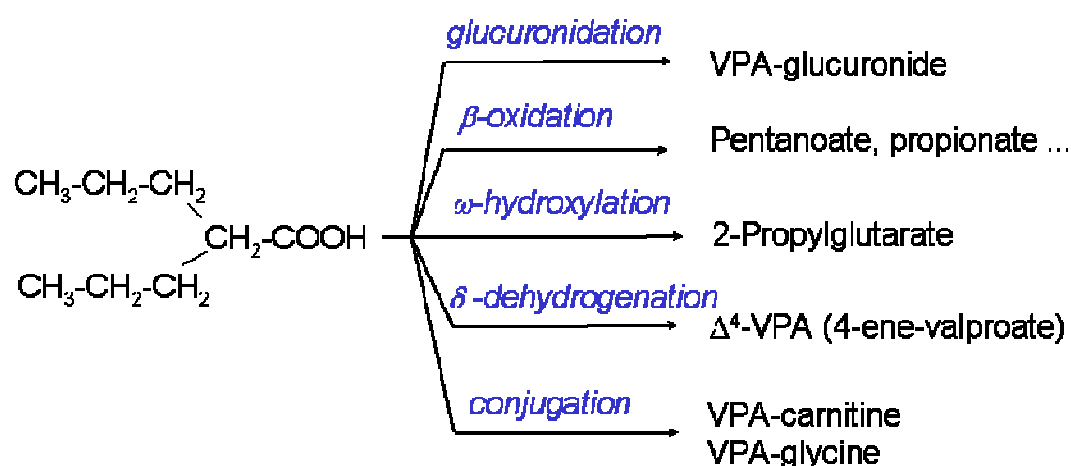
Figure 2. *Metabolism of valproate*. Valproate is a medium-chain, branched fatty acid, which is primarily metabolized by glucuronidation and conjugation with carnitine or glycine. In addition, valproate can be degraded by β-oxidation, which produces odd-chain fatty acids such as propionate and pentanoate. It can also be metabolized to a ω-hydroxy derivative, which can be converted to 4-ene-valproate. These fatty acid derivatives and/or their corresponding CoA-esters can inhibit mitochondrial functions, in particular mitochondrial β-oxidation.

Amiodarone

Amiodarone is a class III antiarrhythmic used widely to treat cardiac arrhythmias particularly in patients with coronary heart disease. In patients and animals, amiodarone can be associated with hepatocellular injury, which may be due to liver steatosis [38]. In mice and rats, it has been shown that amiodarone uncouples oxidative phosphorylation and inhibits β-oxidation of liver mitochondria [39, 40].

Regarding amiodarone, we were interested to find out the structure which is finally responsible for its mitochondrial toxicity, and whether it is possible to obtain a pharmacologically active amiodarone derivative (block of hERG channels) without mitochondrial toxicity. In a first study, we confirmed amiodarone's mitochondrial toxicity in rats, and could demonstrate the importance of the configuration of the diethylaminoethoxy side chain for its mitochondrial toxicity [41]. These data allowed us to synthesize additional derivatives with alterations in the side chain, rendering it more hydrophilic (see Figure 3). Indeed, we were able to detect two derivatives, which were lacking almost any mitochondrial toxicity. These derivatives contain only an ethoxy or an acetoxy group in the side chain attached to the benzoyl moiety (see Figure 3, unpublished results). The composition of this side chain appears therefore to be critical for mitochondrial toxicity of amiodarone derivatives. Further studies will have to show, whether these derivatives can block the hERG channels, and whether their activity to toxicity profile is favorable as compared to amiodarone.

Benzbromarone and bromarone

Benzbromarone and bromarone are amiodarone derivatives (see Figure 3). For both substances, hepatotoxicity has been shown, in some patients with a fatal outcome [42]. Because of the structural similarity with amiodarone, we hypothesized that the toxicity of these two substances may also have a mitochondrial mechanism.

We could indeed show that both drugs decrease the mitochondrial membrane potential, inhibit the activity of the respiratory chain and uncouple oxidative phosphorylation. In addition, both drugs impaired mitochondrial β-oxidation [43].

Since inhibition of the electron transport chain can be associated with increased formation of oxygen radicals, we speculated that benzbromarone and benzarone could open the membrane permeability transition pore, leading to dissipation of the mitochondrial membrane potential and possibly initiating apoptosis. Indeed, we could demonstrate increased reactive oxygen species (ROS) formation in the presence of these substances, and opening of the membrane permeability transition pore; as well as mitochondrial swelling and cellular spillage of cytochrome c due to rupture of the outer mitochondrial membrane. This initiated either apoptosis or necrosis, depending on the cellular ATP content [43].

Amiodarone

Benzarone
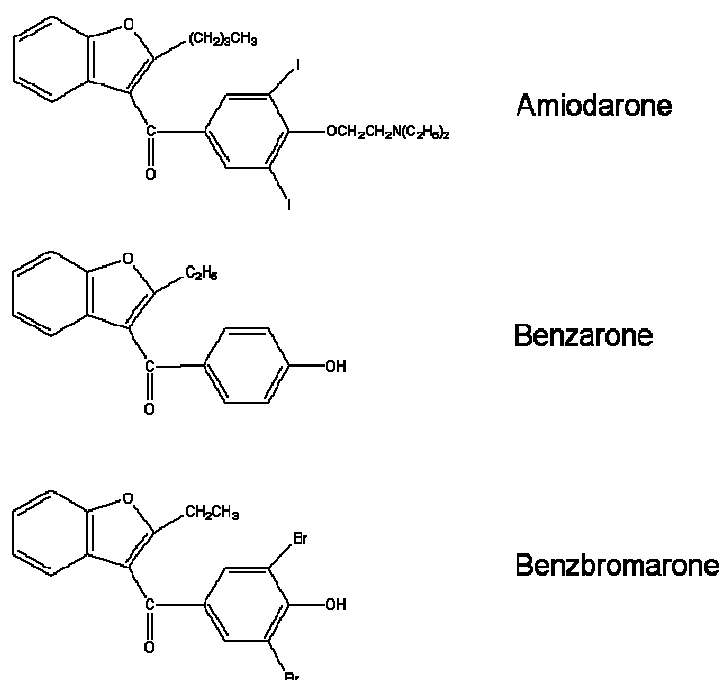
Benzbromarone

Figure 3. *Structure of amiodarone and amiodarone derivatives investigated*. Amiodarone, benzbromarone and benzarone are 3-benzoyl-benzofuran derivatives. All of these three substances are mitochondrial toxins, mainly affecting the respiratory chain and β-oxidation. While amiodarone carries a diethylaminoethoxy side chain at the benzoyl moiety, this side chain is lacking for benzarone and benzbromarone. Alterations of this side chain, e.g. replacement by an ethoxy or acetoxy group, is reducing the mitochondrial toxicity of amiodarone.

3.3.4. Conclusions

Many drugs can affect mitochondrial function and can, thereby, lead to cellular and/or organ damage. Important mechanisms include inhibition of the respiratory chain, uncoupling of oxidative phosphorylation and inhibition of mitochondrial β-oxidation. These primary effects can secondarily lead to a decrease in the mitochondrial ATP content, increased production of ROS and opening of the mitochondrial membrane permeability transition pore, with consecutive mitochondrial swelling, rupture of the outer membrane and cellular spillage of cytochrome c. These events can end in apoptosis or necrosis of the affected cells, depending on the cellular ATP content.

3.4. Toxicity of statins on rat skeletal muscle mitochondria

Priska Kaufmann, Michael Török, Anja Zahno, Katri Maria Waldhauser, Karin Brecht, Stephan Krähenbühl

Division of Clinical Pharmacology & Toxicology and Department of Research, University Hospital Basel, Switzerland

3.4.1. Summary

We investigated mitochondrial toxicity of four lipophilic (cerivastatin, fluvastatin, atorvastatin, simvastatin) and one hydrophilic statin (pravastatin). In L6 cells (rat skeletal muscle cell line), the four lipophilic statins (100µmol/L) induced death in 27 to 49% of the cells. Pravastatin was not toxic up to 1mmol/L. Cerivastatin, fluvastatin and atorvastatin (100µmol/L) decreased the mitochondrial membrane potential by 49 to 65%, whereas simvastatin and pravastatin were less toxic. In isolated rat skeletal muscle mitochondria, all statins, except pravastatin, decreased glutamate-driven state 3 respiration and respiratory control ratio. Beta-oxidation was decreased by 88 to 96% in the presence of 100µmol/L of the lipophilic statins, but only at higher concentrations by pravastatin. Mitochondrial swelling, cytochrome c release and DNA fragmentation was induced in L6 cells by the four lipophilic statins, but not by pravastatin. Lipophilic statins impair the function of skeletal muscle mitochondria, whereas the hydrophilic pravastatin is significantly less toxic.

3.4.2. Introduction

Statins (3-hydroxy-3-methyl-glutaryl coenzyme A reductase inhibitors, HMG-Co A reductase inhibitors) impair hepatocellular cholesterol production by inhibiting the synthesis of mevalonate, a critical intermediary product in the cholesterol pathway. They are generally well tolerated, but can produce a variety of skeletal muscle-associated, dose-dependent adverse reactions, ranging from muscle pain to frank rhabdomyolysis. Rhabdomyolysis is a serious adverse reaction of these drugs for both patients and the pharmaceutical industry, as evidenced by numerous case reports and case series [44, 45] and the withdrawal from the market of cerivastatin in August 2001 [46] .

The frequency of rhabdomyolysis is low, with a reported incidence of approximately 1:10,000 patient years [47] and a death rate 0.15 per million prescriptions [46, 48]. The fact that the frequency of myotoxicity observed for cerivastatin was higher than for the other statins raised the question of whether there are differences in the myotoxic potential of the statins and whether such differences are related to their physicochemical properties. As shown in Table 1, differences in the physicochemical properties of statins can result in a variable kinetic behavior, including bioavailability, tissue distribution and metabolism, which may affect their toxic potential on skeletal muscle [49]. For example, inhibition of cytochrome P450 (CYP) isozymes can lead to increased bioavailability of lipophilic statins [50], thereby elevating the potential for myotoxicity. However, since myotoxicity has been reported with all statins on the market, the variability in their pharmacokinetic properties does not adequately explain the susceptibility to develop statin-induced myotoxicity.

Little is known regarding the mechanisms by which statins produce skeletal muscle injury. HMG-CoA reductase catalyses the formation of mevalonate from HMG-CoA. Mevalonate is an important precursor not only of cholesterol but also of ubiquinone, dolichols and other isoprenoids [51]. All of these compounds are involved in various essential cell functions. A deficit in them may therefore adversely affect myocytes, rendering them vulnerable to myotoxic events [51, 52]. This hypothesis was strengthened by the observation that the myotoxicity of statins on myocytes *in vitro* could be decreased by the addition of mevalonate [53, 54]. Ubiquinone, whose biosynthesis is reduced in the presence of statins [51, 52], is utilized by mitochondria for the transport of electrons between enzyme complexes of the electron transport chain. Reduced levels of ubiquinone are present in specific forms of mitochondrial myopathies and are considered to result in impaired mitochondrial electron transport chain function and decreased adenosine triphosphate (ATP) synthesis [55, 56]. Regarding statins and mitochondria, light microscopic changes observed in muscle biopsies of patients with statin-associated myopathy were similar to the findings in patients with mitochondrial myopathies [57-60]. In a patient with rhabdomyolysis associated with simvastatin, MELAS syndrome manifested in the recovery phase, suggesting that so far unnoticed mitochondrial diseases may represent

risk factors for statin-associated myopathy [61]. Furthermore, in a recent study, Vladutiu et al. described biochemical and/or genetic abnormalities of proteins or genes involved in skeletal muscle energy metabolism in more than 50% of patients with statin-associated myopathy [62]. Recent *in vitro* investigations indicate that simvastatin interferes with mitochondrial calcium homeostasis and inhibits complex I of the electron transport chain [63].

On the basis of these reports, we hypothesized that statins could act as mitochondrial toxins and that the patients with an underlying mitochondrial disease could react preferentially with myopathy. Since the data about toxicity of statins on mitochondria are still rare, we decided to investigate the effects of several statins on isolated rat skeletal muscle mitochondria and on L6 cells, a rat skeletal muscle cell line.

Table 1

Physiochemical properties, pharmakokinetic parameters and metabolism of the statins studied. [48, 52]

Statin	Lipophi-licity	Hepatic extraction [%]	Bioavaila-bility [%]	Protein binding [%]	Volume of distribution (L)	Metabolism	Renal/ fecal elimina tion [%]
Cerivastatin	high	< 40	60	99	21	[1]Cyp3A4/2C8	30 / 70
Fluvastatin	high	> 68	6	98	30	Cyp2C9/3A4	6 / 90
Atorvastatin	high	> 70	12	80	381	Cyp3A4	2 / 70
Simvastatin	high	~ 80	5	95	[2]nk	Cyp3A4	13 / 58
Pravastatin	low	44-66	18	50	35	Conjugation	20 / 71

[1]CYP = cytochrome P450, [2]nk = not known

3.4.3. Materials and Methods

3.4.3.1. Materials

Fluvastatin was a gift from Novartis Pharma (Basel, Switzerland), simvastatin from Merck Sharp & Dohme (Rahaway, NJ, USA), cerivastatin from Bayer (Zürich, Switzerland) and pravastatin from Bristol-Myers Squibb (Sankyo, Japan). Atorvastatin was provided by Prof J. Drewe (University Hospital Basel, Switzerland). Simvastatin lactone was converted to the corresponding acid as described previously. [64] JC-1 was obtained from Alexis Biochemicals (Lausen, Switzerland) and [1-^{14}C]palmitic acid from Amersham (Dübendorf, Switzerland). FAS ligand was prepared as described previously [65].

Fetal calf serum, all supplements and the culture medium were from Gibco (Paisley, UK). The 96-well plates were purchased from Becton Dickinson (Franklin Lakes, NJ, USA) and the 8-chamber slides from Nalge Nunc (Rochester, NY, USA). The Vybrant[TM] Apoptosis Assay

Kit #2 was purchased from Molecular probes (Eugene, OR, USA). All other chemicals used were of best quality available and purchased from Sigma–Aldrich (Schnelldorf, Germany).

3.4.3.2. Animals

Male Sprague Dawley rats (Charles River, Les Onins, France) were used for all experiments. They were fed *ad libitum*, hold on a 12-hour dark and light cycle and weighed before their use. The study protocol had been accepted by the local Animal Ethics Committee.

3.4.3.3. Cells

L6 cell lines (rat skeletal muscle myoblasts) were obtained from LGC Promochem (Wesel, Germany). The cell line was cultured in Dulbecco's Modified Eagle's Medium (Gibco 61965026; with 4mmol/L GlutaMAX®, 4.5g/L glucose and sodium bicarbonate) supplemented with 10% heat inactivated fetal calf serum, 1mmol/L sodium pyruvate and 5μL/mL penicillin-streptomycin. Culture conditions were 5 % CO_2 and 95 % air atmosphere at 37°C.

3.4.3.4. Isolation of rat skeletal muscle mitochondria

At the time of killing, the rat weight averaged 389g. The animals were first treated with carbon dioxide and then killed by decapitation. The skeletal muscle of the hind legs (mean 19.0g) was removed, freed from fat and connective tissue, minced with scissors and homogenized according to Kerner and Hoppel [66]. From this homogenate, skeletal muscle mitochondria were isolated according to Palmer et al. [67].
The mitochondrial protein content was determined using the biuret method with bovine serum albumin (BSA) as a standard [68].

3.4.3.5. In vitro cytotoxicity assays

Cell injury was assessed by the determination of the activity of lactate dehydrogenase (LDH) in the supernatant of statin-treated as compared to LDH activity in the supernatant of lysed cells (Triton X-100 0.8%) [65]. LDH activity was analyzed as described by Vassault [69]. Different concentrations of the compounds investigated and 100mmol/L mevalonate (only to selected incubations, see Results) were added to the cell cultures in a 96-well-plate for 24 hours before the supernatants were harvested and analyzed. Control incubations were treated with the vehicle used to dissolve the substances investigated.

3.4.3.6. Mitochondrial membrane potential ($\Delta\Psi$m)

Cells were detached from the cell culture flasks by adding 10mmol/L ethylenediamine-tetraacetic acid (EDTA) in phosphate buffered saline pH 7.4 (PBS). After filtration, cells were adjusted to a density of 0.5 x 10^6 cells/mL and incubated in complete medium in the dark. Before incubation, test substances, JC-1 (4µg/mL) and 100µmol/L mevalonate (only to selected incubations, see Results) were added. Flow cytometry was performed after an incubation time of 10min using a FACS Calibur flow cytometer (Becton Dickinson, San José, CA, USA). Changes in $\Delta\Psi_m$ could be monitored by measuring the JC-1 fluorescence using FL-1 and FL-2. FL denotes the measured fluorescence intensity in the respective channel (FL-1 = 530 ± 15nm, FL-2 = 585 ± 21nm). Dinitrophenol (an uncoupler) and benzbromarone (depolarizes the mitochondrial membrane potential [65]) served as controls.

3.4.3.7. Oxygen consumption

Oxygen consumption was monitored polarographically using a 1mL chamber equipped with a Clark-type oxygen electrode (Yellow Springs Instruments, Yellow Springs, OH, USA) at 30°C as described previously [70]. The final concentration of L-glutamate was 20mmol/L.

Oxygen consumption by intact mitochondria: The respiratory control ratio (RCR) was calculated according to Estabrook [71]. The RCR represents the ratio between the rate of oxygen consumption in the presence of a substrate and ADP (state 3) and the rate after complete conversion of ADP to ATP (state 4).

The test compounds were added to the mitochondrial incubations before the addition of the respective substrate. Control experiments were carried out in the presence of the solvent (1% DMSO) containing no inhibitor.

Oxygen consumption of L6 muscle cells: 1 x 10^6 cells were treated with oligomycin (final concentration 5µg/mL) in order to inhibit F_1F_0-ATPase. After 2 minutes, test compounds were added to the incubation chamber and the oxygen consumption was determined. Control experiments were carried out with solvent (1% DMSO).

3.4.3.8. Activity of NADH-oxidase

The activity of NADH-oxidase was determined at 30°C using freeze-thawed mitochondria as described originally by Blair et al. [72] with the modifications described earlier [73].

3.4.3.9. In vitro mitochondrial β-oxidation and carnitine palmitoyltransferase (CPT) activity

The β-oxidation of [1-^{14}C] palmitic acid by skeletal muscle mitochondria was assessed according to Sherratt et al. [74]. The incubation vials, which contained 500µg mitochondrial

protein in 900μl incubation solution, were closed with a rubber stopper and incubated for 15min at 30°C. A scoop containing a filter paper soaked with 90μl of 0.1mol/L KOH was fixed at the rubber stopper and was used to trap the volatile $^{14}CO_2$.

CPT activity was measured by the formation of palmitoyl-[^{3}H]-carnitine from palmitoyl-CoA and [^{3}H]-L-carnitine [75], a reaction mainly reflecting activity of CPT1. Palmitoylcarnitine was extracted with 1.4mL of water-saturated 1-butanol, which was washed with 600μL butanol-saturated water [76] and quantified by liquid scintillation counting.

3.4.3.10. Activities of mitochondrial β-oxidation enzymes

All enzyme activities were determined using spectrophotometric assays at 37°C. Freeze-thawed mitochondria were treated 1:1 with 5% cholic acid in order to disrupt the mitochondrial membranes. The solution was then diluted one hundred times with 50mmol/L potassium phosphate buffer (pH 7.4). Acyl-CoA dehydrogenase was determined according to Hoppel et al. [70], using palmitoyl-CoA as a substrate. Beta-hydroxy-acyl-CoA dehydrogenase was determined in the reverse direction according to Brdiczka et al. using acetoacetyl-CoA as substrate [77]. Beta-ketothiolase was determined using acetoacetyl-CoA as a substrate according to Hoppel et al. [70].

3.4.3.11. Mitochondrial swelling

Mitochondrial swelling was monitored by measuring the decrease in light scattering at 540nm using a SpectraMAX 250 plate reader (Paul Bucher Analytik und Biotechnologie, Basel, Switzerland). The decrease in light scattering has been shown to correlate closely with the percentage of the mitochondrial population undergoing permeability transition [78]. Freshly isolated mitochondria were suspended in isotonic swelling buffer (pH 7.3; 150mmol/L KCl, 20mmol/L MOPS, 10mmol/L Tris(hydroxymethyl)-aminomethan (TRIS), 2mmol/L nitrilotriacetic acid and 2μmol/L calcium ionophore A23187) and exposed to test compounds at room temperature. Swelling was calculated from the slope between 60 and 2000 sec of exposure.

3.4.3.12. Cytochrome c immunocytochemistry

For immunocytochemistry, cells were grown in an 8 chamber-slide for 24 hours at 37°C and then treated with the test compounds for 24 hours. Cytochrome c was visualized by immunocytochemistry as described previously [65].

3.4.3.13. Cellular ATP content

Rat myoblasts (500'000 L6 cells/well) were transferred into a 12-well plate and treated for 24 hours with test compounds. Following treatment, cells were collected and the ATP content measured as described previously [65]. ATP concentrations were calculated using an ATP standard curve.

3.4.3.14. Determination of apoptosis

Both assays were performed using L6 muscle cells cultured on poly-D-lysine coated (0.1mg/mL, 30min) cell culture dishes.

Hoechst 33342 nuclear staining: A confluent cell layer was treated for 24h with test compounds, then incubated for 30 minutes at room temperature with Hoechst 33342 dye (50µmol/L in PBS) and visualized by fluorescence microscopy (Olympus IX 50, Hamburg, Germany).

Annexin V and propidium iodide (PPI) staining: An *in situ* apoptosis detection kit was used for Annexin V binding and propidium iodide staining (Vybrant™ Apoptosis Assay Kit #2). After a 24h incubation with the test compounds, cells were stained with 25µL Annexin V-Alexa Fluor® 488 and 2µL PPI (final concentration: 1.5µg/L). After 15 minutes of incubation at room temperature, samples were analyzed by flow cytometry, using a FACS Calibur flow cytometer (Becton Dickinson, San José, USA).

3.4.4. Statistical analysis

Data are presented as mean ± standard error of the mean (SEM). For statistical comparisons, data of groups were compared by analysis of variance (ANOVA). The level of significance was $p \leq 0.05$. If ANOVA revealed significant differences, comparisons between the control and the other incubations were performed by Dunnett's post test procedure. A t-test (unpaired, two-tailed) was performed if only two groups were analyzed.

3.4.5. Results

3.4.5.1. In vitro cytotoxicity

Cytotoxicity was investigated by treating L6 cells with various concentrations of the different statins for 24 hours. As shown in Figure 1, 100µmol/L cerivastatin, fluvastatin, atorvastatin or simvastatin showed significant toxicity. In contrast, pravastatin did not cause any cell damage up to 1mmol/L. Statin-associated cytotoxicity could not be prevented by the addition of 100µmol/L mevalonate to the incubations. Since lipophilic statins were toxic to muscle cells, further experiments were performed to find out the mechanisms for cytotoxicity.
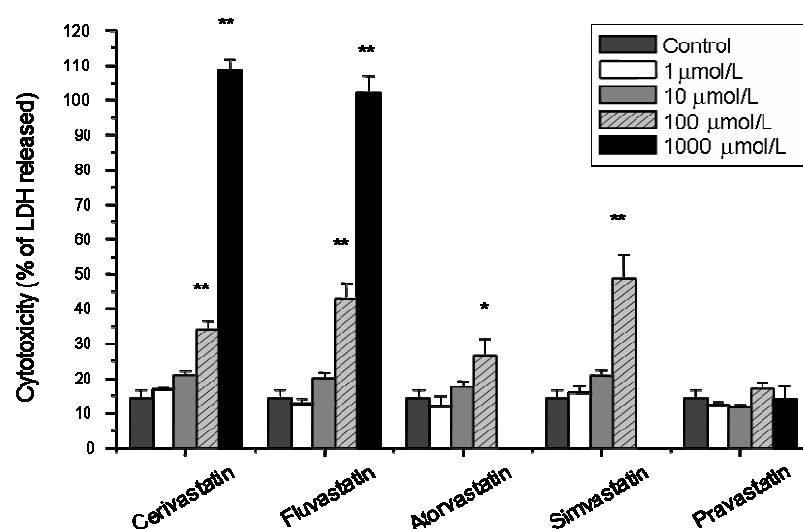
Figure 1

Cytotoxicity of the test compounds. Cerivastatin, fluvastatin, atorvastatin and simvastatin caused a concentration-dependent release of LDH from L6 cells into the cell culture media. In contrast, the cells were not destroyed by pravastatin up to 1mmol/L. Data are expressed as the percentage of total LDH activity released into the cytoplasm and are presented as mean ± SEM of at least three individual experiments. *$p < 0.05$ vs. control, **$p < 0.01$ vs. control.

3.4.5.2. Mitochondrial membrane potential

Since statin-induced myopathy has been shown to be associated with mitochondrial dysfunction [57, 58], we first focused on mitochondria. In a first step, we measured the mitochondrial membrane potential, since this potential is critical for myocyte survival [79] and its dissipation can be associated with induction of apoptosis [80]. As shown in Figure 2, at a concentration of 100µmol/L, 35% of the cells showed a dissipated mitochondrial membrane potential in the presence of cerivastatin, and 51%, 20% or 26% in the presence of fluvastatin, atorvastatin or simvastatin, respectively. The dissipation of the mitochondrial membrane potential could not be prevented by the addition of 100µmol/L mevalonate to the incubations (data not shown).
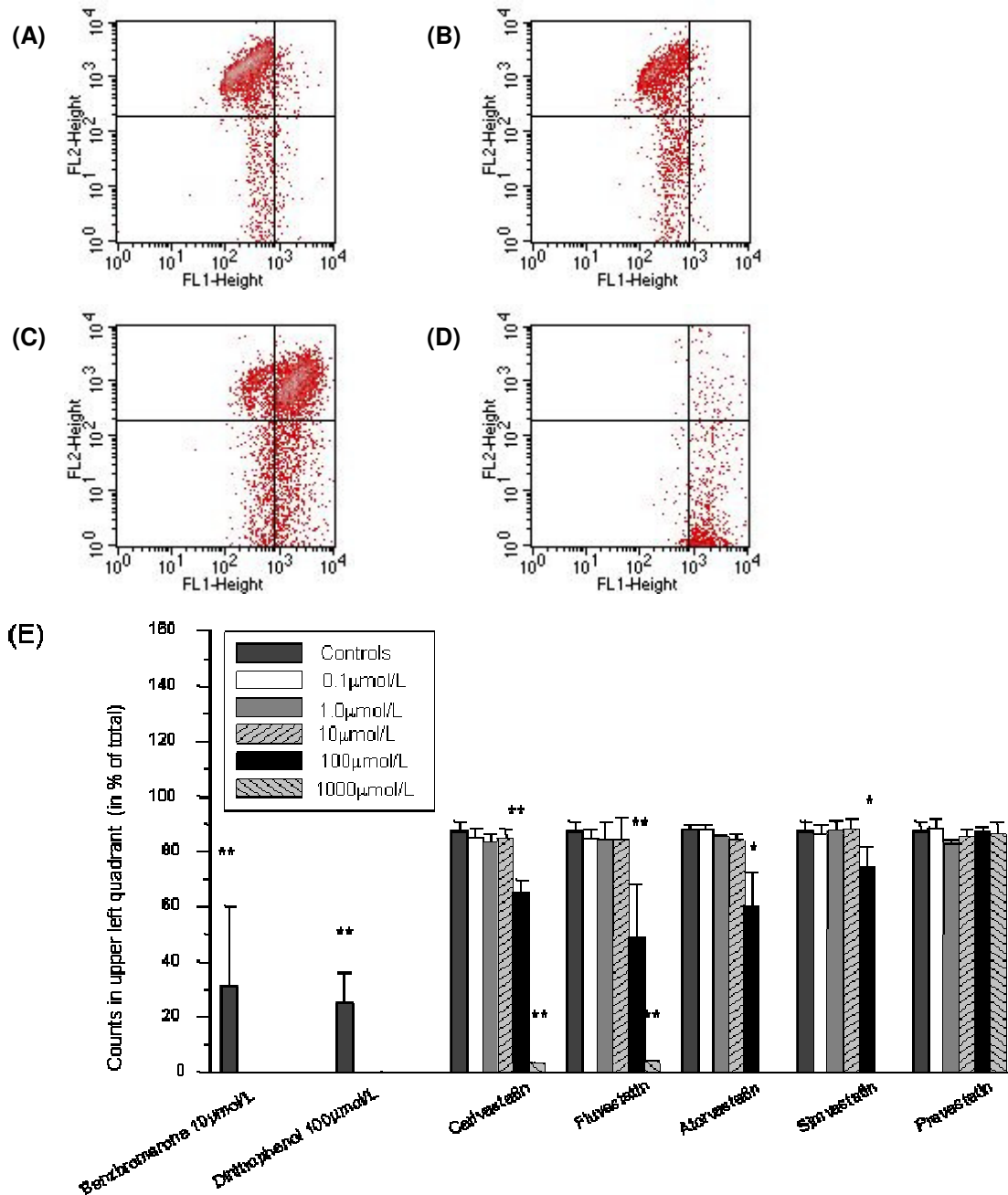
Figure 2

Assessment of the mitochondrial membrane potential. After labelling the cells with JC-1, mitochondrial depolarization could be visualized by a shift of the fluorescence emission from green to red. In the upper left quadrant, cells with polarized mitochondria are located (panel A; DMSO 1%), whereas cells with dissipated potential are found in the upper or lower right panels (panel B, C or D; fluvastatin 10µmol/L, 100µmol/L or 1000µmol/L, respectively). In panel E, the counts retrieved in the upper left quadrant are given as the percentage of total counts (defined as 100%). Data are given as mean ± SEM of at least three individual experiments. *p<0.05 vs. control, **p<0.01 vs. control.

3.4.5.3. Mitochondrial respiration

In order to further specify the mitochondrial defects, we assessed the toxicity of the statins on oxidative metabolism of isolated rat skeletal muscle mitochondria. In the presence of L-glutamate as a substrate, cerivastatin, fluvastatin, atorvastatin and simvastatin induced a progressive depression of the RCR, which reflects the activity of the electron transport chain and the tightness of the coupling of oxidative phosphorylation (see Table 2). The concentrations associated with a 50% decrease in the RCR were: 57µmol/L for cerivastatin, 72µmol/L for fluvastatin, 113µmol/L for atorvastatin and 78µmol/L for simvastatin. In contrast, pravastatin did not significantly affect the RCR up to 400µmol/L.

Table 2

Effects of cerivastatin, fluvastatin, atorvastatin, simvastatin and pravastatin on oxidative metabolism of L-glutamate by isolated rat skeletal muscle mitochondria. See method section for experimental details. Mean ± SEM of at least 3 experiments using different mitochondrial preparations.

	State 3	State 4	RCR
Control (no inhibitor)	233 ± 21	66 ± 14	3.7 ± 0.8
Cerivastatin (µmol/L)			
2	256 ± 23	69 ± 10	4.0 ± 0.6
5	240 ± 31	69 ± 6	3.5 ± 0.4
25	289 ± 35	88 ± 10	3.4 ± 0.5
50	274 ± 35	137 ± 15*	2.0 ± 0.0
100	187 ± 19	187 ± 19**	1.0 ± 0.0**
Fluvastatin (µmol/L)			
5	241 ± 15	63 ± 7	3.9± 0.2
25	224 ± 8	42 ± 21	3.5 ± 0.3
50	266 ± 24	65 ± 6	2.3 ± 0.4
100	192 ± 41	126 ± 28*	1.7 ± 0.5*
200	31 ± 17**	116 ± 11*	1.0 ± 0.0**
Atorvastatin (µmol/L)			
5	171 ± 28	49 ± 3	3.4 ± 0.3
25	173 ± 20	56 ± 1	3.1 ± 0.3
50	161 ± 45	45 ± 9	3.5 ± 0.6
100	149 ± 6*	71 ± 11	2.2 ± 0.3*
200	45 ± 5**	45 ± 5	1.0 ± 0.0**
Simvastatin (µmol/L)			
5	200 ± 32	56 ± 6	3.0 ± 0.3
25	213 ± 56	74 ± 16	2.8 ± 0.4
50	157 ± 41	86 ± 18	1.9 ± 0.5*
100	123 ± 15*	80 ± 13	1.7 ± 0.5*
200	83 ± 9*	83 ± 9	1.0 ± 0.0**
Pravastatin (µmol/L)			
50	272 ± 25	92 ± 10	3.0 ± 0.4
100	338 ± 41	95 ± 28	2.9 ± 0.5
200	271 ± 36	82 ± 5	3.4 ± 0.5
300	247 ± 41	90± 12	2.7 ± 0.1
400	278 ± 73	88 ± 10	3.1 ± 0.5

*p < 0.05 vs. control; ** p < 0.01 vs. control

While the depression of the RCR by fluvastatin, atorvastatin and simvastatin was mainly due to inhibition of state 3 respiration (inhibition of the electron transport chain), for cerivastatin, the decrease was mostly due to acceleration of state 4, suggesting uncoupling. We therefore determined oxygen consumption by L6 cells in the presence of oligomycin, an inhibitor of F_1F_0ATPase (Figure 3). Under these conditions, only cerivastatin showed an increase in state 4 respiration, demonstrating that cerivastatin uncouples oxidative phosphorylation.
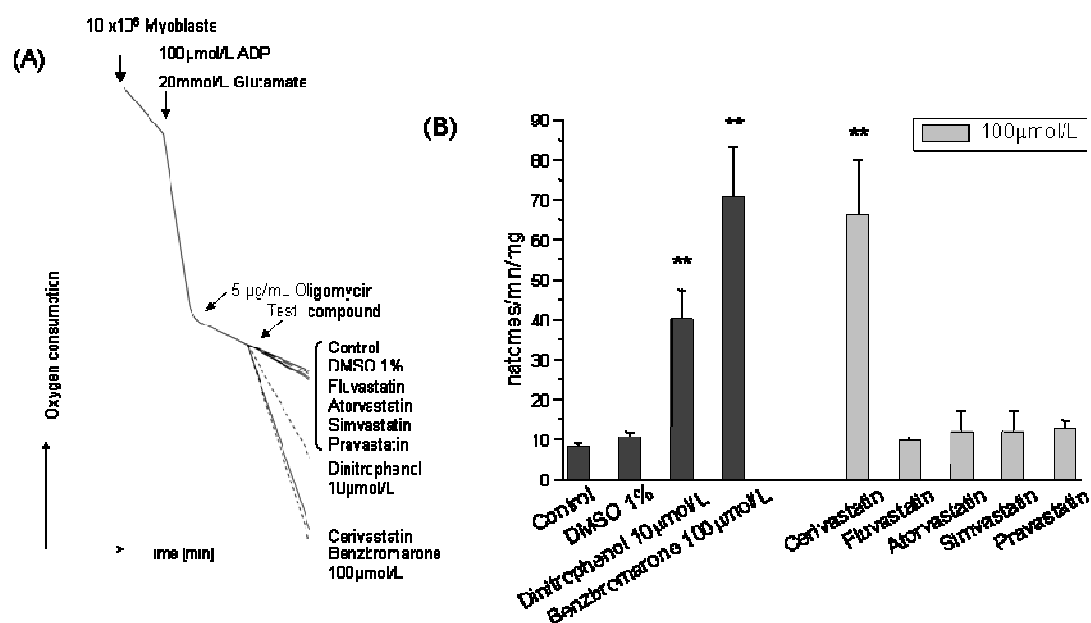
Figure 3

Uncoupling effect of statins. Uncoupling was determined by assessing the effect of statins on state 4 respiration in the presence of L-glutamate and oligomycin using L6 cells. In coupled mitochondria, blocking of the F_1F_0-ATPase by oligomycin results in a restricted electron transport and oxygen consumption similar to state 4. If a test compound works as an uncoupler, oxygen consumption increases, in spite of inhibited phosphorylation (panel A). Of the tested statins, only cerivatstatin worked as an uncoupler, whereas the other statins did not increase oxygen consumption. Dinitrophenol and benzbromarone served as positive controls. *p<0.05 vs. control, **p<0.01 vs. control.

In order to exclude the possibility that the observed lack of toxicity of pravastatin is due to its hydrophilicity, which could impair membrane permeation, the activity of the mitochondrial NADH oxidase (reflecting activities of complex I, III and IV) was measured using broken mitochondria. Also in the absence of membrane barriers, pravastatin up to 1mmol/L did not impair the activity of the electron transport chain, whereas the lipophilic statins revealed significant inhibitory effects at ≥ 100µmol/L (results not shown).

3.4.5.4. Fatty acid metabolism

For the assessment of β-oxidation by skeletal muscle mitochondria, both the formation of acid soluble products and CO_2 were determined. [74] As shown in panel A of Figure 4, cerivastatin (100µmol/L), fluvastatin, atorvastatin and simvastatin (each 200µmol/L) inhibited mitochondrial β-oxidation between 82 and 96%. For pravastatin, a significant inhibition of β-oxidation was found at (300µmol/L). The corresponding IC_{50} were: 14µmol/L for cerivastatin, 9.0µmol/L for fluvastatin, 29µmol/L for atorvastatin, 75µmol/L for simvastatin and 300µmol/L for pravastatin.

In order to localize the inhibitory effect of β-oxidation in more detail, three enzymes of the β-oxidation were investigated. Acyl-CoA dehydrogenase was inhibited by 30-40% in the presence of 100µmol/L cerivastatin, 200µmol/L fluvastatin, atorvastatin or simvastatin, or 400µmol/L pravastatin, and β-hydroxy-acyl-CoA dehydrogenase by 10-20% in the presence of 100µmol/L cerivastatin, 200µmol/L fluvastatin, atorvastatin or simvastatin, or 400µmol/L pravastatin. In contrast, β-ketothiolase was not significantly inhibited by the statins used at the same concentrations as above.

Since there was some discrepancy between the inhibition of the β-oxidation pathway (using intact mitochondria) and individual enzymes (using disrupted mitochondria), we also determined the activity of CPT, which can be rate-limiting for fatty acid oxidation. [81] As shown in panel B of Figure 4, fluvastatin and cerivastatin inhibited CPT1 activity, whereas the other statins revealed no significant inhibitory effect up to 200µmol/L (atorvastatin) or 1mmol/L (simvastatin, pravastatin).
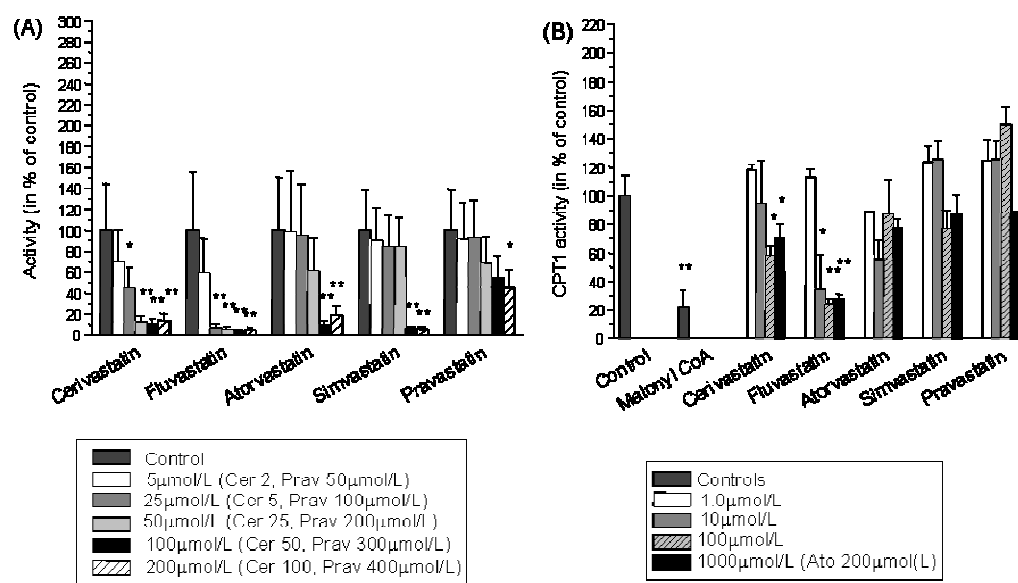
Figure 4

Effect of statins on β-oxidation and CPT1 activity. Fatty acid oxidation (panel A) was determined using isolated rat skeletal muscle mitochondria and was impaired by all lipophilic statins in a concentration-dependent manner (IC_{50} 9.9 – 76µmol/L). In contrast, pravastatin inhibited fatty acid oxidation with an IC_{50} of 300µmol/L. Data are given relative to control values (100% activity corresponds to 3.90nmol/mg mitochondrial protein/min). In panel B, the effect of statins on CPT1 activity using isolated mitochondria was determined. Cerivastatin and fluvastatin are inhibitors of CPT1, whereas the other 3 statins investigated do not affect CPT1 activity. Data are given relative to control values (100% activity corresponds to 6.45nmol/mg mitochondrial protein/min). Data are given as mean ± SEM of at least three individual experiments. *p<0.05 vs. control, **p<0.01 vs. control.

3.4.5.5. Mitochondrial swelling and release of cytochrome c

As already demonstrated, statins did cause a loss of the mitochondrial membrane potential. We therefore hypothesized that statins might induce mitochondrial permeability transition, which can result in mitochondrial swelling and cytochrome c release [82]. As shown in Figure 5, cerivastatin, fluvastatin, atorvastatin and simvastatin were inducing mitochondrial swelling in a concentration-dependent manner, whereas pravastatin did not cause an opening of the mitochondrial permeability transition pore.
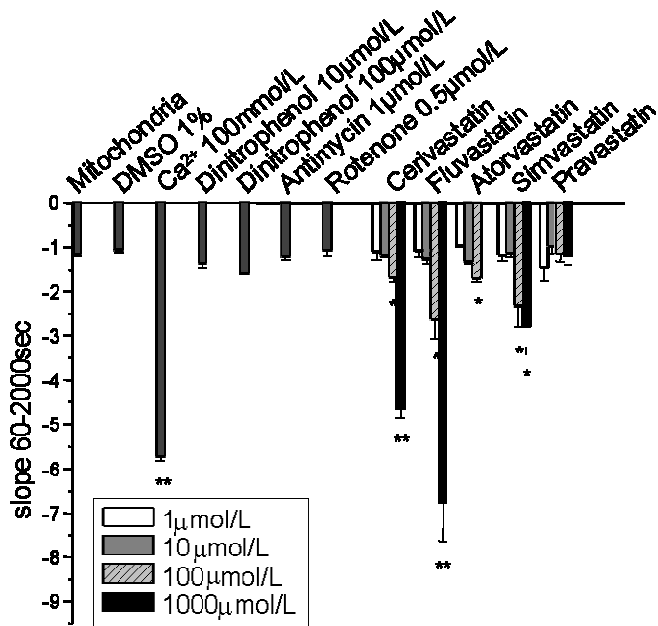
Figure 5

Induction of mitochondrial permeability transition. Mitochondrial permeability transition was monitored as a decrease in absorbance at 540nm. Upon pore opening, osmotically driven influx of water into the mitochondrial matrix leads to mitochondrial swelling, causing a change in the light scattering properties of mitochondria. Ca^{2+} was used as positive control. Among the tested statins, only pravastatin did not induce mitochondrial permeability transition, whereas all lipophilic statins caused a concentration-dependent increase in mitochondrial size. * $p < 0.05$ vs. control; ** $p < 0.01$ vs. control.

As a consequence of the mitochondrial permeability transition pore opening, cytochrome c release from the mitochondrial intermembrane space into the cytoplasm can occur, which can trigger the mitochondrial pathway of apoptosis [83]. To assess this possibility, cytochrome c release into cytoplasm was determined. As shown in Figure 6, only pravastatin did not induce a release of cytochrome c from the mitochondria, whereas in the presence of the lipophilic statins, cytochrome c was spilled into the cytoplasm.
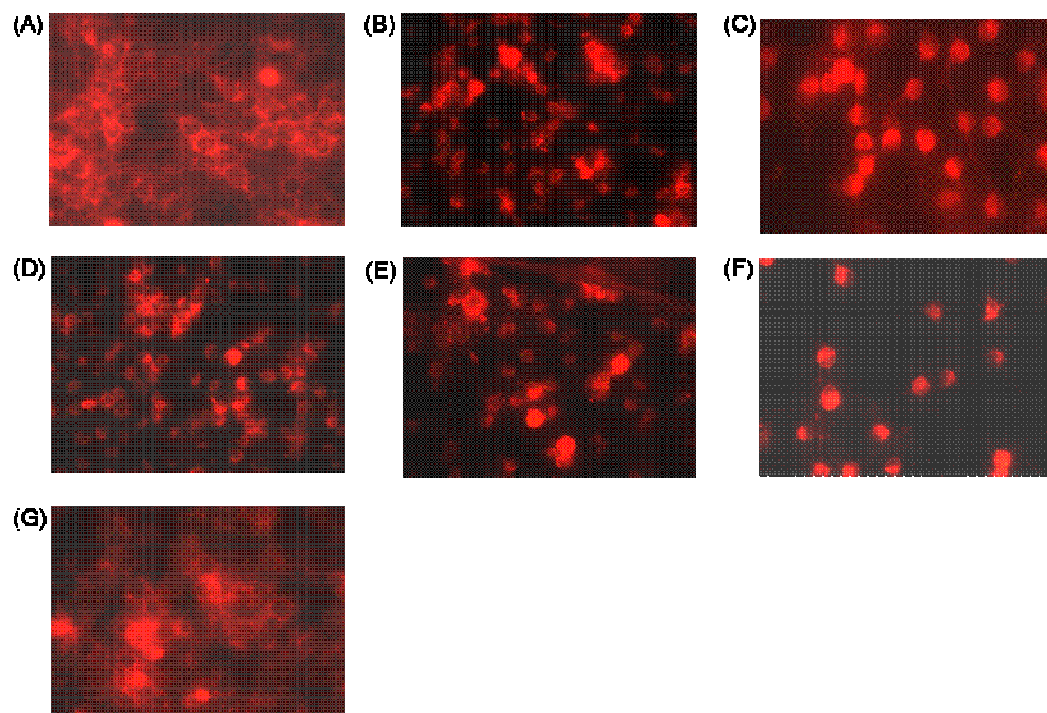
Figure 6

Mitochondrial release of cytochrome c. L6 cells were incubated with test compounds (each 100µmol/L) for 24 hours and cytochrome c was detected by immunocytochemistry. In the presence of 1% DMSO (panel A, negative control) or pravastatin (panel G), no leakage into the cytoplasm occurred (the nuclei are clearly visible and cytochrome c is distributed in the cytoplasm with a granular pattern). After treatment with benzbromarone (positive control, panel B), cerivastatin (panel C), fluvastatin (panel D), atorvastatin (panel E) or simvastatin (panel F), cytochrome c was released from the mitochondrial intermembrane space into the cytoplasm (most nuclei covered by cytochrome c and the cytoplasm stained diffusely).

3.4.5.6. Mechanisms of cell death

Cytoplasmic cytochrome c can activate caspases and induce apoptosis [84]. DNA fragmentation occurring during apoptosis can be visualized by fluorescence microscopy using dyes intercalating with DNA. As shown in Figure 7, untreated cells showed an apoptosis rate of 1.1%. At a concentration of 100µmol/L, the proportion of apoptotic cells was 13% for cerivastatin, 11% for fluvastatin, 6% for atorvastatin, 6% for simvastatin and 1% for pravastatin.

Another hallmark of the early stages of apoptosis is the translocation of phosphatidylserine from the inner to the outer leaflet of the plasma membrane, what can be detected by Annexin V. Cells were co-stained with PPI as a marker of cell membrane permeability, which increases during the later stages of apoptosis and also in necrosis. Since PPI only enters cells with already disintegrated membranes, early apoptotic cells can be distinguished from late apoptotic and necrotic cells. Similar to the stainings with Hoechst 33342, flow cytometric analysis of the cells revealed a progressive increase of the Annexin V signal (early apoptotic cells) with increasing concentrations of lipophilic statins. At 100µmol/L of these compounds, between 9

and 17% of cells underwent early apoptotic changes. In contrast, only 3% of cells treated with 100µmol/L pravastatin were Annexin V-positive (data not shown). Fas ligand, used as a positive control for apoptosis induction, induced early apoptosis in 12% of cells. Similarly, only the lipophilic statins, but not pravastatin, caused late apoptosis/necrosis (data not shown).
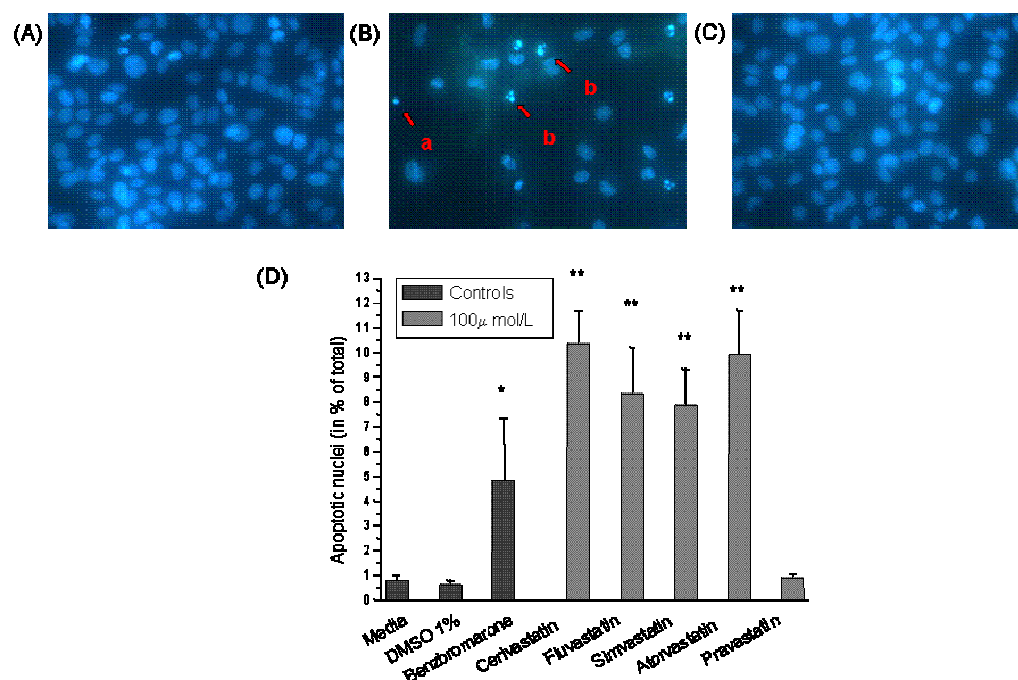
Figure 7

Detection of apoptosis by staining with Hoechst 33342. L6 cells were treated with test compounds at a concentration of 100µmol/L for 24 hours and subsequently stained with Hoechst 33342. The cell nuclei were visualized using fluorescence microscopy. Panel (A) control, panel (B) atorvastatin, panel (C) pravastatin. Apoptotic cells were characterized by DNA condensation (panel B, arrow a) and/or DNA fragmentation (panel B, arrow b). Panel (D) summarizes the percentage of cells undergoing apoptosis. Pravastatin was the only statin not inducing apoptosis. * $p < 0.05$ vs. control; ** $p < 0.01$ vs. control.

Since ATP is essential for executing apoptosis [82, 85], the cellular ATP content was assessed. The ATP content in control incubations was 1.26 ± 0.08µmol/10^6 myocytes and remained stable in presence of 100µmol/L fluvastatin, atorvastatin, simvastatin or pravastatin. In the presence of 100µmol/L cerivastatin, it dropped to 0.16 ± 0.09µmol/10^6 myocytes, suggesting that also necrosis occurred.

3.4.6. Discussion

Our investigations demonstrate that lipophilic statins are mitochondrial toxins affecting the electron transport chain, coupling of oxidative phosphorylation and/or mitochondrial β-oxidation. These alterations in mitochondrial function are associated with dissipation of the electric

potential across the inner mitochondrial membrane. The mitochondrial membrane potential is mainly maintained by a proton gradient generated by the proton pump activity of complexes I, III and IV of the electron transport chain. Any perturbation of these enzyme complexes and/or uncoupling of oxidative phosphorylation can be expected to dissipate the mitochondrial membrane potential, which can therefore be regarded as a marker of mitochondrial function and integrity. A decrease in the mitochondrial membrane potential can lead to mitochondrial membrane permeabilization, which is considered to be a point-of-no-return for initiating apoptotic cell death [84, 86]. Mitochondrial membrane permeabilization can culminate in rupture and therefore loss of barrier function of the outer mitochondrial membrane, with consequent release of apoptosis-inducing proteins (e.g. cytochrome c) from the mitochondrial intermembrane space.

Our study shows that lipophilic statins are acting along this entire sequence: they inhibit the function of the electron transport chain, impair mitochondrial β-oxidation (limited availability of NADH for the function of complex I of the electron transport chain), uncouple oxidative phosphorylation (cerivastatin), decrease the mitochondrial membrane potential, and induce mitochondrial swelling and apoptosis. The induction of apoptosis by statins may not only be initiated by the mitochondrial pathway, however. Due to inhibition of the conversion of HMG-CoA to mevalonate, not only the synthesis of cholesterol, but also of intermediates between HMG-Co A and cholesterol and products of these intermediates (e.g. ubiquinone and dolichols) is reduced [51]. As a consequence, cells may become poor in prenylated (farnesylated or geranylated) small GTP-proteins, such as Rho, Ras or Rac, which promote cell maintenance and cell survival [46, 87, 88]. Since mevalonate could not prevent statin- associated mitochondrial damage and cytotoxicity, mitochondrial toxicity, and not impaired prenylation of GTP-proteins, appears to initiate apoptosis of L6 cells. Patients treated with statins may have an increased basal rate of apoptotic cell death, which is compensated by cell proliferation under normal conditions. In the case an additional insult, e.g. a large increase in the statin plasma and tissue concentrations due to a drug-drug interaction and/or an underlying metabolic disease [62], there may be a massive increase in apoptotic cell death, possibly leading to organ damage such as rhabdomyolysis.

Our findings support the results of Kubato et al. [89], who showed that lipophilic statins can cause apoptosis of hepatocytes. Also in these experiments, pravastatin did neither reduce cell viability nor induce apoptosis. Since a reduction in cholesterol synthesis could also be shown for pravastatin, also the hydrophilic pravastatin had to have entered the hepatocytes in order to execute its pharmacological action. At least in hepatocytes, inhibition of cholesterol synthesis is therefore not sufficient to induce apoptosis.

Although all lipophilic statins tested induced apoptosis of skeletal muscle cells, their effects on mitochondrial function differed among each other. For instance, only cerivastatin uncoupled oxidative phosphorylation (see Figure 3). The uncoupling capacity of cerivastatin is obviously

not related to its pharmacological action, but may offer an explanation for its higher myotoxicity compared to the other statins [45, 48, 49, 90]. When mitochondrial uncoupling occurs, protons are transported into the mitochondrial matrix by bypassing the F_1F_0-ATPase. As a consequence, the mitochondrial membrane potential is dissipated and mitochondrial ATP synthesis is decreased, possibly leading to cellular ATP depletion and cytotoxicity [82]. Furthermore, uncouplers may be transported into and accumulate within the mitochondrial matrix, what could enhance their toxicity. The higher myotoxicity of cerivastatin compared to other statins may therefore be explained by its higher bioavailability (see Table 1) and by its capability to uncouple oxidative phosphorylation of skeletal muscle mitochondria.

Having investigated muscle toxicity of statins *in vitro*, the question arises, to what extent our findings are relevant for the *in vivo* situation. For atorvastatin, pravastatin and atorvastatin, typical plasma concentrations after oral doses of 20-40 mg are in the range of 0.1µmol/L [48, 91], which is considerably lower than the toxic concentrations determined in our investigations. Since data of statin concentrations in skeletal muscle of humans are so far lacking, possible tissue concentrations reached have to be estimated. The volume of distribution of lipophilic statins (Table 1) is high for atorvastatin, low for the statins with high protein binding (cerivastatin and fluvastatin) and unknown for simvastatin (intermediate protein binding). At least for atorvastatin (and possibly also for simvastatin), accumulation in peripheral tissues can be assumed, possibly also in skeletal muscle. Furthermore, most cases of rhabdomyolysis with statins have been described in patients having a drug-drug interaction [44], leading to plasma (and possibly also tissue) concentrations which are higher (in some cases ten-fold or even more [92]) than normal concentrations. Since it is known that even in the presence of a drug-drug interaction, only a minority of the patients develop rhabdomyolysis [93], patients affected by muscular problems may have an underlying (possibly mitochondrial) disease, rendering them more sensitive to lower statin concentrations [62]. Taken together, our findings may be relevant for the *in vivo* situation in sensitive humans, although the statin concentrations associated with mitochondrial toxicity found in our study appear to be high.

Similar to the study of Kubota et al. [89], our investigations do not offer an explanation for *in vivo* skeletal muscle toxicity of pravastatin, which appears to have an equal frequency as for atorvastatin and simvastatin [47]. In our assays, pravastatin revealed only a slight inhibition of mitochondrial β-oxidation at high concentrations, but did not induce apoptosis or necrosis of L6 cells. A lack of access to cell organelles can be excluded by our own studies (NADH oxidase) and also by the studies of Kubota et al. [89]. The possibilities remain that a metabolite of pravastatin is the culprit or that L6 cells are not a suitable cell system to show toxicity for this particular statin.

In conclusion, the lipophilic statins impair several functions of skeletal muscle mitochondria, whereas as the hydrophilic pravastatin does not reveal a relevant mitochondrial toxicity *in vitro*. Although the toxic concentrations of the statins on isolated mitochondria and L6 cells are

considerably higher than their plasma concentrations in humans, mitochondrial toxicity may trigger rhabdomyolysis in sensitive patients. Since the hydrophilic pravastatin is also associated with rhabdomyolysis, additional mechanisms may exist.

4. Aims of the thesis

The main focus of this thesis lies on a known mitochondrial toxin, amiodarone, and especially on its chemical structure – effect relationship. Amiodarone is a potent antiarrhytmic agent which use is unfortunately limited subsequent to the numerous side effects it can provoke. Despite these unwanted adverse effects including pulmonary, thyroidal, hepatic and numerous others amiodarone mostly remains the drug of choice when life-threatening arrhytmias are treated. The aim of the first project of this thesis was to find out more about the amiodarone molecule in order to predict which part of it is responsible for its hepatotoxic effect. Amiodarone, three metabolites of amiodarone and five derivatives differing from each other only by their side chain were chosen for the studies. The investigations were accomplished using freshly isolated rat liver mitochondria, primary rat hepatocytes and HepG2 cells. Once a non-toxic molecule was found, it was tested on its ability to block potassium channels, as a test system CHO cells stably expressing the hERG potassium channel. Currents were measured by means of the patch-clamp technique in the whole-cell configuration. As an outcome of this study, we hoped to find a non-toxic but still pharmacologically active amiodarone derivative and to learn more about the amiodarone molecule itself.

The second project concentrates on studying the overall toxicity of amiodarone, its two main metabolites and five derivatives on pulmonary and hepatoma cell lines (A549 and HepG2 cells, respectively), and on predicting their inhibitory effect on the hERG channel, by means of *in vitro* examinations and an *in silico* approach. We hoped to provide further pharmacological and toxicological knowledge about the amiodarone molecule, especially about its behaviour towards the potassium channel.

The third project concerns dermal fibroblasts derived from patients suffering from two different mitochondrial malfunctions. These primary cells were used to study the possible link between an underlying mitochondrial defect and an unexpected toxicity of a drug leading to apoptosis or necrosis of a cell. The drugs chosen for these studies were benzbromarone and simvastatin, both known to be the cause of an idiosyncratic reaction, which is an unexpected toxic response to a drug. Benzbromarone is a uricosuric agent known for its hepatocellular toxicity that led to its withdrawal from the market. Simvastatin belongs to the group of the HMG-CoA reductase inhibitors used for the treatment of hypercholesterolemia. Myotoxicity, especially rhabdomyolysis, is a rare but severe problem associated with simvastatin use. Our main interest was to find out if the mitochondrial defect would predispose the fibroblasts to higher toxicity when treated with benzbromarone or simvastatin.

5. Hepatocellular toxicity and pharmacological effect of amiodarone and amiodarone derivatives

Katri Maria Waldhauser, Michael Török, Huy-Riem Ha, Urs Thomet, Daniel Konrad, Karin Brecht, Ferenc Follath, Stephan Krähenbühl

Division of Clinical Pharmacology & Toxicology and Department of Research (KMW, MT, KB, SK), University Hospital Basel, Cardiovascular Therapy Research Unit (HRH, FF), University Hospital of Zürich, [3]Bsys Ltd (UT, DK), Witterswil, Switzerland

5.1. Abstract

The aim of this work was to compare hepatocellular toxicity and pharmacological activity of amiodarone (2-n-butyl-3-[3,5 diiodo-4-diethylaminoethoxybenzoyl]-benzofuran = B2-O-Et-N-diethyl) and of eight amiodarone derivatives. Three amiodarone metabolites were studied, namely mono-N-desethylamiodarone (B2-O-Et-NH-ethyl), di-N-desethylamiodarone (B2-O-Et-NH_2) and B2 carrying an ethanol side chain (B2-O-Et-OH). In addition, five amiodarone analogues were investigated, namely N-Dimethylamiodarone (B2-O-Et-N-dimethyl), N-Dipropylamiodarone (B2-O-Et-N-dipropyl), B2-O carrying an acetate side chain (B2-O-Acetate), B2-O-Et- carrying an propionamide side chain (B2-O-Et-propionamide) and B2-O- carrying an ethyl side chain (B2-O-Et). A concentration-dependent increase in LDH leakage from HepG2 cells and isolated rat hepatocytes was observed in the presence of amiodarone and of most analogues, confirming their hepatocellular toxicity. Using freshly isolated rat liver mitochondria, amiodarone and most analogues showed a dose-dependent toxicity on the respiratory chain and on β-oxidation, significantly reducing the respiratory control ratio and oxidation of palmitate, respectively. The ROS concentration in hepatocytes increased time-dependently and apoptotic/necrotic cell populations were identified using flow cytometry and annexinV/propidiumiodide staining. The effect of the three least toxic amiodarone analogues on the hERG channel was compared to amiodarone. Amiodarone, B2-O-Acetate and B2-O-Et-N-dipropyl (each 10 µmol/L) significantly reduced the hERG tail current amplitude, whereas B2-O-Et (10 µmol/L) displayed no detectable effect on hERG outward potassium currents. In conclusion, three amiodarone analogues (B2-O-Et-N-dipropyl, B2-O-Acetate and B2-O-Et) showed a lower hepatocellular toxicity profile than amiodarone and two of these analogues (B2-O-Et-N-dipropyl and B2-O-Acetate) retained hERG channel interaction capacity, suggesting that amiodarone analogues with class III antiarrhythmic activity and lower hepatic toxicity could be developed.

5.2. Introduction

Amiodarone (2-n-butyl-3-[3,5 diiodo-4-diethylaminoethoxybenzoyl]-benzofuran, B2-O-Et-N-diethyl) is a class III antiarrhythmic used in the treatment of a wide spectrum of cardiac arrhythmias [94]. Amiodarone has been shown to be at least as efficacious as sotalol in patients with atrial fibrillation [95] and to reduce mortality in patients with a high risk for of arrhythmia, e.g. patients with severe congestive heart failure [96] or after acute myocardial infarction [97]. Amiodarone is a class III antiarrhythmic drug which blocks hERG channels, leading to prolongation of the refractoriness and resulting in QT prolongation [94]. In addition, it has an inhibitory effect on fast sodium as well as on calcium channels [94]. Similar to its pharmacological action, amiodarone's adverse reaction profile is complex, ranging from thyroidal [98] to pulmonary [99], ocular [100] and/or liver toxicity [38, 101]. Amiodarone is a mitochondrial toxicant, uncoupling oxidative phosphorylation and inhibiting the electron transport chain and ß-oxidation of fatty acids [39-41, 43].

Amiodarone is composed of a benzofuran ring carrying a C_4H_9 side chain and a highly lipophilic di-iodobenzene ring (B2) with a diethylaminoethoxy side chain (see Table 1). It is metabolized by desalkylation of the diethylaminoethoxy group to mono-N-desethylamiodarone (B2-O-Et-NH-ethyl) [102] and to di-N-desethylamiodarone (B2-O-Et-NH$_2$) [103], which may be transaminated and reduced to B2-O-Et-OH (see Table 1) [103].

In earlier studies, we have investigated the significance of the 2-butyl-benzofuran group and O-dealkylation of the amiodarone molecule with respect to mitochondrial toxicity [41]. These studies revealed that the benzofuran ring and the presence of iodines were important for mitochondrial toxicity. More recent studies [43] showed, however, that not the benzofuran ring alone is responsible for hepatocellular toxicity of amiodarone, but that a side chain in position 2 and/or 3 of the benzofuran ring was necessary.

The principal aim of the current studies was to find out amiodarone derivatives without or with minimal mitochondrial toxicity, but still exhibiting inhibitory activity towards the hERG channel. We therefore synthesized eight amiodarone derivatives (including 3 metabolites) with different lipid solubilities (see Table 1). All of the derivatives synthesized contained a benzofuran ring carrying a butyl group and differed from each other only by their side chain. Amiodarone (B2-O-Et-N-diethyl), B2-O-Et-NH-ethyl, B2-O-Et-NH$_2$, B2-O-Et-N-dimethyl, B2-O-Et-N-dipropyl and B2-O-Et-propionamide had side chains differing from each other by the substituents coupled to the nitrogen atom (see Table 1). In comparison, B2-O-Acetate, B2-O-Et-OH and B2-O-Et did not carry a nitrogen atom in the side chain coupled to the diiodophenyl ring (see Table 1). Hepatocellular toxicity was studied using freshly isolated rat liver mitochondria, primary rat hepatocytes and HepG2 cells. The effect on the blockade of the voltage-gated potassium channel hERG was tested for amiodarone and the least toxic analogues (B2-O-Et-N-dipropyl, B2-O-Et and B2-O-Acetate) in order to estimate their class III antiarrhythmic activity.

B2
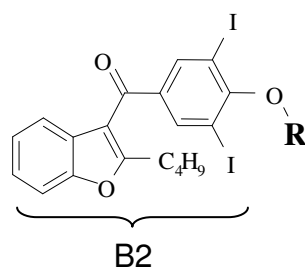
Compound	R	ClogP	logP
B2-O-Et-N-diethyl (amiodarone)	CH_2—N(Et)$_2$	7.3	4.92±0.25
B2-O-Et-NH-ethyl	CH_2—NH—Et	6.6	4.47±0.12
B2-O-Et-NH$_2$	CH_2—NH$_2$	5.9	3.83±0.10
B2-O-Et-N-dimethyl	CH_2—N(CH$_3$)$_2$	6.7	4.40±0.07
B2-O-Et-N-dipropyl	CH_2—N(CH(CH$_3$)$_2$)$_2$	8.2	5.51±0.12
B2-O-Acetate	CH_2—C(=O)—OH	6.4	4.69±0.08
B2-O-Et-Propionamide	CH_2—NH—C(=O)—C$_2$H$_5$	6.3	4.31±0.16
B2-O-Et	CH_2—CH$_3$	7.0	4.83±0.06
B2-O-Et-OH	CH_2—OH	6.2	4.18±0.15

5.3. Materials and methods

5.3.1. Amiodarone and amiodarone derivatives

Amiodarone hydrochloride was purchased from Sigma-Aldrich (Buchs, Switzerland). All of the amiodarone metabolites or analogues were synthesized starting from B2 as shown in Figure 1.

Chemistry, General Methods. All chemicals used in the synthesis work were purchased from Aldrich (Buchs, Switzerland) and were used without further purification. All melting points given are uncorrected. NMR spectra were obtained for all substances synthesized and will be reported elsewhere.

Synthesis of (2-Butyl-benzofuran-3-yl)-(4-hydroxy-3,5-diiodophenyl)-methanone (B2). This compound was prepared with a yield of 60% as described previously [104]. Melting point (146.4-146.9°C) and NMR data (not shown) were in agreement with the previous report. As shown in Figure 1, B2 is the origin of the synthesis of all amiodarone metabolites and analogues used in this study.

	R1	R2		R3
B2-O-Et-NH-ethyl	H	C_2H_5	B2-O-Et	CH_3
B2-O-Et-N-dimethyl	CH_3	CH_3	B2-O-Et-OH	CH_2OH
B2-O-Et-N-dipropyl	$CH(CH_3)_2$	$CH(CH_3)_2$		
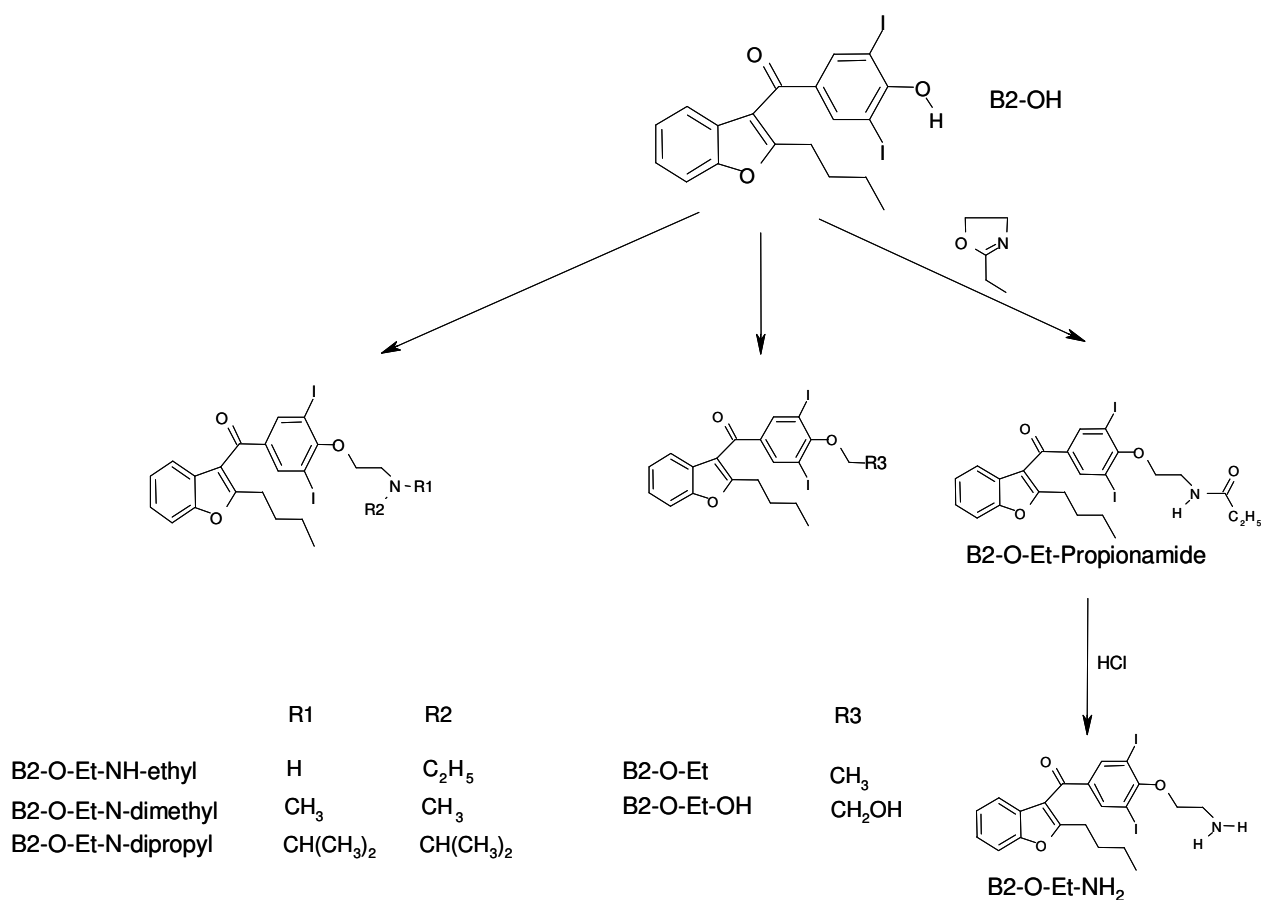
Figure 1.

General scheme of the synthesis of amiodarone derivatives. All the amiodarone metabolites or derivatives used were synthesized from B2. B2 was synthesized as described previously [104]. The derivatives B2-O-Et-NH-ethyl, B2-O-Et-NH_2, B2-O-Et-N-dimethyl, and B2-O-Et-N-dipropyl were prepared by condensing B2 with the respective 2-chloroethyl amine hydrochloride salts in the presence of K_2CO_3. Using the same procedure, B2-O-Et-OH, B2-O-Acetate and B2-O-Et were obtained from the reaction of B2 with iodoethanol, alpha-bromo-ethylacetate (subsequently hydrolyzed in 0.1M NaOH) and iodoethyl, respectively. The compound B2-O-Et-NH-Propionamide was synthesized from B2 and 2-ethyl-2-oxazoline. The yields of the reactions were between 70 and 85% and the purity of the final substances was ≥ 97% as assayed by HPLC. See Method section for more details on synthesis and characterization of the compounds.

Synthesis of (2-Butyl-benzofuran-3-yl)-4-[2-(ethylamino-ethoxy)-3,5-diiodophenyl]-methanone • hydrochloride (B2-O-Et-NH-ethyl). To a mixture of B2 (2g, 3.66mmol) and K_2CO_3 (1.66g, 12mmol) in toluene:water (2:1, v/v, total volume 75mL) heated to 55-60 °C N-ethyl-2-chloroethylamine hydrochloride (2.66g, 18.5mmol) was added portionwise. N-ethyl-2-chloroethylamine hydrochloride had been prepared by Lasselle's method [105]. After the addition, the temperature was raised to reach reflux over 30 minutes, until the yellow color of B2

had disappeared. The reaction was refluxed for 1 additional hours and the phases were separated quickly by a separation funnel at 60°C. The toluene phase was washed three times with 25mL of water at this temperature. The organic phase was evaporated to dryness; the residue suspended in 10mL of 5% NH_3 and B2-O-Et-NH-ethyl was extracted three times with 15mL toluene. The organic phases were separated by centrifugation, combined and evaporated to dryness under reduced pressure. Two mL of 10N HCl and 15mL of toluene were added, and the liquids were removed under reduced pressure at 80°C. A white solid was obtained after three additional treatments with 10mL toluene. The obtained residue was then crystallized from toluene, yielding 1.55g (65%) of analytically pure B2-O-Et-NH-ethyl. The melting point was 176.8-177.7°C.

Synthesis of (2-Butyl-benzofuran-3-yl)-4-[2-(dimethylamino-ethoxy)-3,5-diiodophenyl]-methanone • hydrochloride (B2-O-Et-N-dimethyl) and (2-Butyl-benzofuran-3-yl)-4-[2-(dipropylamino-ethoxy)-3,5-diiodophenyl]-methanone • hydrochloride (B2-O-Et-N-dipropyl). B2-O-Et-N-dimethyl and B2-O-Et-N-dipropyl were prepared in a similar manner as described for B2-O-Et-NH-ethyl, but 2-(dimethylamino)ethyl chloride and 2-(diisopropylamino)ethyl chloride were used instead of N-ethyl-2-chloroethylamine hydrochloride. For B2-O-Et-N-dimethyl, the melting point was 89.5-89.7°C and for B2-O-Et-N-dipropyl 146.8-148.7°C.

Synthesis of [4-(2-Aminoethoxy)-3,5-diiodophenyl]-(2-butylbenzofuran-3-yl)-methanone • hydrochloride (B2-O-Et-NH$_2$). A mixture of B2 (1.2g; 2mmol), 2mL (20mmol) of 2-ethyl-2-oxazoline and 3mL of toluene was heated at reflux for 1h and cooled to room temperature. The mixture was taken up in 10mL methylene chloride, washed with 4N potassium hydroxide (3x20mL), dried (Na_2CO_3) and concentrated in vacuo to give brown oil. The oil was solidified by trituration with petroleum ether followed by recrystallization from ethyl acetate:hexane to give a white solid. Thin layer chromatography analysis using Merck precoated silica gel 60-F_{254} plates and hexane:isopropyl alcohol:25% NH_3 (84:15:1 v/v) as an eluant revealed only one spot with an Rf value of 0.42 with UV detection at 254 nm. The corresponding Rf value of B2 was 0.05. This intermediate compound corresponded to B2-O-Propionamide (see Figure 1) by NMR analysis (data not shown).

To this compound 10mL of 6N HCl were added. The mixture was heated to 130°C for 3.5h and then cooled to room temperature. Impurities were washed out by diethyl ether until the organic phase was colorless (5 x 5mL). The precipitate was collected by filtration and washed with water. The compound was flash-chromatographed using silica gel Merck 60 (40-60μm, 230–400 mesh) with hexane:isopropyl alcohol:25% NH_3 (84:15:1 v/v) as an eluant, yielding 0.6g (60%) of hydrochloride salt of B2-O-Et-NH$_2$ as a white solid with a melting point of 200.5-201.4°C. B2-O-Et-NH$_2$ was found as a minor metabolite of amiodarone in humans, and its spectroscopic data have been reported in a previous study [103].

Synthesis of (2-Butyl-benzofuran-3-yl)-(4-ethoxy-3,5-diiodophenyl)-methanone (B2-O-Et). To a mixture of B2 (2.0g, 3.66mmol) in dry acetone (50mL) iodoethyl (2.34g, 15mmol) was

added over 20min. The reaction was stirred at 50°C for 16h. The insoluble salt was removed by filtration and the filtrate concentrated in vacuo to give 1.7g (yield 75%) of B2-O-Et as a white solid. The melting point was 67.0-69.4°C.

Synthesis of (2-Butyl-benzofuran-3-yl)-[4-(2-hydroxyethoxy)-3,5-diiodophenyl]-methanone (B2-O-Et-OH). This compound was prepared in a similar manner as B2-O-Et, but iodoethyl was replaced by 2-chloroethanol. The final product was obtained as an oil. When stored in a closed vial at room temperature, it solidified after 10 days. The melting point was 69.6-72.9°C. B2-O-Et-OH was found as a minor metabolite of amiodarone in humans, and its spectroscopic data have been reported in a previous study [103].

Synthesis of [4-(2-butyl-benzofuran-3-carbonyl)-2,6-diiodophenyl]-acetic acid (B2-O-Acetate). The ethyl ester of B2-O-Acetate (not shown in Figure 1) was prepared from B2 and α-bromoethyl acetate as described by Carlsson et al. [106]. The hydrolysis of the ester was performed in the presence of 0.1M NaOH at 22°C for 16 h. The melting point of the product was 186.4-187.8°C.

Amiodarone and the analogues were dissolved in dimethylsulfoxide (DMSO). The end concentration of DMSO in the experiments never exceeded 1% and control incubations contained the same DMSO concentration.

Determination of the octanol/water partition coefficient of amiodarone and derivatives

The octanol/water partition of the compounds synthesized was determined using reversed phase HPLC as described by Braumann [107]. HPLC of the substances was performed at 37°C using different 0.005M phosphate buffer (pH7.4)/methanol mixtures as an eluant. The octanol/water partition of a substance can be calculated based on the retention times obtained in the presence of different concentrations of methanol in the eluant [107].

5.3.2. Other chemicals

1-[^{14}C]Palmitic acid was purchased from Amersham Pharmacia Biotech (Dübendorf, Switzerland), collagenase type 2 from BioConcept (Allschwil, Switzerland). Propidium iodide was from Molecular Probes (Eugene, OR, USA) and Alexa Fluor 633 labeled annexin V was a generous gift from Dr. Felix Bachmann, Aponetics Ltd. (Witterswil, Switzerland). All other chemicals were purchased from Sigma-Aldrich (Buchs, Switzerland) and were of best quality available when not otherwise stated. All cell culture media, all supplements and fetal calf serum were from Gibco (Paisley, UK), except for Williams E, which was purchased from Cambrex Bio Science (Verviers, Belgium). The 96-well-plates and the 12-well-plates were purchased from Beckton Dickinson (Franklin Lakes, NJ, USA).

5.3.3. Animals

Male Sprague-Dawley rats were purchased from Charles River Laboratories (L'Arbresle, France), and kept in the animal facility of the University Hospital Basel, Switzerland. Rats were kept in a temperature-controlled environment with a 12-h light-dark cycle and food and water ad libitum. The study protocol had been accepted by the Animal Ethics Committee of the Canton Basel Stadt.

5.3.4. Isolation of rat hepatocytes

The isolation of rat hepatocytes by a two step collagenase perfusion was based on a method described by Berry [108] and performed as described earlier [43]. Cell viability was determined by trypan blue exclusion and was always greater than 80%. Cells were seeded into cell culture dishes in Williams E medium supplemented with 10% heat-inactivated fetal calf serum, 10mmol/L HEPES buffer (pH 7.4), 2mmol/L GlutaMax$^{®}$ and 1000U/mL penicillin/streptomycin. The mean rat weight was 395 ± 115g.

5.3.5. Isolation of rat liver mitochondria

Rat liver mitochondria were isolated by differential centrifugation according to the method of [70]. The mitochondrial protein content was determined using the biuret method with bovine serum albumin as a standard [68]. The mean rat weight was 343 ± 91g and the mean rat liver weight was 14.12 ± 2.81g.

5.3.6. Cell lines and cell culture

HepG2 cells were kindly provided by Professor Dietrich von Schweinitz (University Hospital Basel, Switzerland). The cell line was cultured in Dulbecco's Modified Eagle Medium supplemented with 10% (v/v) inactivated fetal calf serum, 10mmol/L HEPES buffer (pH 7.4), 2mmol/L GlutaMAX (Invitrogen, Basel, Switzerland), nonessential amino acids, and penicillin/streptomycin (100U/mL). The culture conditions were 5% CO_2 and 95% air atmosphere at 37°C.

5.3.7. Cell viability

Lactate dehydrogenase (LDH) leakage in the supernatant was determined as a measure of cell viability as described by Vassault [69] and calculated as described by Huang et al. [109]. LDH leakage from the cells treated with the test compounds was compared to the LDH leakage

of cells lysed with the detergent NP40 (0.01% w/v). The activity in the supernatant of lysed cells was set at 100%.

5.3.8. Apoptosis and necrosis detection by annexin V binding and propidium iodide uptake

After an 18-h-incubation with the test compounds, hepatocytes were stained with 0.5µl Alexa Fluor 633 labeled annexin V and 2µl propidium iodide (final concentration: 1.5µg/L). After 15 minutes of incubation at 37ºC, the cells were analyzed by flow cytometry (FACS Calibur flow cytometer: Beckton Dickinson, San José, CA, USA). As positive controls for apoptosis, deoxycholic acid (100µmol/L) was used. As a positive control for necrosis, cells were treated with the surfactant NP40 (final concentration 0.1%, v/v).

5.3.9. ATP content of the cells

Freshly isolated hepatocytes were seeded on a 12-well-plate (200,000 cells/well). Subsequently, they were treated for 18 hours with the test compounds. After the incubation, cells were trypsinized, the pellet was resuspended in 600µL reagent grade water and snap-frozen in liquid nitrogen [110]. Intracellular ATP concentration of the cells was determined using a luciferin-luciferase assay (Sigma, Deissenhofen, Germany).

5.3.10. Measurement of reactive oxygen species (ROS)

A fluorescence-based microplate assay [111] was used for the evaluation of oxidative stress in primary hepatocytes treated with the test compounds. DCFH-DA is a membrane permeable, non-polar and non-ionic molecule. In the cytoplasm, it is hydrolyzed by intracellular esterases to non-fluorescent DCFH, which is oxidized to fluorescent dichlorofluorescein in the presence of reactive oxygen species (H_2O_2 and $O_2^{\cdot-}$). Hepatocytes were simultaneously exposed to test compounds and to DCFH-DA dissolved in ethanol (final concentration 5µmol/L) and incubated for 2, 4, 6 and 18 hours. The fluorescence was measured using a microtiter plate reader (HTS 700 Plus Bio Assay Reader, Perkin Elmer, Buckinhamshire, UK) in incubations containing cells and exposure medium at an excitation wavelength of 485nm and an emission wavelength of 535nm.

5.3.11. Oxygen consumption and β-oxidation of intact mitochondria

Oxygen consumption by intact mitochondria was measured in a chamber equipped with Clark-type oxygen electrode (Yellow Springs Instruments, Yellow Springs, OH) at 30ºC [70]. The final concentration of L-glutamate was 20mmol/L. The mitochondrial respiratory control

ratio (RCR) as well as state 3 and state 4 of respiration were determined according to Estabrook [112] and as described by Krähenbühl et al. [73]. Uncoupling of the oxidative phosphorylation was investigated by monitoring oxygen consumption in the presence of test substances and oligomycin, an inhibitor of F_1F_0-ATPase (final concentration of 5µg/mL) [43].

5.3.12. Mitochondrial β-oxidation

Mitochondrial β-oxidation of [1-^{14}C] palmitic acid in the presence of test compounds was determined usingg freshly isolated liver mitochondria according to the method of Freneaux et al. [113] with some modifications as described by Spaniol et al. [41].

5.3.13. Effect of amiodarone, B2-O-Et-N-dipropyl, B2-O-Acetate and B2-O-Et on the inhibition of hERG currents

5.3.13.1. CHO hERG cells

The 3 least toxic compounds (B2-O-Et-N-dipropyl, B2-O-Acetate and B2-O-Et) and amiodarone were chosen for examination concerning their antiarrhythmic effect. The interaction of the test substances (final concentration 10µmol/L) with the hERG channel was examined using CHO cells stably expressing this potassium channel. Briefly, two separate human cardiac plasmid cDNA libraries were prepared from freshly isolated tissue and the hERG alpha subunit PCR product released from the pCR2.1-TOPO vector (Invitrogen, Basel, Switzerland) for ligation into a modified pcDNA5/FRT/TO vector (Invitrogen, Basel, Switzerland) with excluded BGH site. Restriction analysis and complete sequencing confirmed the correct composition and expression of the hERG alpha subunit in the plasmid. CHO cells were transfected with the calciumphosphate precipitation method (Invitrogen, Basel, Switzerland). Clones were selected with 700µg/mL Hygromycin B (Invitrogen, Basel, Switzerland) and checked back electrophysiologically for the presence of sufficient potassium current, longterm recording stability and sealing properties. Using limited dilution, clone CHO hERG K2, which displayed an average tail current amplitude of approximately 700-1500pA, was isolated. This clone was successfully cultivated over 40 passages without detectable loss of current density and was used in the current studies. The cells were generally maintained and passaged in HAM/F12 with GlutaMax I (GIBCO, Paisley, UK) supplemented with 9% fetal bovine serum (GIBCO, Paisley, UK), 0.9% Penicillin/Streptomycin solution (GIBCO, Paisley, UK) and 500µg/mL Hygromycin B (Invitrogen, Basel, Switzerland). For electrophysiological measurements, the cells were seeded onto 35mm sterile culture dishes containing 2mL culture medium (without antibiotics or antimycotics). Confluent clusters of CHO cells are electrically coupled. Because responses in distant cells are not adequately voltage clamped and because of uncertainties about the extent

of coupling, cells were cultured at a density enabling single cells (without visible connections to neighbouring cells) to be used for the experiments.

5.3.13.2. Electrophysiology

hERG currents were measured by means of the patch-clamp technique in the whole-cell configuration. The incubation buffer contained (in mmol/L) NaCl 137, KCl 4, CaCl$_2$ 1.8, MgCl$_2$ 1, D-glucose 10, HEPES 10, pH (NaOH) 7.40. The pipette solution consisted of (in mmol/L) KCl 130, MgCl$_2$ 1, MgATP 5, HEPES 10, EGTA 5, pH (KOH) 7.20. After formation of a Gigaohm seal between the patch electrodes and individual hERG stably transfected CHO cells, the cell membrane across the pipette tip was ruptured to assure electrical access to the cell interior. All solutions applied to cells were continuously perfused (1mL/min) and maintained at room temperature. As soon as a stable seal could be established, hERG outward tail currents were measured upon depolarization of the cell membrane to +20mV for 3 s (activation of channels) from a holding potential of -80mV and subsequent partial repolarization to -40mV for 4 s. This voltage protocol was run a minimum of 10 times at intervals of 10 s before application of the test compound. After equilibration (typically taking approximately 3 min), the voltage protocol was run continuously until the steady state level of current block was reached. At least three individual measurements were run per test compound. The steady state level currents were compared to those from control conditions (0.01% DMSO) and the residual current calculated as percentage of control.

5.4. Statistical methods

Data are presented as mean ± standard error of the mean (SEM) of at least three individual experiments. Differences between groups (control and test compound incubations) were analyzed by analysis of variance (ANOVA) and Dunnett´s post hoc test was performed if ANOVA showed significant differences. A p value ≤ 0.05 was considered to be significant.

5.5. Results

5.5.1. Oxygen consumption

Oxygen consumption by isolated mitochondria can roughly be divided into two states. In state 3, a substrate donates electrons to the electron transport chain and ADP is being phosphorylated to ATP. In state 4, ADP is depleted and therefore no ATP can be produced. Since the RCR is the ratio between these two states, a decrease in the RCR can be due to reduced state 3 of respiration (impairment of the function of electron transport chain) or an

increase in state 4 of respiration (in most cases uncoupling of the activity of electron transport chain from production of ATP).

In order to get an overview about the effect on mitochondria, the influence of 1, 10 and 100µmol/L amiodarone and analogues on oxidative metabolism on isolated rat liver mitochondria was tested in the presence of L-glutamate as a substrate (see table 2). For all test compounds, the RCR decreased dose-dependently, and for all compounds, except for B2-O-Et, the decrease was statistically significant in comparison to control incubations. B2-O-Et did not have a significant effect on mitochondrial respiration at any concentration.

Most of the analogues and amiodarone were associated with an increase in state 4 respiration, suggesting uncoupling properties. In order to test this possibility, oxygen consumption was studied in the presence of test compounds and oligomycin. Oligomycin is an inhibitor of the F_1F_0-ATPase, and induces a so called state 4u when incubated with mitochondria. Under these conditions, an increase in oxygen consumption can only reflect uncoupling and not production of ADP by other mechanisms. After an incubation in the presence of oligomycin, amiodarone, B2-O-Et-N-dimethyl, B2-O-Et-N-dipropyl and B2-O-Acetate significantly increased oxygen consumption at 10µmol/L, and B2-O-Et-N-dipropyl and B2-O-Et-propionamide at 100µmol/L (data not shown). In contrast, B2-O-Et-OH did not change the state 4u significantly up to 100µmol/L. B2-O-Et was not investigated, since it did not change the RCR (see Table 2). These data match well with the observed effect on state 4 respiration (compare with data in Table 2).

Table 2.

Effects of amiodarone, and amiodarone metabolites and analogues on oxidative metabolism in isolated rat liver mitochondria. The values represent mean±SEM of at least three experiments. All incubations contained 1%DMSO; *p<0.05 and **p<0.01 versus control incubations.

	State 3	State 4	RCR
	natoms O x min^{-1} x mg^{-1}		
Control (1%DMSO)	78.9 ± 15.0	2.30 ± 0.37	7.91 ± 1.28
B2-O-Et-N-diethyl (amiodarone)(µmol/L)			
1	72.9 ± 9.3	2.5 ± 0.5	6.60 ± 0.53
10	72.2 ± 7.7	4.17 ± 1.53*	4.21 ± 1.38**
100	64.5 ± 8.1	9.83 ± 2.25**	1.52 ± 0.31**
B2-O-Et-NH-ethyl (µmol/L)			
1	68.5 ± 16.9	3.67 ± 2.25	5.06 ± 2.17*
10	69.7 ± 8.0	3.33 ± 1.44	5.10 ± 1.42*
100	3.7 ± 1.3**	3.72 ± 1.29	1.00± 0.00**
B2-O-Et-NH$_2$ (µmol/L)			
1	76.7 ± 3.2	2.50 ± 0.5	7.07 ± 1.5
10	75.2 ± 8.8	2.50 ± 0.5	7.01 ± 2.09
100	3.4 ± 1.6**	3.37 ± 1.61	1.00± 0.00**
B2-O-Et-N-dimethyl (µmol/L)			
1	75.1 ± 12.3	2.67 ± 0.58	6.40 ± 0.66
10	66.8 ± 6.0	3.67 ± 0.58**	4.15 ± 0.67**
100	5.2 ± 1.3**	5.20 ± 1.29**	1.00 ± 0.00**
B2-O-Et-N-dipropyl (µmol/L)			
1	77.3 ± 11.4	3.17 ± 0.29	5.55 ± 1.24*
10	72.1 ± 10.1	3.67 ± 1.26	4.70 ± 1.31**
100	68.4 ± 3.4	5.17 ± 2.08**	3.32 ± 1.27**
B2-O-Acetate (µmol/L)			
1	69.1 ± 8.9	2.50 ± 0.87	6.50 ± 1.39
10	49.1 ± 10.2**	3.67 ± 0.58**	3.00 ± 0.38**
100	9.7 ± 5.2**	5.13 ± 1.15**	1.25 ± 0.43**
B2-O-Et-propionamide (µmol/L)			
1	63.2 ± 26.1	2.5 ± 2.71	5.67 ± 2.34*
10	63.9 ± 9.3	3.83 ± 0.29	3.77 ± 0.79**
100	47.6 ± 6.8*	47.57 ± 6.81**	1.00 ± 0.00**

B2-O-Et (µmol/L)			
1	84.7 ± 21.3	2.33 ± 0.29	8.40 ± 3.22
10	81.0 ± 15.2	2.50 ± 0.00	7.27 ± 1.36
100	73.6 ± 19.8	2.67 ± 0.29	6.12 ± 0.99
B2-O-Et-OH (µmol/L)			
1	72.9 ± 13.4	2.50 ± 0.50	6.55 ± 0.18
10	75.8 ± 7.7	2.67 ± 0.29	6.37 ± 0.04
100	20.0 ± 3.2**	20.07± 3.15**	1.00 ± 0.00**

5.5.2. Mitochondrial β-oxidation

Since amiodarone is known to impair mitochondrial β-oxidation [39, 43], the effect on the metabolism of palmitate was investigated. In comparison to the control incubations, amiodarone and most of the derivatives significantly decreased palmitate metabolism in a dose-dependent fashion (Figure 2). The exceptions were B2-O-Et-N-dipropyl and B2-O-Et, which did not affect mitochondrial β-oxidation up to 100µmol/L.
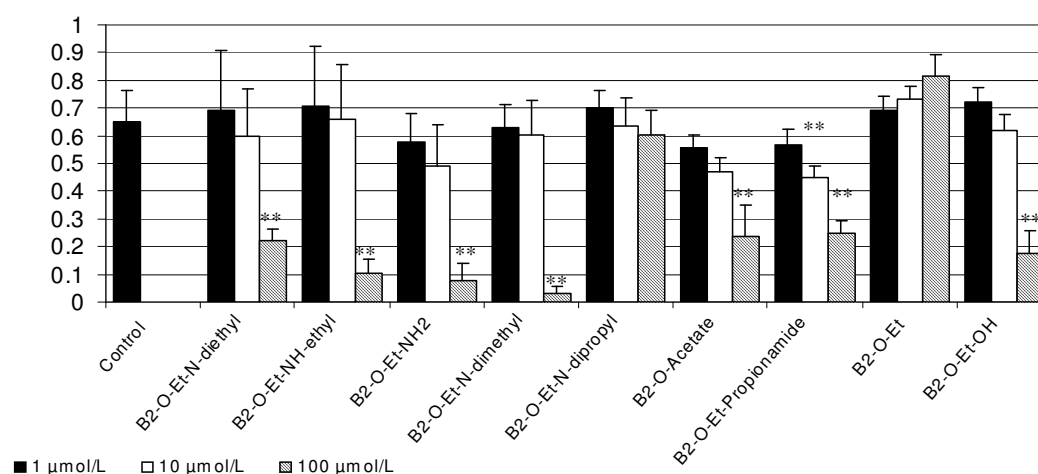
Figure 2.

Effect of amiodarone and its analogues on ß-oxidation by isolated rat liver mitochondria. With the exception of B2-O-Et-N-dipropyl and B2-O-Et, amiodarone (B2-O-Et-N-diethyl) and all amiodarone derivatives impaired mitochondrial β-oxidation at a concentration of 10 to 100µmol/L. Incubations were performed as described in the Method section. Results are expressed as acid soluble products produced from [^{14}C]-palmitic acid and represent mean ± SEM of at least 4 experiments. All incubations contained 1% DMSO; *p<0.05 and **p<0.01 versus control incubations.

5.5.3. Production of ROS

Since increased ROS formation can be one of the consequences of the inhibition of the electron transport chain [43], this was determined using isolated rat hepatocytes. ROS formation was measured after incubation for 2, 4, 6 or 18 hours with 100µmol/L amiodarone or its analogues. The emitted fluorescence increased time-dependently for all derivatives and for amiodarone as shown in Figure 3. After 18 hours of incubation, ROS production was significantly increased in comparison to control incubations for all compounds except for B2-O-Et-N-dipropyl and B2-O-Et.
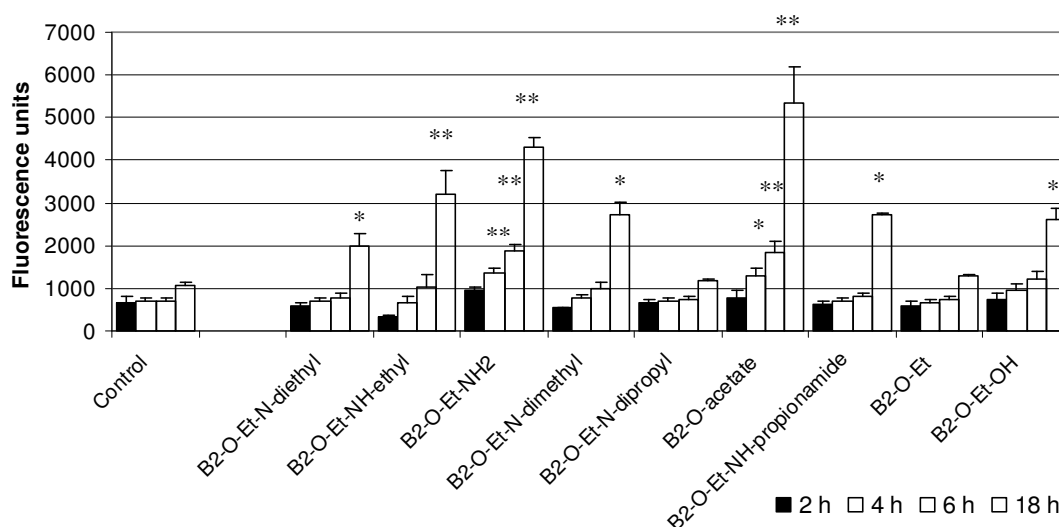
Figure 3.

ROS formation by primary hepatocytes. ROS formation by primary hepatocytes treated with 100 µmol/L amiodarone and analogues increased time-dependently for all compounds tested, reaching statistical significance for amiodarone, B2-O-NH-ethyl, B2-O-Et-NH$_2$, B2-O-Et-N-dimethyl, B2-O-Acetate, B2-O-Et-propionamide and B2-O-Et-OH. Incubations were performed as described in Methods. Results are shown as mean ± SEM of at least three individual experiments in quadruplicate. All incubations contained 1% DMSO; *p<0.05 and **p<0.01 versus control incubations.

5.5.4. Cell viability

Impaired mitochondrial ß-oxidation and/or impaired function of oxidative phosphorylation with ROS production can be associated with necrosis and apoptosis of the affected cells [43]. In order to investigate these possibilities, HepG2 cells or primary rat hepatocytes were treated for 18 hours with amiodarone or its analogues in rising concentrations (1, 10 and 100µmol/L) and the extracellular LDH activity was measured in the supernatant as a marker of cell death (see Figure 4 for HepG2 cells). Amiodarone, its metabolites B2-O-Et-NH-ethyl, B2-O-Et-NH$_2$ and B2-

O-Et-OH, as well as B2-O-Et-N-dimethyl, B2-O-Acetate and B2-O-Et-propionamide showed a dose-dependent toxicity, which, at a concentration of 10 and/or 100µmol/L, was significant in comparison to control incubations. A similar pattern was obtained, when this experiment was repeated with primary rat hepatocytes (results not shown).
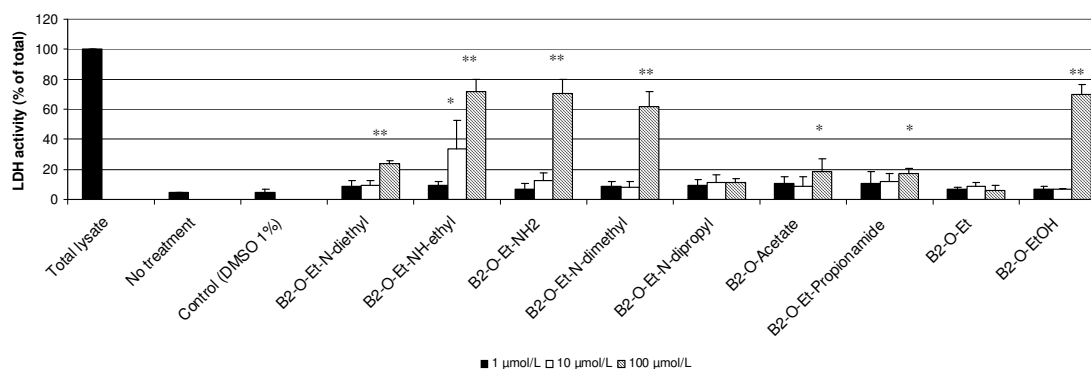
Figure 4.

Cytotoxicity of amiodarone and amiodarone derivatives. Cytotoxicity was studied using HepG2 cells under the conditions described in the Method section. Amiodarone (B2-O-Et-N-diethyl), B2-O-Et-NH-ethyl, B2-O-Et-NH$_2$, B2-O-Et-N-dimethyl, B2-O-Acetate, B2-O-Et-propionamide and B2-O-Et-OH increased the LDH leakage into the cell culture media dose-dependently after an incubation for 18 hours. In contrast, for B2-O-Et-N-dipropyl and B2-O-Et, the cell membrane remained tight under each concentration used for the incubations. Similar data were obtained using primary rat hepatocytes. Data are given as mean±SEM of at least three individual experiments in triplicates. All incubations (except "no treatment") contained 1% DMSO; *p<0,05 and **p<0.01 versus control incubations.

5.5.5. Mechanism of cell death

The mechanism of cell death was investigated using staining with annexin V/PI, which can differentiate between early apoptosis and late apoptosis/necrosis [43]. After 18 hours of incubation, hepatocytes showed a significant increase in late apoptosis/necrosis for all substances investigated, except for B2-O-Et-N-dimethyl, B2-O-Et-N-dipropyl, B2-O-Acetate and B2-O-Et (Figure 5). In agreement with these findings, the ATP content of the hepatocytes was reduced at this time point in the incubations containing amiodarone, B2-O-Et-NH-ethyl, B2-O-Et-NH$_2$, B2-O-Et-propionamide and B2-O-Et-OH (data not shown). With the exception of B2-O-Et-N-dimethyl (significant LDH release and non-significant increase in late apoptosis/necrosis), these findings agree well with the results of the LDH leakage assay. The discrepancy between LDH release and annexin V/PI staining may be associated with extent of cell damage needed to obtain a positive result.
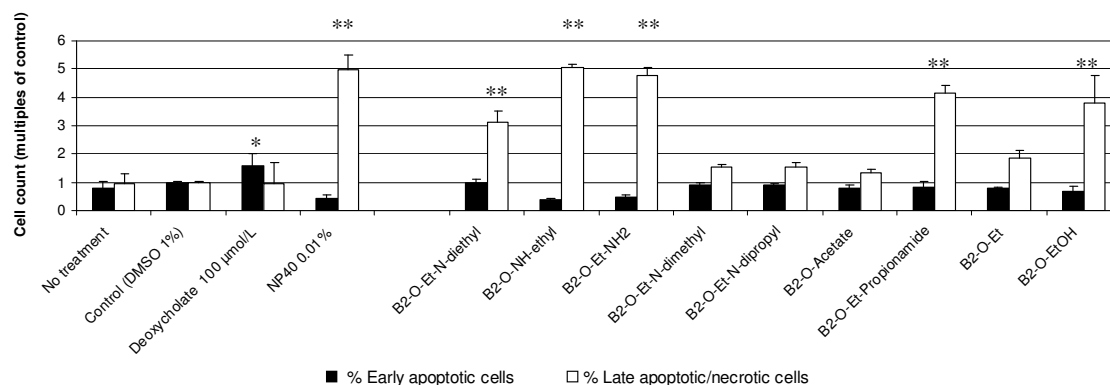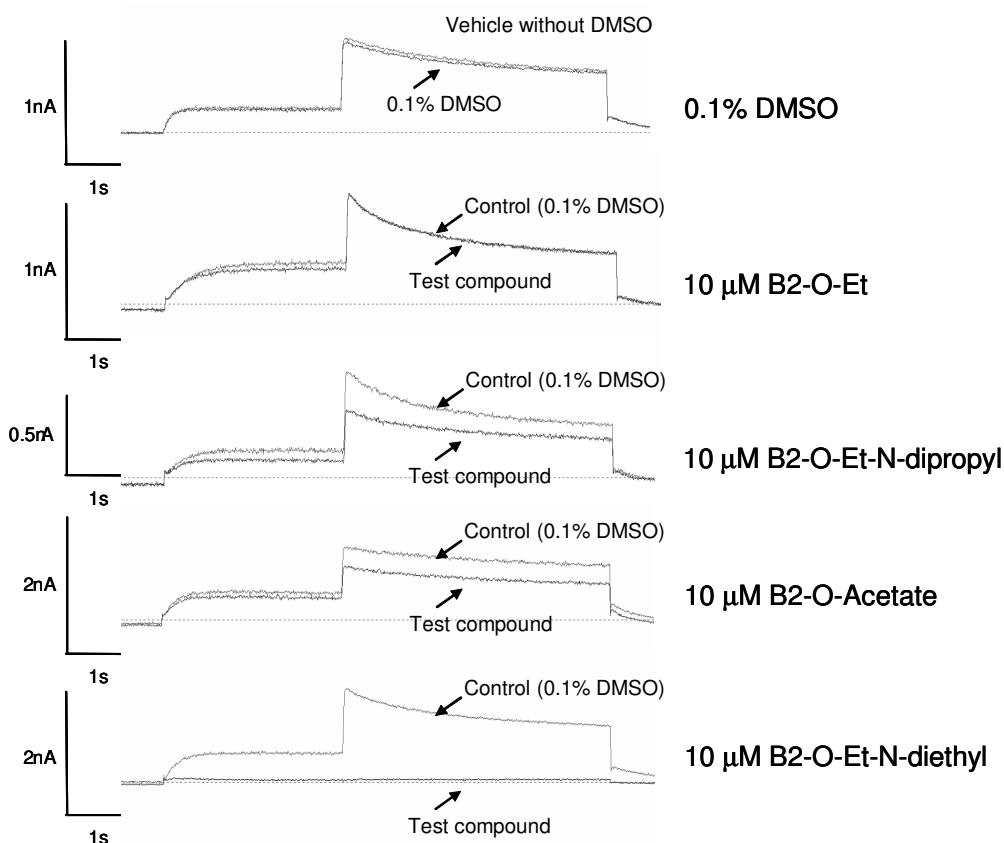
Figure 5.

Mechanism of cell death in primary hepatocytes. Cell death was assessed using staining with Annexin V/propidiumiodide followed by flow cytometry. The assays were carried out as described in the Method section and quantified as described previously [43]. Deoxycholate (100µmol/L) was used as a positive control for early apoptosis and the detergent NFP40 (0.01%, v/v) as a positive control for late apoptosis/necrosis. During apoptosis, phosphatidylserine is externalized and can be bound by Annexin V, which can be detected by flow cytometry. During late apoptosis or necrosis, propidiumiodide is able to enter the cells across disintegrated membranes and to stain DNA, which can be differentiated by flow cytometry from early apoptosis [43]. After 18 hours of incubation with the compounds shown in figure, the positive control (deoxycholate 100µmol/L) was associated with early apoptosis, but none of the test compounds investigated. In comparison, late apoptosis/necrosis was detected in the presence of the positive control (NP40 0.01%, v/v), and also in the presence of amiodarone (B2-O-Et-N-diethyl), B2-O-Et-NH-ethyl, B2-O-Et-NH$_2$, B2-O-Et-propionamide and B2-O-Et-OH (all at a concentration of 100µmol/L). The results are presented as mean±SEM of three individual experiments. With the exception of the incubation labelled "no treatment", all incubations contained 1% DMSO; *p<0,05 and **p<0.01 versus control incubations.

5.5.6. Effects on the cardiac rapid delayed rectifier K$^+$ current (IKr)

Since one of the important antiarrhythmic mechanisms of amiodarone is the inhibition of hERG channels, the effect of amiodarone and of the three least toxic amiodarone derivatives (B2-O-Et-N-dipropyl, B2-O-Acetate and B2-O-Et) on the K$^+$ current was investigated in CHO cells overexpressing hERG channels. As shown in Figure 6, amiodarone (10µmol/L) rapidly and robustly blocked hERG tail currents (6.28 ± 4.05% tail current relative to control, mean ± SEM of n=3 experiments). The derivatives B2-O-Acetate (10µmol/L) and B2-O-Et-N-dipropyl (10µmol/L) also significantly inhibited the tail current, but less than amiodarone (remaining tail current 81.9 ± 2.6% and 76.2 ± 6.5%, respectively, relative to control values, mean ± SEM of n=3 experiments). No significant effect was observed for 10µmol/L B2-O-Et (94.6 ± 3.5% tail current relative to control, mean ± SEM of n=3 experiments). As expected, at higher concentrations (≥30µmol/L) the inhibitory effects of B2-O-Acetate and B2-O-Et-N-dipropyl was more pronounced with the exception of B2-O-Et, which again displayed no significant hERG blockage

(data not shown). Also the vehicle (0.01% DMSO) did not interfere with hERG channel activity (96.70 ± 0.49%, relative tail current, mean ± SEM of n=3 experiments).

<u>Figure 6.</u>

Inhibition of potassium current. Representative current traces of potassium currents through hERG channels stably expressed in CHO cells are shown. Measurements were accomplished in the whole-cell patch-clamp configuration at room temperature. Outward currents were activated upon depolarization of the cell membrane from -80mV to +20mV for 3 s. Partial repolarization to -40mV for 4 s evoked large tail currents. At least three cells were recorded per test compound. The vehicle (0.1% DMSO) as well as 10µmol/L B2-O-Et had no significant effect on hERG channel activity (traces at the top). In contrast, amiodarone, B2-O-Acetate and B2-O-Et-N-dipropyl had a clear inhibitory effect on the hERG channels. The upper line in the figures depicts the control incubations (0.1% DMSO) and the lower line the incubations containing the test compounds.

5.6. Discussion

In our current studies, amiodarone and most of its analogues demonstrated a similar toxicity pattern towards hepatic mitochondria as described earlier in similar investigations [39, 40, 43, 114]. As shown in Table 3, amiodarone and its analogues inhibited the function of the respiratory chain, impaired mitochondrial β-oxidation and/or uncoupled oxidative phosphorylation. Most substances were cytotoxic, exceptions were B2-O-Et and B2-O-Et-N-dipropyl.

Regarding B2-O-Et and the B2-O-Et-NR_2 derivatives, the pattern of cytotoxicity (strong cytotoxicity of the amiodarone metabolites B2-O-Et-NH-ethyl and B2-O-Et-NH_2, lower cytotoxicity for amiodarone and very low or lacking cytotoxicity for B2-O-Et) was very similar to the toxicity found on alveolar macrophages, as reported in a recent investigation [115]. As shown for B2-O-Et-N-dipropyl, uncoupling of the respiratory chain was not sufficient to induce cytotoxicity. Incomplete uncoupling (mitochondria are still able to produce some ATP) and extramitochondrial production of ATP (e.g. by glycolysis) could serve as explanations for this finding. As evidenced e.g. by amiodarone and by the amiodarone metabolites B2-O-Et-NH-ethyl and B2-O-Et-NH_2, cytotoxicity is associated primarily with substances that affect the function of the respiratory chain and/or mitochondrial β-oxidation. Inhibition of the respiratory chain can be associated with ROS production [43], which can trigger opening of the mitochondrial permeability transition pore, leading to the release of cytochrome c and other substances into the cytoplasm and triggering apoptosis and/or necrosis, depending on the ATP content of the cell [116, 117]. In combination with the concomitant drop in the cellular ATP content, the results in Figure 4 therefore indicate that after 18 hours of incubation most hepatocytes had undergone necrosis in the presence of 100µmol/L amiodarone, B2-O-Et-NH-ethyl, B2-O-Et-NH_2, B2-O-Et-propionamide or B2-O-Et-OH.

Amiodarone and the amiodarone metabolites B2-O-Et-NH-ethyl and B2-O-NH_2 were shown to be strong inhibitors of mitochondrial β-oxidation and of the respiratory chain (B2-O-Et-NH-ethyl and B2-O-NH_2) or uncouplers of oxidative phosphorylation (amiodarone). Regarding amiodarone, mitochondrial toxicity explains the histological findings in liver biopsies from patients [118] and mice [39] with amiodarone-associated hepatotoxicity, revealing micro- and macrovesicular accumulation of fat in hepatocytes as a hallmark of their toxicity. Accumulation of small lipid droplets in hepatocytes (microvesicular steatosis) is considered to be a consequence of the inhibition of β-oxidation in hepatocellular mitochondria [28]. It can therefore be predicted that beside amiodarone, also its metabolites B2-O-Et-NH-ethyl, B2-O-Et-NH_2 and B2-O-Et-OH as well as the other amiodarone analogues synthesized and tested (all of them except B2-O-Et and B2-O-Et-N-dipropyl) will most probably be associated with microvesicular steatosis. For amiodarone, it has been shown that inhibition of carnitine palmitoyltransferase I (CPT I) is a mechanism for the inhibition of β-oxidation [119]. This may also be the case for the amiodarone metabolites and analogues, but formal proof is so far lacking.

For amiodarone, the toxicity found in the current investigations (strong uncoupling activities and inhibition of mitochondrial β-oxidation) is in agreement with previous investigations [40, 41, 43]. Since the two metabolites B2-O-Et-NH-ethyl and B2-O-NH_2 are strong inhibitors of the respiratory chain and are both associated with ROS production (which may be a consequence of the inhibition of the respiratory chain [43]) and with a remarkable cytotoxicity, it appears to be possible that they are at least partially responsible for the hepatic toxicity in patients treated with amiodarone. If this were the case, induction of CYP3A4, the main CYP

isozyme responsible for amiodarone deethylation [120], may be a risk factor for hepatotoxicity associated with amiodarone. While a high dosage and/or high plasma levels of amiodarone are considered to represent risk factors for hepatotoxicity associated with this drug [121, 122], induction of CYP3A4 has so far not been reported to be a risk factor for amiodarone-associated liver injury [38, 123, 124]. Since CYP3A4 inducers (e.g. antiepileptics such as phenytoin, phenobarbital and carbamazepine as well as rifampicin) are used quite frequently and since hepatotoxicity associated with amiodarone is potentially fatal [38], this question is clinically important and should therefore be investigated and answered.

As shown in Table 3, the toxicity of the investigated substances showed tendencies but no clear correlation with their lipophilicity profile. Inhibition of the respiratory chain (state 3 respiration), of mitochondrial β-oxidation, ROS production and cytotoxicity were preferentially associated with less lipophilic substances. On the other hand, uncoupling of oxidative phosphorylation was associated preferentially with substances showing a higher lipophilicity. Since all substances investigated showed some mitochondrial toxicity (at least uncoupling of oxidative phosphorylation or inhibition of β-oxidation), all of the compounds studied had to be able to penetrate the inner mitochondrial membrane. Lack of penetration of the mitochondrial membranes is therefore no probable explanation for a low toxicity.

Table 3

Overview of the toxicological properties of amiodarone and analogues and of their effect on hERG channels. The compounds are listed with increasing lipophilicity. The graduation was as follows. For state3, state4, state4u, β-oxidation and cytotoxicity: + = $p<0.05$ at 100µmol/L, ++ = $p<0.01$ at 100µmol/L and +++ = $p<0.05$ at 10µmol/L. For ROS production: + = $p<0.05$ at 18h, ++ = $p<0.05$ at 6h and +++ = $p<0.05$ at 4h. For the effect on hERG channels: + = $p<0.05$ at 10µmol/L, ++ = $p<0.01$ at 10µmol/L and +++ = $p<0.001$ at 10µmol/L.

	logP	State3	State4	State4u	β-oxida-tion	ROS	Cytotoxi-city[1]	Effect on hERG channels
B2-O-Et-NH₂	3.83	++	0	ND	++	+++	++	ND
B2-O-Et-OH	4.18	0	0	0	++	+	++	ND
B2-O-Et-Pro-pionamide	4.31	+++	+++	++	+++	+	+	ND
B2-O-Et-N-dimethyl	4.40	++	+++	+++	++	+	++	ND
B2-O-Et-NH-ethyl	4.47	++	0	ND	++	+	+++	ND
B2-O-Acetate	4.69	+	++	+++	++	+++	+	+
B2-O-Et	4.83	++	++		0	0	0	0
B2-O-Et-N-diethyl (Amiodarone)	4.92	0	+++	+++	++	+	++	+++
B2-O-Et-N-dipropyl	5.51	0	++	+++	0	0	0	+

[1]Cytotoxicity was determined using the data of Figure 4

The lack of a clear relationship between lipophilicity of the substances and their cytotoxicity may be explained at least partially by the rather small differences in their lipophilicity. The log P values of the substances tested were between 3.83 and 5.51, indicating that all compounds investigated are lipophilic, and that the most lipophilic substance (B2-O-Et-N-dipropyl) has an approximately 50 times lower solubility in water than the compound with the lowest lipophilicity (B2-O-Et-NH₂). In addition to their lipophilicity profile, the observed differences in hepatic mitochondrial toxicity between the compounds tested may therefore reflect also the composition of the side chain attached to B2. This is for instance substantiated by B2-O-Et, which has a quite high lipophilicity (log P 4.83), but almost no cytotoxicity. The cytotoxicity increases, however, when functional groups are attached to B2-O-Et, e.g. a hydroxyl group or an amino group with or without substituents. Regarding the amino groups, alkylation gradually decreases its toxicity (as shown by the comparison of the -NH₂, -N-dimethyl, -N-diethyl and -N-dipropyl

derivatives), but increases the uncoupling activity. The increase in the uncoupling activity associated with substituents at the amino group may be explained by the positive inductive effect of the alkyl groups, rendering the amino group more basic and therefore better suitable as a proton carrier. Due to their better lipid solubility, derivatives with large alkyl substituents at the amino group may diffuse better out of the mitochondrial matrix after having been deprotonated in the basic environment of the mitochondrial matrix, thereby explaining as well the observed tendency for a lower toxicity on the electron transport chain and on β-oxidation.

Similar to mitochondrial toxicity, also the effect on hERG channels did not show a clear relation to the lipophilicity of the compounds tested. Although the four substances investigated had a similar lipophilicity profile (log P values between 4.69 and 5.51), their effect on hERG channels was quite different. B2-O-Et had no inhibitory effect, whereas B2-O-Acetate and B2-O-Et-N-dipropyl had a median and B2-O-Et-N-diethyl a strong inhibitory activity on the hERG channels. The functional groups may therefore not only be important for the toxicity of these substances, but also for their inhibitory activity on the hERG channels. Inhibition of hERG channels is associated with prolongation of the refractoriness of cardiac tissue and QT prolongation, resulting in an antiarrhythmic (class III) activity [94]. However, in the case of overdosage and/or presence of certain risk factors such as electrolyte dysbalances, QT prolongation may become excessive and turn into so called torsade de pointes, a specific form of ventricular fibrillation which may be fatal [125].

In conclusion, despite similar lipophilicity profiles, amiodarone and the investigated amiodarone metabolites and analogues show large differences in mitochondrial toxicity and inhibition of hERG channels, accentuating the importance of the functional groups attached to the side chain of B2. Our studies reveal the possibility to detect amiodarone analogues with activity against hERG channels but with a lower mitochondrial toxicity than amiodarone, potentially offering the possibility to find safer antiarrhythmic drugs.

6. hERG channel interaction and cytotoxicity of amiodarone and amiodarone analogues

Katri Maria Waldhauser[1*], Karin Brecht[1*], Simon Hebeisen[3*], Ha Huy Riem[2], Daniel Konrad[3], Daniel Bur[4], Stephan Krähenbühl[1]

[1]Division of Clinical Pharmacology & Toxicology and Department of Research, University Hospital Basel, [2]Cardiovascular Therapy Research Unit, University Hospital of Zürich, [3]Bsys Ltd., Witterswil and [4]Actelion Ltd. Allschwil, Switzerland

*these authors contributed equally to this work

Submitted in 2008

6.1. Abstract

Amiodarone (2-n-butyl-3-[3,5 diiodo-4-diethylaminoethoxybenzoyl]-benzofuran, B2-O-CH$_2$CH$_2$-N-diethyl, (**1**)) is an efficient class III antiarrhythmic drug with a broad field of clinical applications but with potentially life threatening organ toxicities. In order to better characterize hepatic and pulmonary toxicity and to differentiate cytotoxicity from the interaction with the hERG channel, we synthesized amiodarone analogues with or without a positively ionizable nitrogen in the phenolic side chain. After having studied cytotoxicity using HepG2 (a hepatocyte cell line) and A549 cells (a pneumocyte cell line), we studied the interaction of all compounds with the hERG channel using pharmacological and in silico methods. Compared to amiodarone, which displayed only a weak cytotoxicity, the mono- and bis-desethylated metabolites, the further degraded alcohol (B2-O-CH$_2$-CH$_2$-OH), the corresponding acid (B2-O-CH$_2$-COOH) and, finally, the newly synthesized B2-O-CH$_2$-CH$_2$-N-pyrrolidine were equally or more toxic than the parent compound. On the other hand, structural analogues such as B2-O-CH$_2$-CH$_2$-N-diisopropyl and B2-O-CH$_2$-CH$_2$-N-piperidine were significantly less toxic than amiodarone. Cytotoxicity was correlated with a drop in the mitochondrial membrane potential and is therefore most probably of mitochondrial origin. Pharmacological and in silico investigations concerning the interactions of these compounds with the hERG channel revealed that substances carrying a basic nitrogen in the side chain displayed a much higher affinity than those lacking such a group. Specifically, B2-O-CH$_2$-CH$_2$-N-piperidine and B2-O-CH$_2$-CH$_2$-N-pyrrolidine revealed a higher affinity towards hERG channels than amiodarone. Our data reveal the possibility to identify amiodarone analogues with maintained pharmacological activity and improved cytotoxicity profiles compared to the parent compound.

6.2. Introduction

Efficient and safe pharmacological treatment of cardiac arrhythmias is a difficult challenge. One of the most efficient currently used antiarrhythmic drugs is amiodarone (2-n-butyl-3-[3,5 diiodo-4-diethylaminoethoxybenzoyl]-benzofuran, $B2-O-CH_2CH_2-N$-diethyl, (**1**)), a class III antiarrhytmic agent with additional class I and II properties. It blocks human ether-a-go-go (hERG) channels, leading to prolongation of the refractoriness and resulting in QT prolongation [94]. Amiodarone (see Table 1 for chemical structures) is metabolized via mono-[102] and bis-desalkylation [103] to the corresponding secondary ($B2-O-CH_2CH_2-NH$-ethyl, **2**) and primary amine ($B2-O-CH_2CH_2-NH_2$, **3**), respectively. The primary amine **3** can subsequently be transaminated and oxidized to the corresponding acid ($B2-O-CH_2-COOH$, (**5**)) or primary alcohol ($B2-O-CH_2CH_2-OH$, (**6**)) [103].

Amiodarone's therapeutic use is limited because of its numerous side effects that include thyroidal [98], pulmonary [99], ocular [100] and/or liver toxicity [38, 101]. The mechanisms leading to amiodarone's toxicity are not completely understood, but they are assumed to involve accumulation of the parent compound as well as metabolites in cells, resulting in cellular toxicity, for instance by impairing mitochondrial function. Amiodarone uncouples oxidative phosphorylation and inhibits the electron transport chain and ß-oxidation of fatty acids in mitochondria [39-41, 43, 126].

The most serious non-cardiac side effect of amiodarone is pulmonary toxicity, occurring in 5-15% of patients treated with this drug. This toxicity is characterized clinically by progressive dyspnea and impaired alveolar diffusion of oxygen and, finally, also carbon dioxide, and radiologically by interstitial lung damage due to interstitial fibrosis [127-130]. It is possible that alveolar macrophages may play a role in pulmonary fibrosis associated with amiodarone [99]. Interestingly, Bigler et al. [131] were recently able to show that some modifications of the diethyl-amino-ethoxy group of amiodarone reduced its toxicity towards alveolar macrophages.

In earlier studies, we could show that the substituents attached to the benzofuran ring (aliphatic side chain in position 2 and iodinated 4-diethyl-amino-ethoxy-benzoyl chain in position 3) are responsible for mitochondrial toxicity caused by amiodarone [41, 43]. More recent studies focusing on the hepatotoxic profile and the antiarrhythmic effect of amiodarone and amiodarone derivatives again revealed the importance of the topology of the side chain attached to the bicyclic aromatic template (B2, see Table 1) of amiodarone for both interaction with the hERG channel and hepatocellular toxicity [126].

Despite these studies, several questions regarding amiodarone and its metabolites and derivatives with different compositions of the aliphatic side chain attached to B2 remained unanswered. The current study was designed to address following issues: 1. Are amiodarone and related derivatives also toxic to cultured pneumocytes and is this toxicity similar to that on cultured hepatocytes? 2. Is there a correlation between the physicochemical properties of these

compounds and their pharmacological effects and/or cellular toxicity? We therefore synthesized and investigated the ethyl ester B2-O-CH_2-COO-CH_2CH_3 (**11**) of the acid B2-O-CH_2-COOH (**5**), as well as two derivatives with either a terminal pyrrolidine (B2-O-CH_2CH_2-N-pyrrolidine (**8**)) or piperidine (B2-O-CH_2CH_2-N-piperidine (**9**)) group, respectively. In addition, we investigated the two amines **2** and **3** (two amiodarone metabolites), as well as the bis-isopropyl amine B2-O-CH_2CH_2-N-diisopropyl (**4**), three compounds we had investigated already in a previous study [126]. The data of the current investigations could then be compared with those of our previous study [126].

Table 1
Chemical structures and lipophilicity of amiodarone, amiodarone metabolites and amiodarone analogues. LogD was determined using reversed phase HPLC at 37°C as described by Braumann [107]. The mobile phase consisted of different mixtures of 5mmol/L phosphate buffer pH 7.4 and methanol. N=3 determinations per compound, mean ± SEM.

= B2
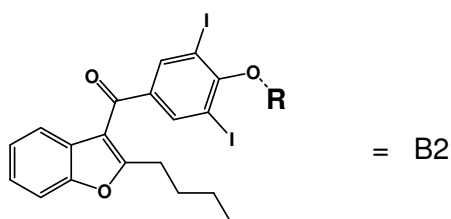
Number	Compound	R	logD
1	B2-O-CH$_2$CH$_2$-N-diethyl (amiodarone)		4.92 ± 0.25
2	B2-O-CH$_2$CH$_2$-NH-ethyl		4.47 ± 0.12
3	B2-O-CH$_2$CH$_2$-NH$_2$		3.83 ± 0.10
4	B2-O-CH$_2$CH$_2$-N-((C(CH$_3$)$_2$)$_2$ (B2-O-CH$_2$CH$_2$-N-diisopropyl)		5.51 ± 0.12
5	B2-O-CH$_2$-COOH		4.69 ± 0.08
6	B2-O-CH$_2$CH$_2$-OH		4.18 ± 0.15
7	B2-O-CH$_2$CH$_2$-NH-CO-CH$_2$CH$_3$		4.31 ± 0.16
8	B2-O-CH$_2$CH$_2$-N-pyrrolidine		7.82 ± 0.05
9	B2-O-CH$_2$CH$_2$-N-piperidine		8.04 ± 0.11
10	B2-O-CH$_2$CH$_3$		4.83 ± 0.06
11	B2-O-CH$_2$-COO-CH$_2$CH$_3$		4.67 ± 0.08

6.3. Materials and Methods

6.3.1. Amiodarone and Amiodarone Derivatives

Amiodarone hydrochloride was from Sigma-Aldrich (Buchs, Switzerland). All amiodarone analogues were synthesized starting from B2 [104] as shown in Table 1 and as described earlier for B2-O-CH$_2$CH$_2$-NH-ethyl (**2**), B2-O-CH$_2$CH$_2$-NH$_2$ (**3**), B2-O-CH$_2$CH$_2$-N-diisopropyl (**4**), B2-O-CH$_2$-COOH (**5**), B2-O-CH$_2$CH$_2$-OH (**6**), B2-O-CH$_2$CH$_2$-NH-CO-CH$_2$CH$_3$ (**7**) and B2-O-CH$_2$CH$_3$ (**10**) [126] and for B2-O-CH$_2$-COO-CH$_2$CH$_3$ (**11**) [103]. The remaining two amiodarone derivatives were synthesized as follows:

B2-O-CH$_2$CH$_2$-N-piperidine [4-(2-butyl-benzofuran-3-yl)-[3,5-diiodophenyl-4-(2-piperidinoethoxy)phenyl]-methanone hydrochloride] (**9**)

To a mixture of B2 (2g, 3.66mmol) and K$_2$CO$_3$ (3.45g, 25mmol) in toluene:water (2:1v/v, total volume: 75mL) heated to 55-60 °C small portions of about 0.2g 1-(2-chlorethyl) piperidine monohydrochloride (3.41g, 18.5mmol) were added. After the addition, the temperature was risen to reach reflux over 30min. The yellow color of B2 disappeared. After having refluxed the reaction mixture for 1 additional hour, the phases were quickly separated using a separation funnel at 60°C. The toluene phase was washed three times with 25mL water at this temperature, and the organic phase was afterwards evaporated to dryness. The residue was suspended in 10mL 5% NH$_3$, and B2-O-Et-NH-ethyl was extracted three times with 15mL toluene. The organic phase was separated by means of centrifugation and evaporated to dryness under reduced pressure. Then, 2mL 10N HCl and 15mL toluene were added to the residue, and the liquids were removed under reduced pressure at 80°C. A white solid residue was obtained after three additional treatments with 10mL toluene. The residue was then crystallized from toluene and yielded 1.62g (64%) of the target product. Analytically pure (**9**) was obtained by silica gel – low pressure chromatography [(30x5 cm i.d.) and mobile phase: methanol: 25% NH$_3$ (99:1 v/v)]. Melting point and NMR, ESI-MS, NMR data of B2-O-Et-N-piperidine (**9**) have been reported already in our previous communication [131].

B2-O-CH$_2$CH$_2$-N-pyrrolidine ([4-(2-butyl-benzofuran-3-yl)-[3,5-diiodophenyl-4-(2-pyrrolidine-1-yl-ethoxy)phenyl]-methanone hydrochloride] (8)

B2-O-CH$_2$CH$_2$-N-pyrrolidine (**8**) (yield 70%) was prepared in the same manner as described for **9**. The ESI-MS, NMR data supporting its chemical structure were published previously [131].

6.3.2. Octanol/water partition coefficient of amiodarone and derivatives

The octanol/water partition of the compounds synthesized was determined using reversed phase HPLC as described by Braumann [132]. HPLC of the substances was performed at 37°C using different 5mM phosphate buffer (pH 7.4)/methanol mixtures as an eluant. The octanol/water partition of a substance can be calculated based on the retention times obtained at different methanol concentrations [107].

6.3.3. Other chemicals

All chemicals used were from Sigma–Aldrich (Buchs, Switzerland) except for JC-1, which was from Alexis Biochemicals (Lausen, Switzerland). All cell culture media were obtained from Gibco (Paisley, UK). The 96-well-plates were from BD Biosciences (Franklin Lakes, NJ).

6.3.4. Cell Lines and Cell Culture

The hepatoma cell line HepG2 was provided by Professor Dietrich von Schweinitz (University Hospital Basel, Switzerland) and HepT1 cells from Professor Torsten Pietsch (University of Bonn, Germany). A549 cells were a generous gift from Dr. Juillerat (University Institute of Pathology, University Hospital Lausanne). HepG2 cells were cultured in Dulbecco's modified Eagle's medium (with 2mmol/L GlutaMAX®, 1.0g/L glucose and sodium bicarbonate) supplemented with 10% (v/v) inactivated fetal calf serum, 10mM HEPES buffer, pH 7.2, 100U/mL penicillin/streptomycin and non-essential amino acids. HepT1 cells were grown in RPMI supplemented with 10% (v/v) inactivated fetal calf serum, 10mM HEPES buffer, pH 7.2, 2mM GlutaMAX® (Invitrogen, Basel, Switzerland) and 100U/mL penicillin/streptomycin. The A549 cell line was cultured in Dulbecco's modified Eagles's medium (with 4mmol/L GlutaMAX®, 4.5g/L glucose and sodium bicarbonate) supplemented with 10% (v/v) inactivated fetal calf serum, 10mM HEPES buffer pH 7.2, nonessential amino acids and 100U/mL penicillin/streptomycin. The culture conditions were 5% CO_2 and 95% air atmosphere at 37°C. Cells were seeded in a density of 70 000 cells/well on a 96-multiwell-plate and let settle over night before the treatment was started.

6.3.5. Adenylate kinase release

The loss of cell membrane integrity results in the release of adenylate kinase (AK), which can be quantified using the firefly luciferase system (ToxiLight® BioAssay Kit, Cambrex Bio Science, Rockland, ME). After an incubation of 4 or 24 hours, 100µL assay buffer was added to 20µL supernatant from cells treated with amiodarone or amiodarone derivates (concentrations

indicated in the Tables and Figures) and the luminescence was measured after 5 minutes of incubation.

6.3.6. Reductive capacity of the cells

The fluorescent dye Alamar Blue[TM] (AbD Serotec, Oxford, UK) was used for this purpose. Proliferating cells cause the change of the oxidized form of blue and non-fluorescent Alamar Blue[TM] (resazurin) to a pink, highly fluorescent and reduced form (resorufin) that can be detected using the fluorescence mode (excitation 560nm; emission 590nm) [133]. The dye was added to the cells together with the test substances in a final concentration of 10% and the fluorescence was measured after 4 and 24 hours.

6.3.7. Mitochondrial membrane potential

The mitochondrial membrane potential was measured with the dye JC-1 according to Current Protocols of Flow Cytometry with minor modifications. HepG2 and A549 cells were harvested by trypsinization and adjusted to 10^5 cells/0.5mL pre-warmed Dulbecco's medium without phenol red containing 1% FCS. The compounds to be tested were then added to the cells and the cells incubated for 24h. After the incubation period, JC-1 stock solution (0.25µg/100µL for 100 000 cells) was added to the incubations and cells were incubated at 37°C in the dark for 10 min. The cell suspension was then washed once by adding 1.5 mL PBS and centrifugation at 500 x g for 4min at room temperature. Cells were resuspended in 0.3mL PBS and analyzed by FACS using the following settings: acquisition = max 300 events/sec; FSC/SSC: E-01 – 5.08 (A549: 6.23)/479 – 1.00; FL1: 400; FL2: 324; compensation: FL2 – 54.4% FL1.

6.3.8. HEK Tet cells expressing hERG channels

The interaction of the test substances with the hERG channel was examined using HEK Tet cells stably expressing this potassium channel. Briefly, a human cardiac plasmid cDNA library was prepared from freshly isolated tissue. The hERG alpha subunit PCR product was released from the pCR2.1-TOPO vector (Invitrogen, Basel, Switzerland) for ligation into a modified pcDNA5/FRT/TO vector (Invitrogen, Basel, Switzerland) with excluded BGH site. Restriction analysis and complete sequencing confirmed the correct composition and expression of the hERG alpha subunit in the plasmid. HEK Tet cells were transfected with the calciumphosphate precipitation method (Invitrogen, Basel, Switzerland). Clones were selected with 200µg/mL hygromycin B and 30µg/mL blasticidin (Invitrogen, Basel, Switzerland) and checked back electrophysiologically. Using limited dilution, clone HEK Tet hERG S12, which displayed an average tail current amplitude of approximately 700-1500pA, was isolated. This clone was successfully cultured over 100 passages without detectable loss of current density and was

used in the current studies. The cells were generally maintained in HAM/F12 with GlutaMax I (GIBCO, Paisley, UK) supplemented with 9% fetal bovine serum (GIBCO, Paisley, UK), 0.9% Penicillin/Streptomycin solution (GIBCO, Paisley, UK) and 100µg/mL hygromycin B and 15µg/mL blasticidin (Invitrogen, Basel, Switzerland). For electrophysiological measurements, the cells were seeded onto 35mm sterile culture dishes containing 2mL culture medium and 1µg/mL tetracycline for induction of channel expression (over night). Confluent clusters of HEK cells are electrically coupled. Because responses in distant cells are not adequately voltage clamped and because of uncertainties about the extent of coupling, cells were cultured at a density enabling single cells to be used for the experiments.

6.3.9. Electrophysiology

hERG currents were measured by means of the patch-clamp technique in the whole-cell configuration as described previously [126].

6.3.10. Molecular Modeling

Model building of hERG was performed on a structure of potassium channel KcsA (PDB-code: 1JVM). Modeling calculations were done on a Dell 670 workstation using the program Moloc [134]. An initial C-alpha model of hERG was built by fitting its aligned sequence on the potassium channel template C-alpha structure followed by optimization of newly introduced loops. Subsequently, a full atom model was generated and newly inserted loops were optimized with the rest of the protein kept stationary. Refinement of the full model with manual removal of repulsive interactions followed and was divided in three subsequent steps. First, only amino acid side chains were allowed to move. In a second step, all atoms except alpha carbons were optimized and, finally, all atoms were allowed to move, however, with positional constraints for alpha carbons. Quality checks were made with Moloc internal programs.

6.3.11. Statistical Analysis

Data are presented as mean ± standard error of the mean (SEM) of at least three individual experiments. Differences between groups (control and test compound incubations) were analyzed by analysis of variance (ANOVA) and Dunnett´s post hoc test was performed if ANOVA showed significant differences. A p value ≤ 0.05 was considered to be significant.

6.4. Results

6.4.1. Toxicity on HepG2 cells

As shown in Figures 1 and 2, the results obtained by two assays used (ToxiLight® and Alamar Blue® assays) are qualitatively comparable. Regarding the ToxiLight® assay, the most toxic compounds tested were the desethylated amiodarone metabolites **2** and **3**, as well as B2-O-CH$_2$-COOH (**5**), which were toxic already in a range of 1 to 10µmol/L. Amiodarone, as well as the piperidine **9** and the pyrrolidine **8** were less toxic, with cytotoxicity starting only at 100µmol/L. For the diisopropyl molecule **4** and the ethyl ester of **5** B2-O-CH$_2$-COO-CH$_2$CH$_3$ (**11**) no cytotoxicity could be demonstrated up to 10µmol/L and only a minor toxicity at 100µmol/L. Beside the concentration, also the time of exposure had a critical influence on toxicity of the individual compounds. For amiodarone (**1**) and the pyrrolidine analogue **8**, an incubation period of 12 hours produced clearly more toxic effects compared to 4 hours.

Interestingly, reductive capacity assessed using the Alamar Blue® Assay increased consistently with the duration of the incubation, irrespective of presence or absence of our compounds (Figure 2). With this assay, toxic effects could be observed for the desethylated amiodarone metabolites **2** and **3**, B2-O-CH$_2$-COOH (**5**) and B2-O-CH$_2$CH$_2$-N-pyrrolidine (**8**), but only at concentrations of 100µmol/L. For amiodarone (**1**), the diisopropyl analogue **4**, the ethylated acid **11** and the piperidine analogue **9**, no toxicity could be demonstrated up to 100µmol/L.

The effect of amiodarone and amiodarone analogues on the mitochondrial membrane potential was comparable to the results obtained by the Alamar Blue® Assay (Table 2). At concentrations of 10µmol/L, the mitochondrial membrane potential was significantly decreased only for the desethylated amiodarone metabolites **2** and **3,** respectively.
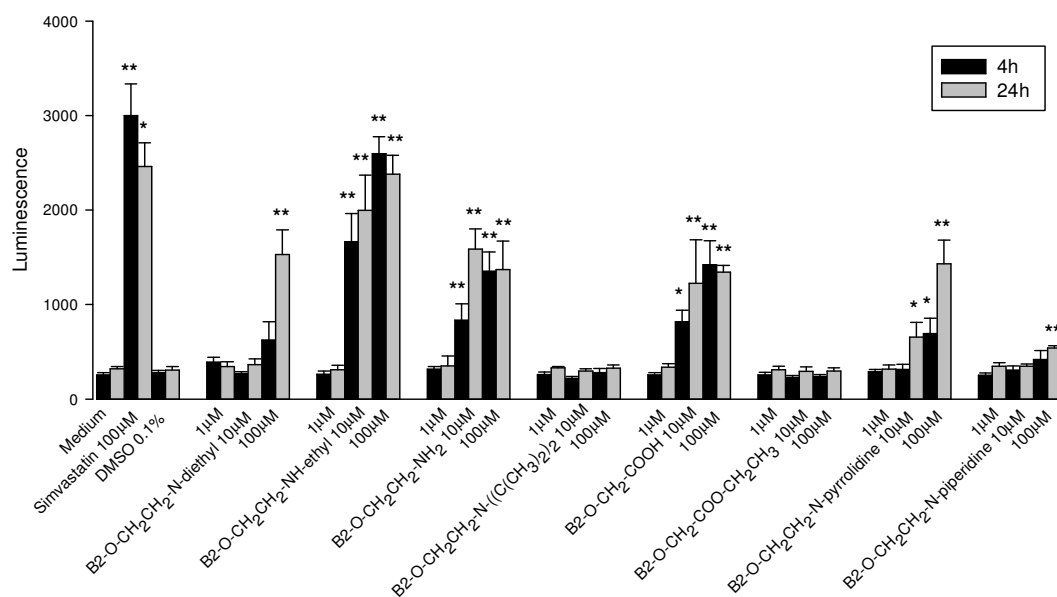
Figure 1.

Adenylate kinase release from HepG2 cells treated with amiodarone or amiodarone analogues. B2-O-CH$_2$CH$_2$-NH-ethyl, B2-O-CH$_2$CH$_2$-NH$_2$, B2-O-CH$_2$-COOH and B2-O-CH$_2$CH$_2$-N-pyrrolidine showed cytotoxicity starting at 10µmol/L, amiodarone and B2-O-CH$_2$CH$_2$-N-piperidine starting at 100µmol/L, and B2-O-CH$_2$CH$_2$-N-diisopropyl and B2-O-CH$_2$-COO-CH$_2$CH$_3$ no cytotoxicity up to 100µmol/L. Simvastatin was used as a positive control. All incubations contained 0.1% DMSO (except medium only). Data are presented as means ± SEM of at least four incubations in triplicate. *P<0.05 and **p<0.01 versus control incubations containing 0.1% DMSO.
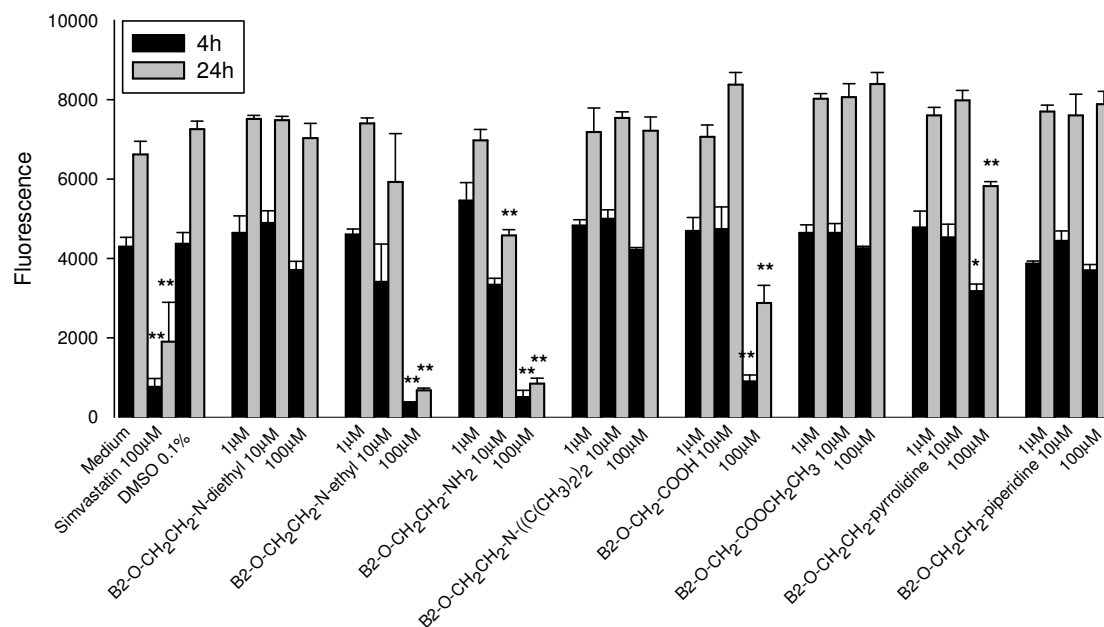
Figure 2.

Inhibition of reductive capacity of HepG2 cells (resazurin reduction test) by amiodarone or amiodarone derivatives. $B2\text{-}O\text{-}CH_2CH_2\text{-}NH_2$ inhibited reductive capacity starting at 10µmol/L, $B2\text{-}O\text{-}CH_2CH_2\text{-}NH\text{-}ethyl$, $B2\text{-}O\text{-}CH_2\text{-}COOH$ and $B2\text{-}O\text{-}CH_2CH_2\text{-}N\text{-}pyrrolidine$ at 100µmol/L, and amiodarone, $B2\text{-}O\text{-}CH_2CH_2\text{-}N\text{-}diisopropyl$, $B2\text{-}O\text{-}CH_2\text{-}COO\text{-}CH_2CH_3$ and $B2\text{-}O\text{-}CH_2CH_2\text{-}N\text{-}piperidine$ revealed no inhibition up to 100µmol/L. Simvastatin was used as a positive control. All incubations contained 0.1% DMSO (except medium only). Data are presented as means ± SEM of at least four incubations in triplicate. *P<0.05 and **p<0.01 versus control incubations containing 0.1% DMSO.

6.4.2. Toxicity on A549 cells

Similar to HepG2 cells, the most toxic compounds tested were the two amines **2** and **3** respectively, with cytotoxicity starting at 10µmol/L. For amiodarone (**1**), $B2\text{-}O\text{-}CH_2\text{-}COOH$ (**5**) and the pyrrolidine derivative **8**, cytotoxicity was detected only at 100µmol/L, whereas the tertiary amine **4**, the esterified acid **11** as well as the piperidine derivative **9** were not toxic up to 100µmol/L. As found for HepG2 cells, amiodarone (**1**) and the cyclic pyrrolidine analogue **8** were clearly more toxic after an incubation period of 12 compared to 4 hours. For the results, see Figure 3.

Regarding reductive capacity (Alamar Blue®), the desethylamine metabolite **2** was toxic already at 10µmol/L for 12 h, whereas the primary amine **3** and $B2\text{-}O\text{-}CH_2\text{-}COOH$ (**5**) impaired reductive

capacity only at 100μmol/L. For amiodarone (**1**), the diisopropyl analogue **4**, the ethylated acid **11** and the pyrrolidine **8** as well as the piperidine derivative **9**, no toxicity could be demonstrated up to 100μmol/L (Figure 4). The results obtained for the mitochondrial membrane potential using the dye JC1 were very similar to those determined in HepG2 cells (Table 2). At concentrations of 10μmol/L, the mitochondrial membrane potential was significantly decreased only by the two desethylated amiodarone metabolites **2** and **3**.

Figure 3.

Adenylate kinase release from A549 cells treated with amiodarone or amiodarone derivatives. B2-O-CH$_2$CH$_2$-NH-ethyl and B2-O-CH$_2$CH$_2$-NH$_2$ showed cytotoxicity starting at 10μmol/L, amiodarone, B2-O-CH$_2$-COOH and B2-O-CH$_2$CH$_2$-N-pyrrolidine at 100μmol/L, and B2-O-CH$_2$CH$_2$-N-diisopropyl, B2-O-CH$_2$-COO-CH$_2$CH$_3$ and B2-O-CH$_2$CH$_2$-N-piperidine no cytotoxicity up to 100μmol/L. Simvastatin was used as a positive control. All incubations contained 0.1% DMSO (except medium only). Data are presented as means ± SEM of at least four incubations in triplicate. *P<0.05 and **p<0.01 versus control incubations containing 0.1% DMSO.
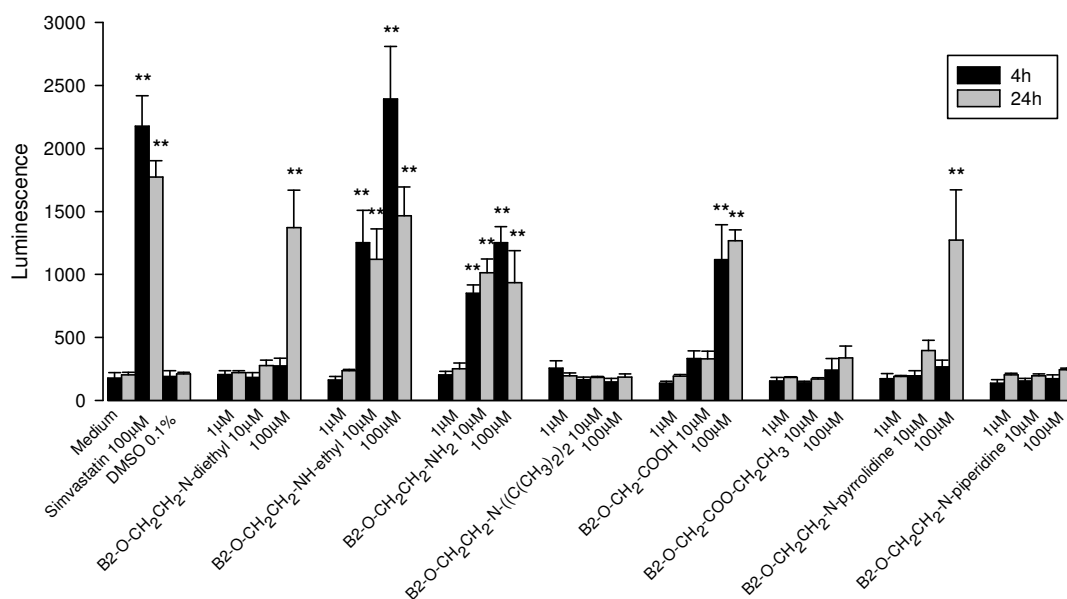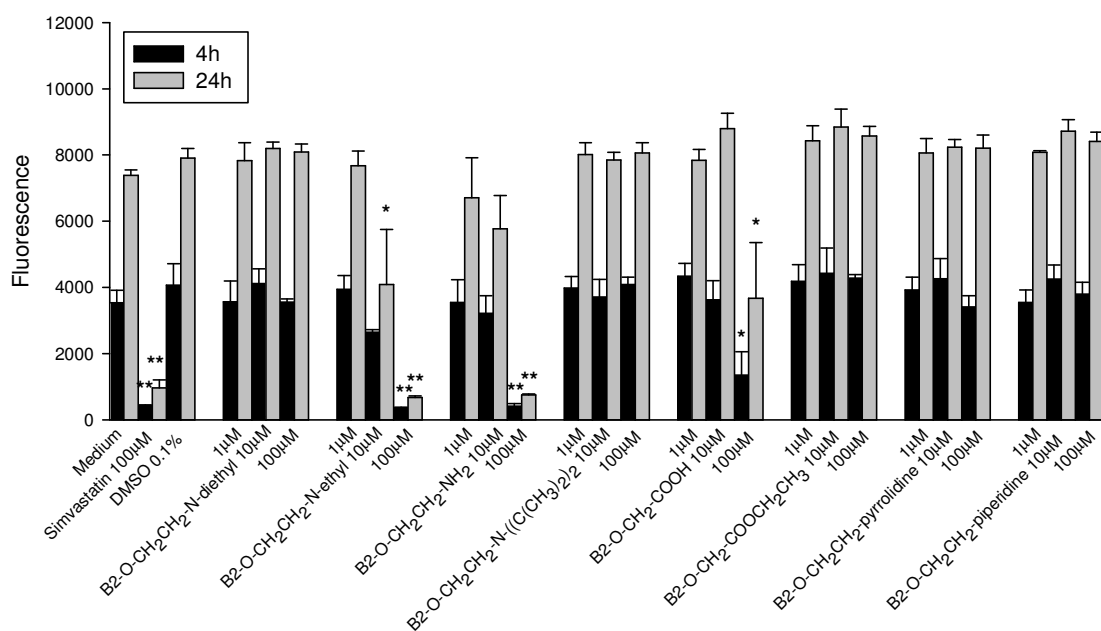
Figure 4.

Inhibition of reductive capacity of A549 cells (resazurin reduction test) by amiodarone or amiodarone derivatives. B2-O-CH$_2$CH$_2$-NH-ethyl inhibited reductive capacity starting at 10µmol/L, B2-O-CH$_2$CH$_2$-NH$_2$ and B2-O-CH$_2$-COOH at 100µmol/L, and amiodarone, B2-O-CH$_2$CH$_2$-N-diisopropyl, B2-O-CH$_2$-COO-CH$_2$CH$_3$, B2-O-CH$_2$CH$_2$-N-pyrrolidine and B2-O-CH$_2$CH$_2$-N-piperidine revealed no inhibition up to 100µmol/L. Simvastatin was used as a positive control. All incubations contained 0.1% DMSO (except medium only). Data are presented as means ± SEM of at least four incubations in triplicate. *P<0.05 and **p<0.01 versus control incubations containing 0.1% DMSO.

Table 2

Effects of amiodarone and analogues on mitochondrial membrane potential in HepG2 and A549 cells. The mitochondrial membrane potential was determined using the dye JC-1 as described in Methods. The concentration of amiodarone and analogues was 10µmol/L. The cells were incubated for 24h with the substances indicated. With the exception of control incubations with culture medium only, all incubations contained 0.1% DMSO. The values represent means ± SEM of at least five experiments. *P<0.05 and **p<0.01 versus control incubations containing 0.1% DMSO.

	HepG2	A549
Cell culture medium	67 ± 3.3	87 ± 2.9
Cell culture medium containing 0.1% DMSO	67 ± 3.5	87 ± 2.9
B2-O-CH_2CH_2-N-diethyl (amiodarone) (1)	71 ± 4.1	86 ± 3.2
B2-O-CH_2CH_2-NH-ethyl (2)	19 ± 4.9 **	9 ± 3.9 **
B2-O-CH_2CH_2-NH_2 (3)	10 ± 1.8 **	8 ± 1.3 **
B2-O-CH_2CH_2-N-diisopropyl (4)	61 ± 2.1	89 ± 2.1
B2-O-CH_2-COOH (5)	58 ± 5.0	74 ± 5.5
B2-O-CH_2CH_2-N-pyrrolidine (8)	69 ± 3.9	83 ± 3.2
B2-O-CH_2CH_2-N-piperidine (9)	60± 3.3	91 ± 1.9
B2-O-CH_2-COO-CH_2CH_3 (11)	59± 4.1	76 ± 7.4

6.4.3. Effects on hERG channels

Amiodarone and its analogues were investigated for their inhibitory effects on hERG potassium channels stably expressed in HEK Tet cells. With the exception of $B2-O-CH_2CH_3$ (**10**) all measured compounds interfered with potassium transport by the hERG channels (Figure 5), with IC_{50} values ranging from 0.05µmol/L to 216µmol/L. The IC_{50} values for amiodarone (**1**), for the two desethylated metabolites **2** and **3**, and for the cyclic analogues **8** and **9** were all lower than 1µmol/L, whereas those for $B2-O-CH_2CH_2-N-diisopropyl$ (**4**) and $B2-O-CH_2CH_2-NH-CO-CH_2CH_3$ (**7**) ranged between 1 and 10µmol/L and the values for $B2-O-CH_2-COOH$ (**5**), $B2-O-CH_2CH_2-OH$ (**6**), $B2-O-CH_2-COO-CH_2CH_3$ (**11**) and $B2-O-CH_2CH_3$ (**10**) exceeded 10µmol/L or were not assessable. Individual traces describing the hERG channels interaction are provided in Figure 6.
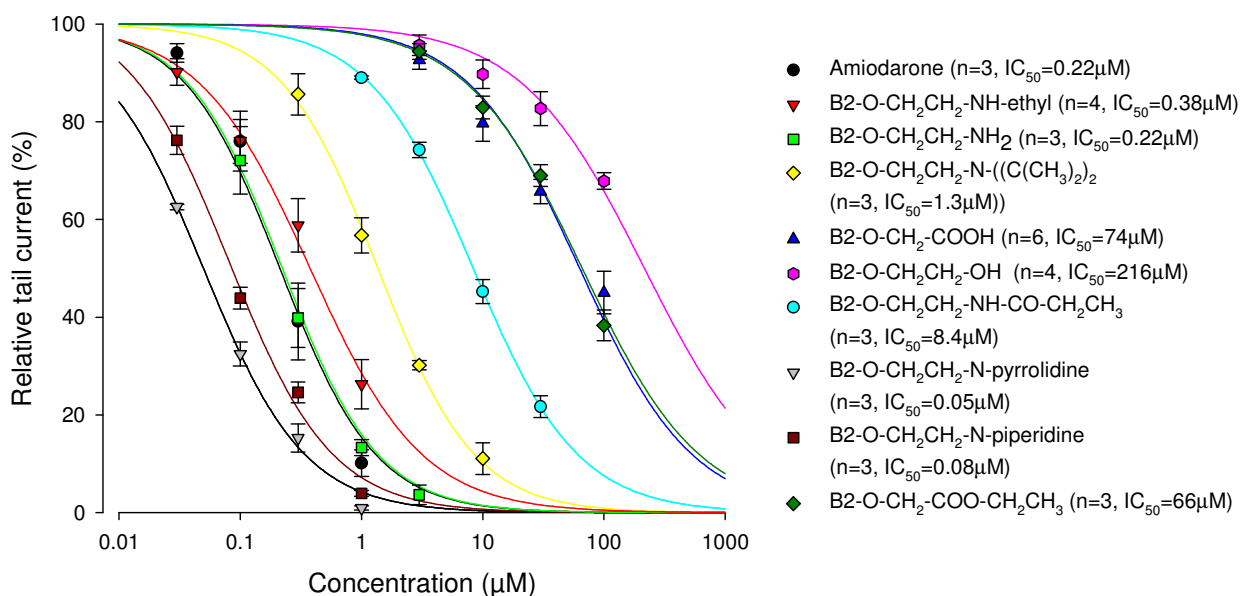
Figure 5.
Dose-response curves of amiodarone and amiodarone derivatives. Amiodarone, the amiodarone metabolites $B2-O-CH_2CH_2-NH-ethyl$ and $B2-O-CH_2CH_2-NH_2$, and the analogues $B2-O-CH_2CH_2-N-$ pyrrolidine and $B2-O-CH_2CH_2-N-piperidine$ revealed strong hERG inhibition with IC_{50} <1µmol/L. B2-O- $CH_2CH_2-N-diisopropyl$ and $B2-O-CH_2CH_2-NH-CO-CH_2CH_3$ were medium strong inhibitors (IC_{50} <1 and <10µmol/L), whereas $B2-O-CH_2-COOH$, $B2-O-CH_2CH_2-OH$, $B2-O-CH_2CH_3$ and $B2-O-CH_2-COO-CH_2CH_3$ showed only a weak or no inhibition. Measurements were accomplished in the whole-cell patch-clamp configuration at room temperature. Outward currents were activated upon depolarization of the cell membrane from -80mV to +20mV for 3 s, whereas partial repolarization to -40mV for 4 s evoked large tail currents. At least three cells were recorded per test compound.
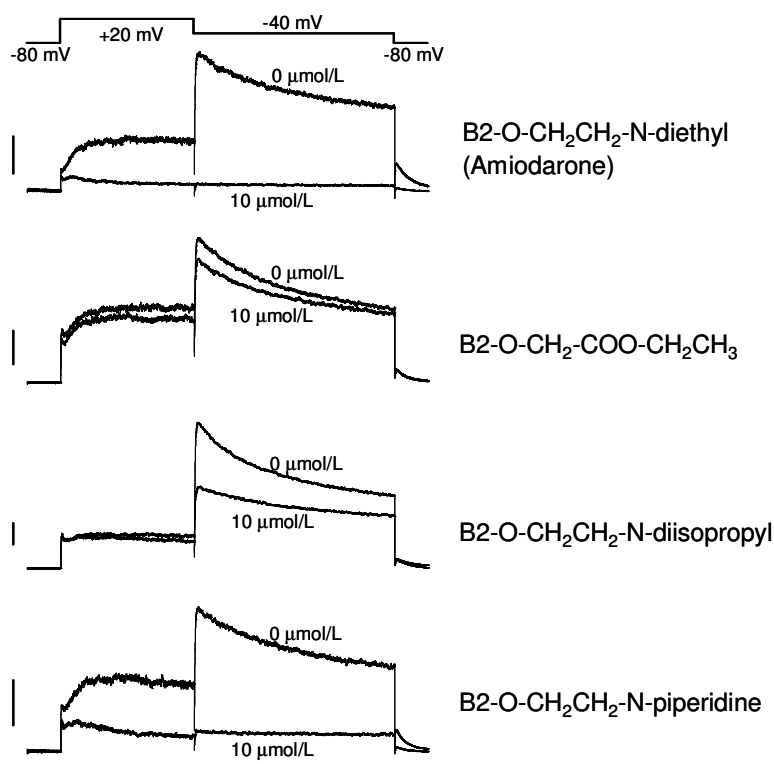
Figure 6

Inhibition of the potassium current by B2-O-CH$_2$CH$_2$-N-diethyl (amiodarone, (1)), B2-O-CH$_2$-COO-CH$_2$CH$_3$ (11), B2-O-CH$_2$CH$_2$-N-diisopropyl (4) and B2-O-CH$_2$CH$_2$-N-piperidine (9). Representative traces of potassium currents across hERG channels stably expressed in HEK Tet cells are shown. Measurements were accomplished in the whole-cell patch-clamp configuration at room temperature. Outward currents were activated upon depolarization of the cell membrane from -80mV to +20mV for 3 s, whereas partial repolarization to -40mV for 4 s evoked large tail currents. At least three cells were recorded per test compound. The vehicle (0.1% DMSO) had no significant effect on hERG channel activity. In contrast, 10µmol/L B2-O-Et-N-diethyl (amiodarone, (1)) as well as 10µmol/L B2-O-CH$_2$CH$_2$-N-piperidine (9) blocked the hERG channel completely. In comparison, the interaction of 10µmol/L B2-O-CH$_2$-COO-CH$_2$CH$_3$ (11) as well as 10µmol/L B2-O-CH$_2$CH$_2$-N-diisopropyl (4) with the hERG channel was less intense. The upper trace in the individual figures depicts the control incubations (0.1% DMSO) and the lower trace the incubations containing the test compounds in 0.1% DMSO.

6.4.4. Molecular modelling of hERG inhibitor interactions

The structure of a tetraethyl ammonium (TEA) inhibited fragment of the KcsA potassium channel resembles roughly an amphora and was reported recently [135]. The sequence alignment of the hERG protein with the KcsA channel suggests that the relevant part of the hERG structure (vestibule and neck of the amphora) are likely to be conserved in both proteins. A model of vestibule and selectivity filter of the hERG channel (neck of the amphora) was therefore produced using the KcsA structure as a structural template (Figure 7). Amiodarone (**1**) and some of its metabolites and/or analogues were docked manually into the hERG-model such that the charged basic nitrogen of **1** could mimic position and function of the ammonium nitrogen of TEA in the KcsA structure (Figure 7A, left panel). Access for solvated potassium ions to the narrow selectivity filter would be blocked by **1** in the energetically most favored inhibitor position. Metabolite B2-O-CH$_2$-COOH (**5**, Figure 7B), which is lacking a positively ionizable nitrogen, but carries a negatively ionizable terminal carboxylate instead, could theoretically assume a similar position inside the rather hydrophobic vestibule. However, the positively charged diethyl-amino group of **1** is replaced by a shorter side chain in **5** that is bearing a terminal negatively ionizable carboxylate. The inversion of charge in the side chain of **5** leads to dramatically lowered attractive interactions with the channel, most likely due to unfavorable electrostatic interferences. The strong affinity of amiodarone (**1**), amiodarone metabolites **2**, **3** and some analogs **8**, **9** is clearly dependent on a positively ionizable group in the side chain (Table 1), while molecules with a neutral or even negatively charged side chain display significantly lowered affinities for the hERG channel.

B2-O-CH$_2$CH$_2$-N-diethyl
(amiodarone)

B2-O-CH$_2$-COOH
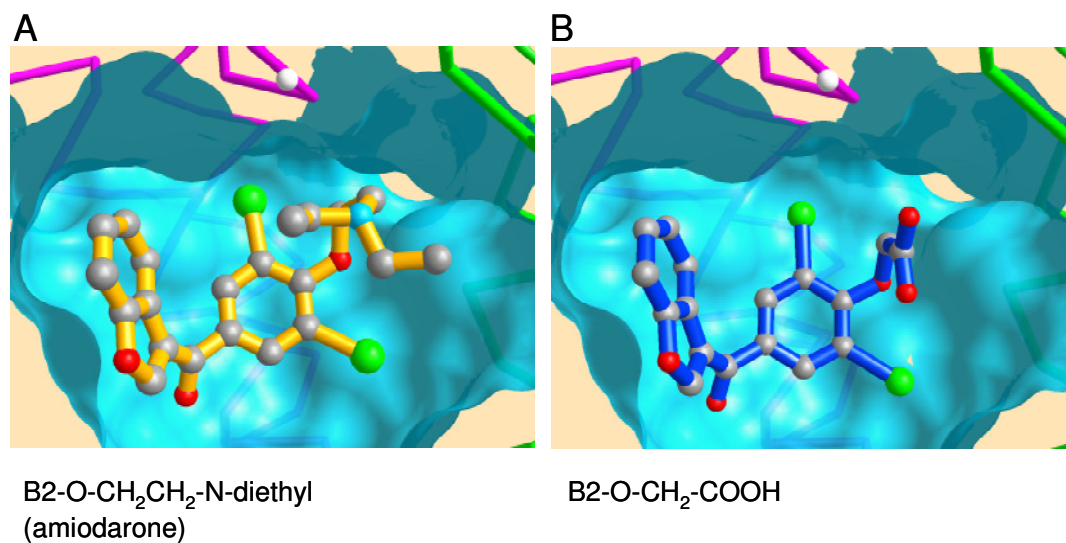
Figure 7

A) Amiodarone (yellow) is docked into the vestibule of a hERG model. Two of the four chains of the hERG homo-tetramer are shown in C-alfa representation (green, magenta). The Connolly surface was produced with a probe radius of 1.4Å. The selectivity filter cannot be displayed in this representation due to its very narrow diameter. A white ball represents a potassium ion in the filter region as found in the KscA structure template.[135]

B) amiodarone derivative **5** (blue) is docked in a hypothetical position similar to the one assumed by **1**. From the apparent positional similarity of **1** and **5** it can be deduced that the positive charged nitrogen as seen in **1** has an attractive effect while the negative charged carboxylate of **5** being in a similar position as the amine nitrogen in **1** induces strong repulsive effects.

Table 3.

Overview of the toxicological and pharmacological effects of amiodarone and the amiodarone analogues investigated. The graduation was as follows. For lactate dehydrogenase leakage: + = $p < 0.05$ at 100µmol/L, ++ = $p < 0.01$ at 100µmol/L and +++ = $p < 0.05$ at 10µmol/L. For adenalyte kinase release: + = $p < 0.05$ at 100µmol/L, ++ = $p < 0.01$ at 100µmol/L and +++ = $p < 0.05$ at 10µmol/L. For reductive capacity: + $p < 0.05$ at 100µmol/L, ++ = $p < 0.05$ at 100µmol/L and +++$p < 0.01$ at 100µmol/L. For mitochondrial membrane potential depolarization: + = $p < 0.05$ and ++ = $p < 0.01$ at 10µmol/L in HepG2 and A549 cell lines. For lipophilicity: + = logP <4.5, ++ = logP 4.5 − 6, +++ = logP >6. Abbreviations: AK, adenylate kinase; ROS, reactive oxygen species; MMP, mitochondrial membrane potential; ND, not determined.

Compound	LDH release (HepG2 cells)[1]	AK release (HepG2 cells)	Resazurin reduction (HepG2 cells)	AK release (A549 cells)	Resazurin reduction (A549 cells)	MMP depolari-zation	IC$_{50}$ hERG channels (µmol/L)
B2-O-CH$_2$CH$_2$-N-diethyl (amiodarone) (1)	++	+	0	+	0	0	0.22
B2-O-CH$_2$CH$_2$-NH-ethyl (2)	+++	+++	+	+++	++	+	0.38
B2-O-CH$_2$CH$_2$-NH$_2$ (3)	++	+++	++	+++	+	+	0.22
B2-O-CH$_2$CH$_2$-N-diisopropyl (4)	0	0	0	0	0	0	1.3
B2-O-CH$_2$-COOH (5)	+	+++	+	++	+	0	74
B2-O-CH$_2$CH$_2$-OH (6)	++	ND	ND	ND	ND	ND	216
B2-O-CH$_2$CH$_2$-NH-CO-CH$_2$CH$_3$ (7)	+	ND	ND	ND	ND	ND	8.4
B2-O-CH$_2$CH$_2$-N-pyrrolidine (8)	ND	++	+	+	0	0	0.05
B2-O-CH$_2$CH$_2$-N-piperidine (9)	ND	+	0	0	0	0	0.08
B2-O-CH$_2$CH$_3$ (10)	0	ND	ND	ND	ND	ND	n.a.[2]
B2-O-CH$_2$-COO-CH$_2$CH$_3$ (11)	ND	0	0	0	0	0	66

[1]obtained from Waldhauser et al.[126]

[2]n.a.: not accessible (no inhibition of hERG channels up to 100µmol/L, higher concentrations not soluble))

6.5. Discussion

The results of our studies demonstrate that cytotoxicity found for amiodarone and some of its analogues do not necessarily parallel their interaction with the hERG channel (see Table 3 for on overview of the results).

For both cell lines investigated, the desethylated amiodarone metabolites **2** and **3** were more toxic than amiodarone itself, a finding of potential clinical importance. Similar observations have been reported in previous studies for HepG2 cells [126] and also for alveolar and bronchiolar epithelial cells [136]. Since mono- and bis-desethylation of amiodarone are primarily performed by CYP3A4 [120, 137], co-administration of CYP3A4 inducers to patients treated with amiodarone may enhance its toxicity. However, clinical evidence for this hypothesis is lacking so far.

Our findings are in line with mitochondrial toxicity being associated with amiodarone and some of its metabolites or analogues. Several studies have already described hepatic mitochondrial toxicity of amiodarone and amiodarone metabolites or analogues *in vivo* [39] and *in vitro* [39-41, 43, 126]. Amiodarone and metabolites appear to target mitochondria also in other organs or cells than liver or hepatocytes, for instance in the lung [136, 138, 139] and in blood cells such as lymphocytes [140]. It is therefore not surprising that the toxic effects observed in our investigations were almost identical in HepG2 and A549 cells.

Pulmonary toxicity exerted by amiodarone is observed with a reported frequency of 5 to 10% for patients treated with this agent [99]. The clinical importance of this adverse drug reaction is given by the fact that morbidity is considerable (patients usually present with coughing and progressive dyspnoea) and may be lethal, if treatment is not stopped early enough. In comparison, symptomatic liver injury appears to be less frequent than pulmonary toxicity, with 1 to 3% of patients being affected [38].

The underlying mechanisms leading to organ damage in patients treated with amiodarone are not fully elucidated. Accumulation of phospholipids (phospholipidosis) occurs in most organs of patients or animals treated with this drug [141] and is considered to reflect impairment of phospholipid breakdown due to inhibition of lysosomal phospholipidases by amiodarone and/or its metabolites [142, 143]. Lipophilic, weak bases such as amiodarone and some of its basic metabolites or analogues are suited for lysosomal trapping [144] and can thereby lead to phospholipidosis. However, the long-term implications of phospholipidosis regarding liver and/or lung damage are not clear yet [144]. While phospholipidosis is a dose-dependent, general phenomenon, lung and liver damage occur only in a small fraction of patients treated with amiodarone, suggesting the necessity of individual risk factors for the manifestation of these adverse reactions.

Mitochondrial toxicity could well explain steatohepatitis observed in patients treated with amiodarone [38, 118], but it is rather difficult to explain the development of pulmonary fibrosis by this mechanism. In hamsters treated intratracheally with amiodarone, pulmonary fibrosis was observed already after 3 weeks of treatment and was preceded by mitochondrial damage (reduced activity of the respiratory chain) and increased expression of transforming growth factor (TGF)-β1 [139, 145]. Interestingly, vitamin E prophylaxis could prevent overexpression of TGF-β1 and subsequent pulmonary fibrosis but not mitochondrial damage. The possibility therefore exists that mitochondrial damage is one of the initial events, eventually associated with progression to pulmonary fibrosis. As observed for other drugs causing mitochondrial toxicity (e.g. valproic acid) [146], pre-existing mitochondrial damage could represent a risk factor organ toxicity. The existence of such risk factors may explain why only a fraction of the patients treated with amiodarone develops symptomatic adverse drug reactions.

Our study demonstrates that the interaction of amiodarone with the hERG channel is strongly favored by the presence of a basic nitrogen connected via a flexible linker to an aromatic moiety in the molecule. The basic nitrogen appears to be crucial for a tight interaction with the protein, since compounds lacking such a basic functionality such as B2-O-CH_2-COOH (**5**), B2-O-CH_2CH_2-OH (**6**), B2-O-CH_2CH_3 (**10**) or B2-O-CH_2-COO-CH_2CH_3 (**11**) displayed significantly higher IC_{50} values (range 66-216µmol/L) than compounds comprising a charged nitrogen (range 0.05-8.4µmol/L). Importantly, cellular toxicity of individual substances did not run in parallel with affinity for hERG channel, as clearly shown for B2-O-CH_2-COOH (**5**) that lacks a basic nitrogen but is highly cytotoxic. Furthermore, desalkylation of the basic nitrogen of amiodarone (**1**) is associated with increased cytotoxicity, but leaves the affinity of the metabolites for the hERG channel unchanged. Most interestingly, the basic piperidine derivative **9** revealed a low cytotoxicity but a very high affinity for the hERG channel (IC_{50} 0.08µmol/L). As also shown for the pyrrolidine derivative **8**, cyclization of the ethyl groups attached to the nitrogen in the side chain of amiodarone may increase the affinity to the hERG channel, but may decrease toxicity. Since metabolism of cyclic compounds *in vivo* may not be associated with the production of N-desalkylated compounds, it can be speculated that such molecules may also *in vivo* be less toxic than amiodarone, but with maintained or even improved antiarrhythmic activity compared to amiodarone.

In conclusion, we can provide quantitative cytotoxicity data for amiodarone, some of its key metabolites that were obtained in hepatic and pulmonary cell lines and several analogues. The affinity of these compounds to the hERG channel critically depends on the presence of a positively ionizable nitrogen in their side chain. Since cytotoxicity and affinity to the hERG channel were not correlated, our results suggest the possibility to develop amiodarone analogues with possibly retained pharmacological activity but decreased toxicity.

Acknowledgements

7. Mitochondrial defects do not predispose dermal fibroblasts to increased toxicity associated with simvastatin or benzbromarone

Katri Maria Waldhauser, Stephan Krähenbühl

Division of Clinical Pharmacology & Toxicology and Department of Research, University Hospital Basel, Switzerland

7.1. Abstract

The unexpected occurrence of an idiosyncratic drug reaction (IDR) during late clinical trials or after a drug has been released can lead to a severe restriction in its use or failure to release/withdrawal. Several attempts have been made to try to predict the potential of drugs to cause such reactions. Since evidence has been gathered that an underlying mitochondrial dysfunction can be the cause of unexpected drug toxicity, we aimed to prove this hypothesis by testing known mitochondrial toxins simvastatin and benzbromarone on dermal fibroblasts from patients suffering from a mitochondrial defect. Comparing these cells with dermal fibroblasts from healthy patients, we discovered that, although dose-dependent, the overall toxicity after a treatment with simvastatin or benzbromarone was not superior, as expected. The test we used was the lactate dehydrogenase (LDH) test. As measured with the formazan formation (MTT) test, the metabolic acitivity of the cells was reduced at high concentrations of simvastatin and benzbromarone. The results between the cell lines were similar. The reactive species (ROS) formation increased time-dependently after simvastatin or benzbromarone treatment in all cell lines but did not differ between them. As a conclusion, we could not affirm the hypothesis of a mitochondrial defect leading to increased unexpected drug toxicity in this cell line. Further examinations with a test system of a better suitability have to be considered.

7.2. Introduction

A drug-caused idiosyncratic adverse reaction (IDR) is non-predictable and can be caused by many different mechanisms, involving immuno-mediated toxicity or abnormalities in biochemical pathways. The common factor combining these mechanisms is that they do not involve the pharmacological effect of the drug [147]. IDRs are rare but when occurring, a remarkable problem that affects the pharmaceutical industry causing unexpected market withdrawals, as an example cerivastatin [148]. Since the IDRs can not be predicted in preclinical or clinical trials there is a great interest in finding the underlying mechanism behind them [149].

Simvastatin belongs to hydroxymethyl glutaryl coenzyme A (HMG-CoA) reductase inhibitors being highly effective in reducing serum cholesterol and low-density lipoprotein cholesterol levels. HMG-CoA reductase inhibitors do not only affect hypercholesterolemia, but also reduce the risk for coronary heart diseases. In overall, statins are considered to be exceptionally safe, but some patients treated with statins suffer under mild, dose-dependent muscle symptoms [150]. The most serious adverse effect associated with the statin therapy is myopathy progressing sometimes to fatal or non-fatal rhabdomyolysis [148, 151, 152]. Several attempts have been made to explain the muscle toxicity of statins. Since statins inhibit the formation of mevalonate (precursor of cholesterol) leading to an impaired formation of ubiquinone, dolichol and other isoprenoids, there are suggestions that the myotoxicity could be caused by the lack or reduced cellular concentration of these substances [153, 154]. As an example, ubiquinone is part of the mitochondrial electron transportation chain, and the inhibition of its biosynthesis leads to reduced production of ATP in the cells. This has been confirmed for simvastatin *in vivo* [155]. In an *in vitro* study of Flint et al. was observed, that the toxicity of statins on muscle cells was decreased by the addition of mevalonate [156], a fact that could not be confirmed in L6 cells in our own study [157]. There are suggestions that an underlying mitochondrial disease (MELAS syndrome) may be an important factor leading to a sudden rhabdomyolysis after a treatment with simvastatin [158]. Light microscopic changes observed in muscle biopsies of patients with statin-associated myopathy were similar to the findings in patients with mitochondrial myopathies [59, 60, 159, 160]. There is evidence about biochemical and/or genetic abnormalities of proteins or genes involved in skeletal muscle energy metabolism in more than 50% of patients associated with myopathy caused by statins [161].

Simvastatin has been shown to inhibit complex I of the electron transport chain and to interfere with mitochondrial calcium homeostasis [162]. Latest *in vitro* studies indicate that lipophilic statins cerivastatin, fluvastatin, simvastatin and atorvastatin are mitochondrial toxins causing apoptosis or necrosis of rat skeletal muscle cells, a fact that could explain myotoxicity [157].

Benzbromarone is a uricosuric agent that reduces the proximal tubular reabsorption of uric acid [163]. Benzbromarone has been associated with hepatic injury. Its hepatotoxic effect can at least partly be explained by its ability to cause mitochondrial toxicity [43].

Lately, mitochondria have been recognized to play an important role in hepatotoxic processes [164]. Mitochondria contain several metabolic pathways responsible for the cellular energy production that makes them a vulnerable target for drug-induced toxicity [165]. One of the newest attempts to explain an idiosyncratic drug reaction involves the mitochondrial abnormalities as a predisposing factor for sudden drug toxicity [9]. This explanation is supported by the fact that many of the drugs that have been implicated to have caused an IDR can impair mitochondrial function. Evidence has been gathered in an *in vivo* study with $Sod2^{+/-}$ mice (an animal model with a defect in the mitochondrial superoxide dismutase 2 protein encoding detoxication of radicals). These mice developed increased mitochondrial damage in comparison to wild-type mice after a long-term treatment with low doses of nimesulide, a COX-2 inhibitor associated with IDR [166].

To provide further evidence for this hypothesis, we studied the overall toxicity of different concentrations of simvastatin and benzbromarone on dermal fibroblasts obtained from patients suffering under a mitochondrial disease [ST cells: An intensive defect on very long chain acyl-CoA dehydrogenase (VLCAD), BL cells: a defect in carnitine palmitoyltransferase 1 (CPT1)] in comparison to dermal fibroblasts obtained from healthy patients (control I and II cell lines). Furthermore, we examined the production of reactive oxygen species after a treatment with simvastatin and benzbromarone.

7.3. Materials and methods

7.3.1. Reagents

All chemicals were purchased from Sigma-Aldrich (Buchs, Switzerland) and were of best quality available when not otherwise stated. Simvastatin lactone was converted into its active form as described earlier [167]. All cell culture media, all supplements and fetal calf serum were from Gibco (Paisley, UK). The 96-well-plates and the 12-well-plates were purchased from Beckton Dickinson (Franklin Lakes, NJ, USA).

7.3.2. Cell culture

The control human fibroblast cell lines I and II from biopsies of healthy patients were a generous gift from Friedel Wenzel from the Department for Medical Genetics (University Children's Hospital Basel). The fibroblast cell line with a defect in VLCAD and the fibroblast cell line with the defect in Cpt1 were received from diagnosed patients from the University Hospital

Zurich. Fibroblasts were cultured in Dulbecco's modified Eagle's medium (with 2mmol/L GlutaMAX®, 1.0g/L glucose and sodium bicarbonate) supplemented with 10% (v/v) inactivated fetal calf serum, 10mM HEPES buffer, pH 7.2, 100U/mL penicillin/streptomycin and non-essential amino acids. Fibroblasts were seeded on a 96-well-plate in a density of 5000 cells/well one day before the experiment was started. Approx. 6 hours prior to the start of the incubation with the test substances and during the incubation and the experiment, a starvation medium containing no glucose or FCS but 5µmol/L BSA-Na-palmitate was used to force the cells to undergo fatty acid metabolism.

7.3.3. Cell viability

The enzymatic activity of lactate dehydrogenase (LDH) in the medium was measured spectrophotometrically at λ340 nm after the method of Vassault et al. [69]. LDH catalyses the oxidation of NADH during the pyruvate-lactate transformation. LDH leakage from the cells treated for 24 hours with the test compounds was compared to the LDH leakage of cells lysed with the detergent Triton X-100 (0.8% w/v). The activity in the supernatant of lysed cells was set at 100%.

7.3.4. Colorimetric tetrazolium measurement (MTT assay)

The metabolic activity of the fibroblasts was measured after the method of Mosmann et al. [168]. After an incubation time of 12 or 24 hours with simvastatin or benzbromarone, sterile filtered MTT (3-(4,5-dimethylthiazol-2-yl)-2,5-diphenyl tetrazolium bromide, 5mg/mL dissolved in PBS) was added to the cells in a final concentration of 10%. MTT is metabolised by living cells resulting in the formation of blue formazan. After 4 hours, the medium was removed and 200µL 1% SDS was added to solubilise the cells. The plates were shaked for 20 minutes after which the colour intensity reflecting cell growth condition was determined by reading optical densities at 550nm (L1) and at 620nm (L2) spectrophotometrically (Spectrophotometer: SofMAXPro 4.5).

7.3.5. Measurement of reactive oxygen species (ROS)

Confluent cultures of fibroblasts were simultaneously exposed to test compounds and to dichlorofluorescine diacetate (DCFH-DA) dissolved in ethanol (final concentration 5µmol/L) and incubated for 24, 48 and 72 hours [169]. The fluorescence was measured using a microtiter plate reader (HTS 700 Plus Bio Assay Reader, Perkin Elmer, Buckinhamshire, UK) in incubations containing cells and exposure medium at an excitation wavelength of 485nm and an emission wavelength of 535nm.

7.4. Results

7.4.1. LDH leakage from the cells

LDH leaks to the supernatant from the cells when the cell membrane integrity is disturbed. In simvastatin treated cells, the absorbance measured and compared to the 1% DMSO treated cells was significant for both control I and II cells and for the ST and BL cells at concentrations 100 and 200µmol/L, as well as at 1mmol/L. There were no differences in the toxicity pattern between the cell lines (Fig.1).
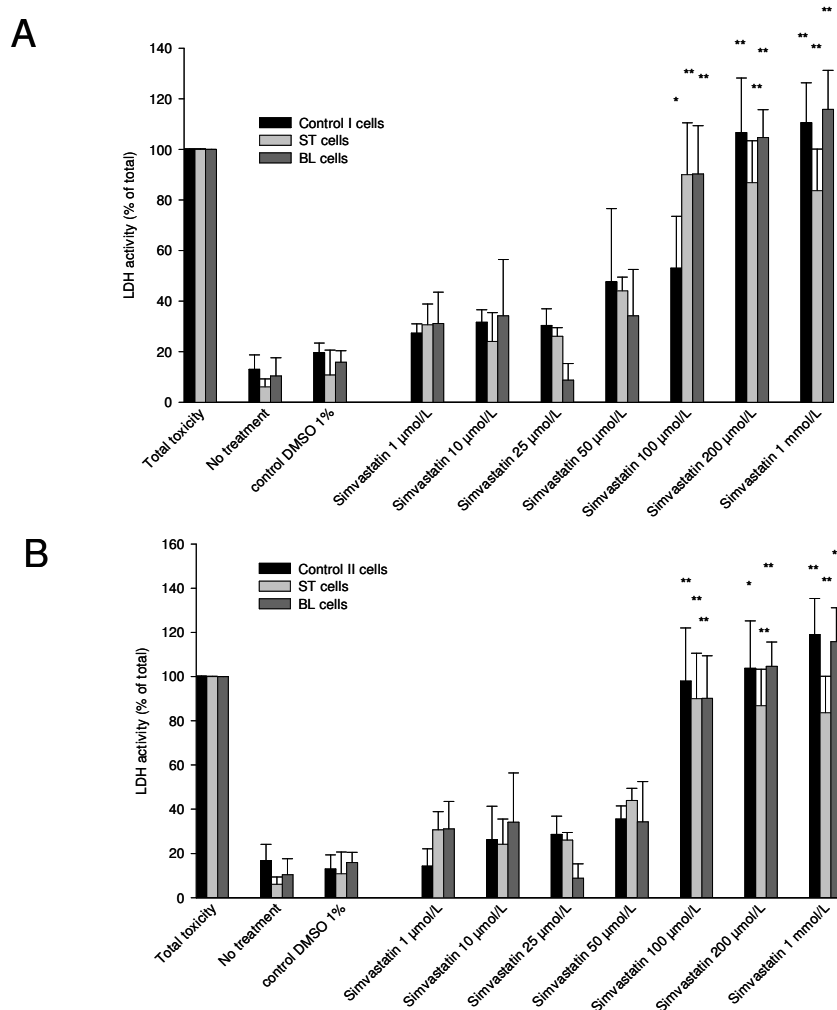
Figure 1. *LDH leakage from fibroblasts after a 24-hour treatment with simvastatin.* (A) ST and BL cells in comparison to control I cells. (B) ST and BL cells in comparison to control II cells. Data are presented as mean ± SEM of at least five independent experiments. *p<0.05 versus 1% DMSO within the cell line, **p<0.01 versus 1% DMSO within the cell line.

As shown in figure 2, after 24 hours, benzbromarone did not show significant toxicity towards the control I cells. For control II cells as well as for the ST and BL cells, the highest concentrations 50 and 100µmol/L caused a significant leakage of LDH into the cytoplasm.

A

B
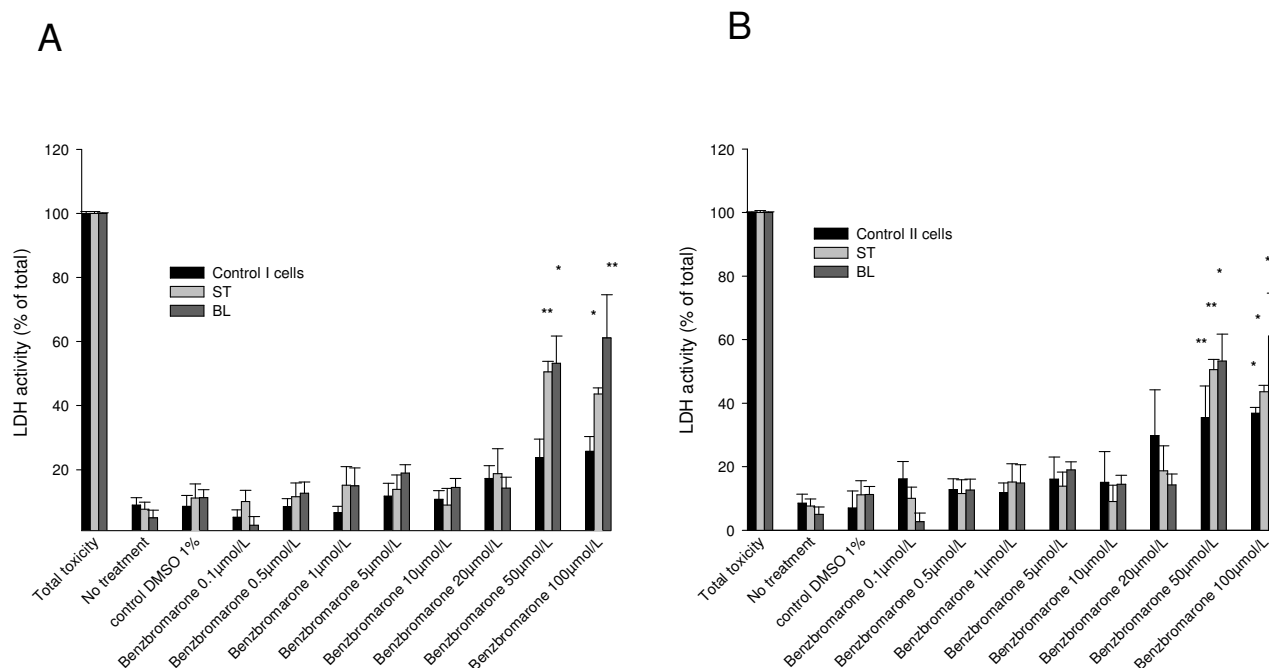
Figure 2. *LDH leakage from fibroblasts after a 24-hour treatment with benzbromarone.* (A) ST and BL cells in comparison to control I cells. (B) ST and BL cells in comparison to control II cells. Data are presented as mean ± SEM of at least four independent experiments. *p<0.05 versus 1% DMSO within the cell line, **p<0.01 versus 1% DMSO within the cell line.

7.4.2. Metabolic activity of the cells

Metabolically active cells are able to convert the MTT dye from its yellow water-soluble tetrazolium salt to its water-insoluble dark blue formazan by reductive cleavage of its tetrazolium ring [168, 170]. The cellular mechanisms involved in this reaction are not completely understood but there are suggestions of the participation of the mitochondrial succinate dehydrogenase system [171]. After 24 hours and for all cell lines, a significant reduction of the formazan formation was measured in the incubations containing 100 and 200µmol/L and 1mmol/L simvastatin (Table 1).

<u>Table 1</u>. *Formazan formation in simvastatin treated fibroblasts.* MTT is converted to blue formazan when incubated with metabolically active cells. 100 and 200 µmol/L, and 1mmol/L simvastatin inhibited the cells significantly from their metabolic activity after 24 hours of treatment. Results are shown as mean ± SEM of at least 4 independent measurements.

	Formazan formation after a 24-hour treatment with simvastatin (in % of control)			
	Control I cells	**Control II cells**	**ST cells**	**BL cells**
No treatment	115 ± 4.7	97 ± 10.7	16 ± 8.7	92 ± 11.7
control DMSO 1%	100 ± 0.0	100 ± 0.0	100 ± 0.0	100 ± 0.0
Simvastatin 1µmol/L	118 ± 1.1	106 ± 12.3	125 ± 10.6	101 ± 10.2
Simvastatin 10µmol/L	124 ± 3.3	115 ± 12.8	122 ± 10.5	121 ± 14.6
Simvastatin 25µmol/L	120 ± 5.3	115 ± 10.2	115 ± 8.6	105 ± 12.6
Simvastatin 50µmol/L	111 ± 8.5	88 ± 14.0	86 ± 14.16	96 ± 6.74
Simvastatin 100µmol/L	51 ± 12.2 *	40 ± 2.8 **	38 ± 9.2 *	47 ± 7.6 *
Simvastatin 200µmol/L	35 ± 1.9 **	36 ± 6.6 **	39 ± 6.4 *	30 ± 6.5 **
Simvastatin 1mmol/L	33 ± 8.1 **	32 ± 4.4 **	38 ± 7.4 *	32 ± 9.1 **

As seen in Table 2, simvastatin treatment for 48 hours resulted in a reduced metabolic activity in cells treated with concentrations higher then 50 µmol/L. This reduction was significant for 100 µmol/L simvastatin in control II and BL cells and in all cell lines for 200 µmol/L and 1 mmol/L.

Table 2. *Effects of different concentrations of simvastatin on the formazan formation from MTT in dermal fibroblasts after an incubation time of 48 hours.* The reduction of the metabolic activity of the cells remained but was significant at a concentration of 50 µmol/L for only control II and ST cells and at a concentration of 100 µmol/L and 1 mmol/L for all cell lines. Means ± SEM of at least 4 independent measurements.

	Formazan formation after a 48-hour treatment with simvastatin (in % of control)			
	Control I cells	**Control II cells**	**ST cells**	**BL cells**
No treatment	115 ± 10.5	123 ± 8.2	137 ± 12.8	130 ± 29.4
control DMSO 1%	100 ± 0.0	100 ± 0.0	100 ± 0.0	100 ± 0.0
Simvastatin 1µmol/	94 ± 15.1	123 ± 7.5	109 ± 5.2	123 ± 17.5
Simvastatin 10µmol/L	104 ± 12.8	111 ± 8.0	113 ± 10.3	97 ± 16.3
Simvastatin 25µmol/L	85 ± 11.4	111 ± 28.0	80 ± 5.8	125 ± 22.0
Simvastatin 50µmol/L	73 ± 7.0	94 ± 9.2	70 ± 3.8	46 ± 9.5
Simvastatin 100µmol/L	47 ± 13.0	52 ± 12.0 *	46 ± 9.4 *	35 ± 6.6
Simvastatin 200µmol/L	51 ± 7.6 *	26 ± 6.3 *	48 ± 10.6 *	25 ± 6.8 *
Simvastatin 1mmol/L	54 ± 14.6 *	38 ± 5.6 *	34 ± 5.0 **	29 ± 7.4 *

Treatment of the fibroblasts with different concentrations of benzbromarone resulted in no significant reduction of the formazan formation after 24 hours of incubation, although a colour change could be observed for the highest concentration (50µmol/L, Table 3). After 48 hours, no significant changes could be observed, either (results not shown).

Table 3. *The colour change from blue to red after a 24-hour-incubation with benzbromarone.* There was a detectable but not statistically significant color change in the wells with 50µmol/L benzbromarone –treated fibroblasts. The results represent means ± SEM of at least 4 independent measurements.

	Formazan formation after a 24-hour treatment with benzbromarone (in % of control)			
	Control I cells	Control II cells	ST cells	BL cells
No treatment	103 ± 6.0	95 ± 4.8	98 ± 2.8	104 ± 3.9
control DMSO 1%	100 ± 0.0	100 ± 0.0	100 ± 0.0	100 ± 0.0
Benzbromarone 0.1µmol/	104 ± 6.7	102 ± 6.1	127 ± 31.8	118 ± 14.4
Benzbromarone 0.5µmol/L	111 ± 3.9	103 ± 8.3	99 ± 5.2	106 ± 5.1
Benzbromarone 1.0µmol/L	102 ± 6.7	115 ± 6.3	99 ± 4.4	100 ± 8.5
Benzbromarone 5µmol/L	119 ± 1.7	128 ± 6.9	113 ± 9.4	124 ± 3.9
Benzbromarone 10µmol/L	130 ± 9.5	132 ± 11.6	111 ± 10.2	151 ± 6.1
Benzbromarone 20µmol/L	135 ± 10.3	137 ± 26.6	132 ± 2.2	141 ± 24.4
Benzbromarone 50µmol/L	69 ± 19.7	70 ± 17.7	51 ± 18.4	61 ± 30.7

7.4.3. ROS formation

Under certain conditions, mitochondria can produce ROS. This happens especially when the electron transportation is uncoupled from the production of ATP in the respiratory chain located in the inner mitochondrial membrane [172]. Since ROS production is claimed to play an important role in the mitochondrial mediated cell death, and since both benzbromarone and simvastatin have been shown to impair the mitochondrial oxidative metabolism [43] [157], the ROS production resulting from the treatment with the test substances was assayed. Especially benzbromarone's uncoupling properties in liver mitochondria refer to an increased electron leakage from the respiratory chain that can lead to increased ROS production

As the figures 3 and 4 show, in all cell lines, a 24-hour incubation with simvastatin did not result in significant ROS production. The ROS production in the control I and BL cell lines caused by a 48-hour simvastatin treatment was not statistically significant in comparison to the control 1% DMSO treated cells even at the highest concentration. In ST cells, 200µmol/L and 1mmol/L simvastatin caused a significant reactice oxygen species formation in comparison to the control treated cells. Surprisingly, also the fluorescence measured for 200µmol/L and 1mmol/L simvastatin in the control II cell line was statistically different in comparison to the control 1% DMSO treated cells. The 72-hour incubation resulted in a significant ROS production only at the highest simvastatin concentration for control I cells. For the other cell lines cells, 200µmol/L and 1mmol/L simvastatin caused a significant increase of the ROS production in comparison to the control 1% DMSO treated fibroblasts. The pattern showing an increased ROS production during the incremental time course was for all cell lines the same.

A

B
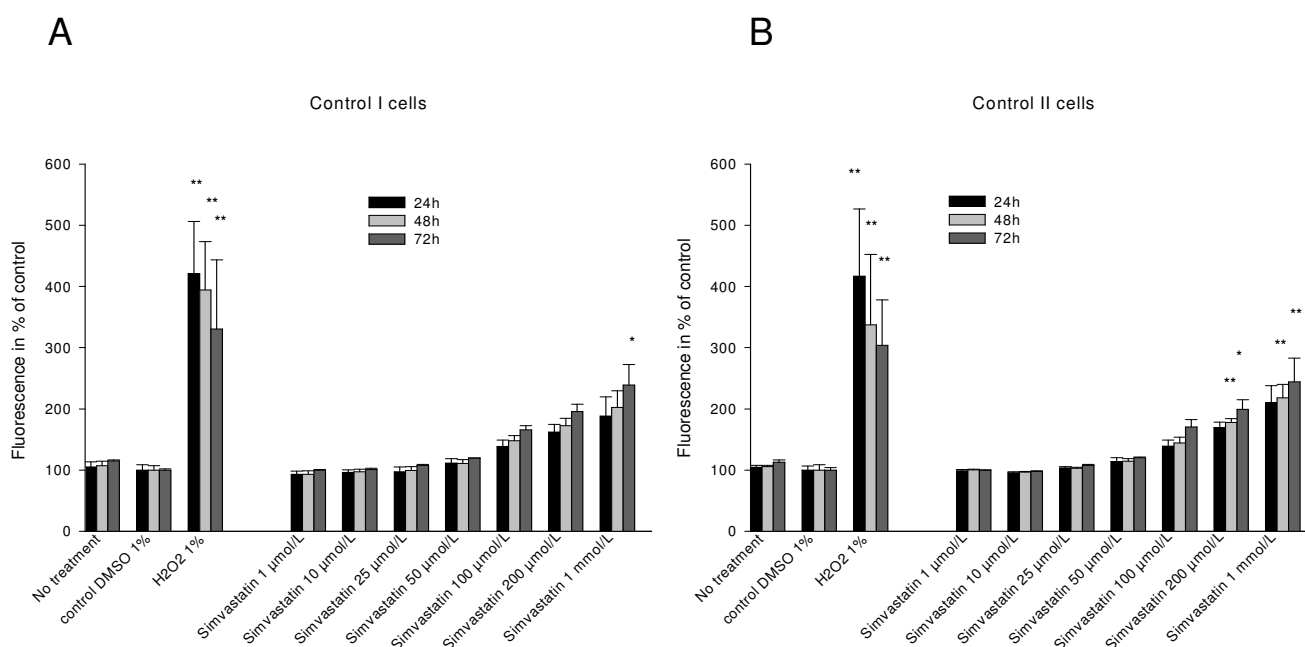
Figure 3. *ROS production in dermal fibroblast control cell lines I and II after a treatment with simvastatin.* The reactive oxygen species formation in simvastatin treated control I cells in comparison to control 1% DMSO treated cells was significant for 1mmol/L after 72 hours of treatment (see panel A). As illustrated in panel B, ROS formation in control II fibroblast cell line increased time-dependently and was statistically significant for 200µmol/L and 1mmol/L simvastatin after 48 hours incubation. The results represent means ± SEM of at least 3 independent measurements in triplicate.

A
B
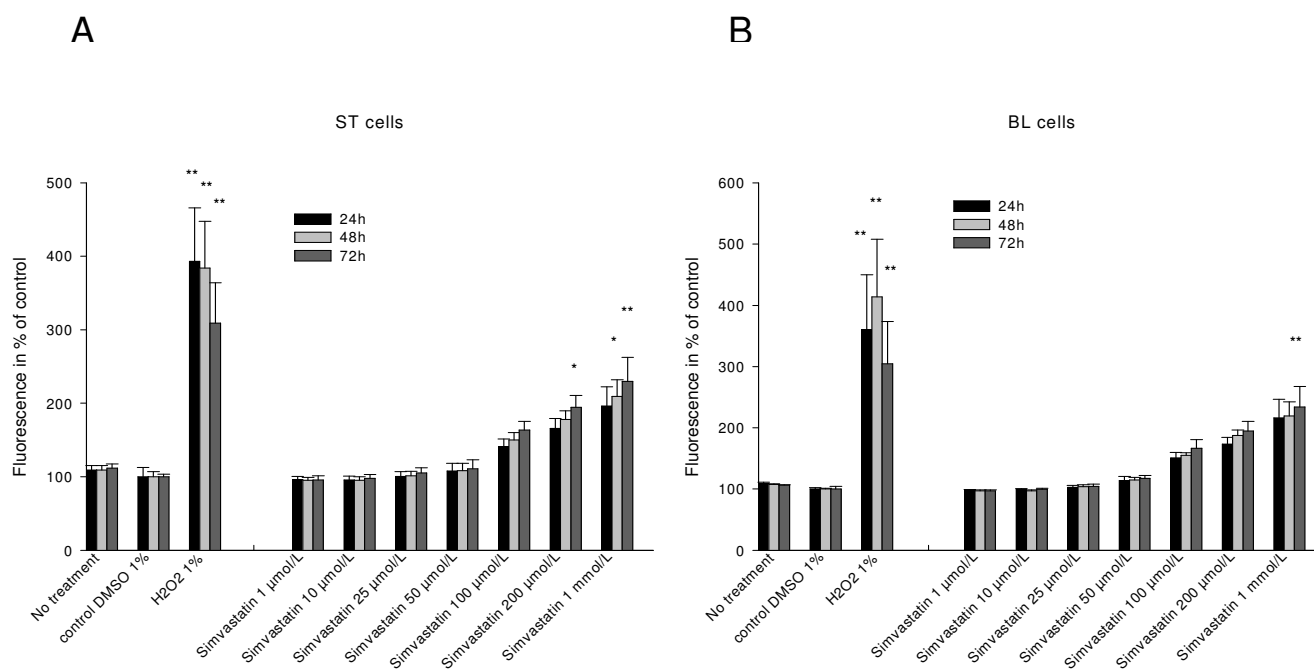
Figure 4. *ROS production in ST and BL cell lines (simvastatin treatment).* After 48 hours, the 1mmol/L simvastatin concentration caused a significant increase of the fluorescence measured in ST cells (panel A) in comparison to 1% DMSO. The 72-hour incubation resulted in a significant fluorescence for 200µmol/L and 1mmol/L simvastatin treated ST cells. For BL cells (panel B), the fluorescence measured increased during the time course but was statistically significant only for the highest simvastatin concentration (1mmol/L) after a 72-hour incubation. Means ± SEM of at least 3 independent measurements in triplicate.

The benzbromarone treatment in control I cells did not cause a remarkable increase in the production of ROS. Still, at the highest concentration (100µmol/L) benzbromarone, the measured fluorescence was statistically different in comparison to control 1% DMSO treatment. In control II cells, ROS production was statistically significant for the highest concentration benzbromarone already after 24 hours. These results are shown in figure 5.

A

B
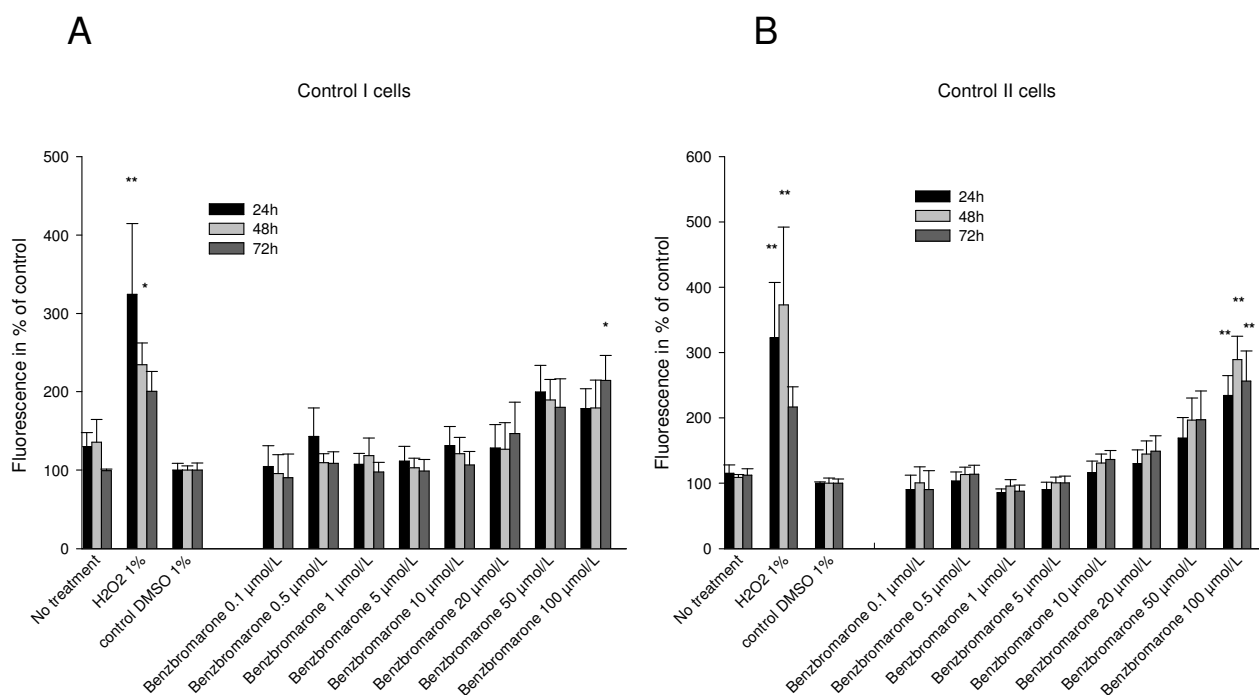
Figure 5. *Production of ROS in benzbromarone-treated control I and II cells.* In control I cells (panel A), only the highest concentration benzbromarone (100µmol/L) caused a statistically significant ROS formation in comparison to control 1% DMSO that was observed after 72 hours whereas for control II cells (see panel B), this concentration was significant already after 24 hours of incubation. Means ± SEM of at least 3 independent measurements in triplicate.

Benzbromarone-treated ST and BL cells did not produce more ROS than the control cell lines (figure 6). ST cells showed no significant increase of ROS production in comparison to control 1% DMSO treatment and BL cells only at the highest concentration (100µmol/L) after 48 hours of treatment.

A

B
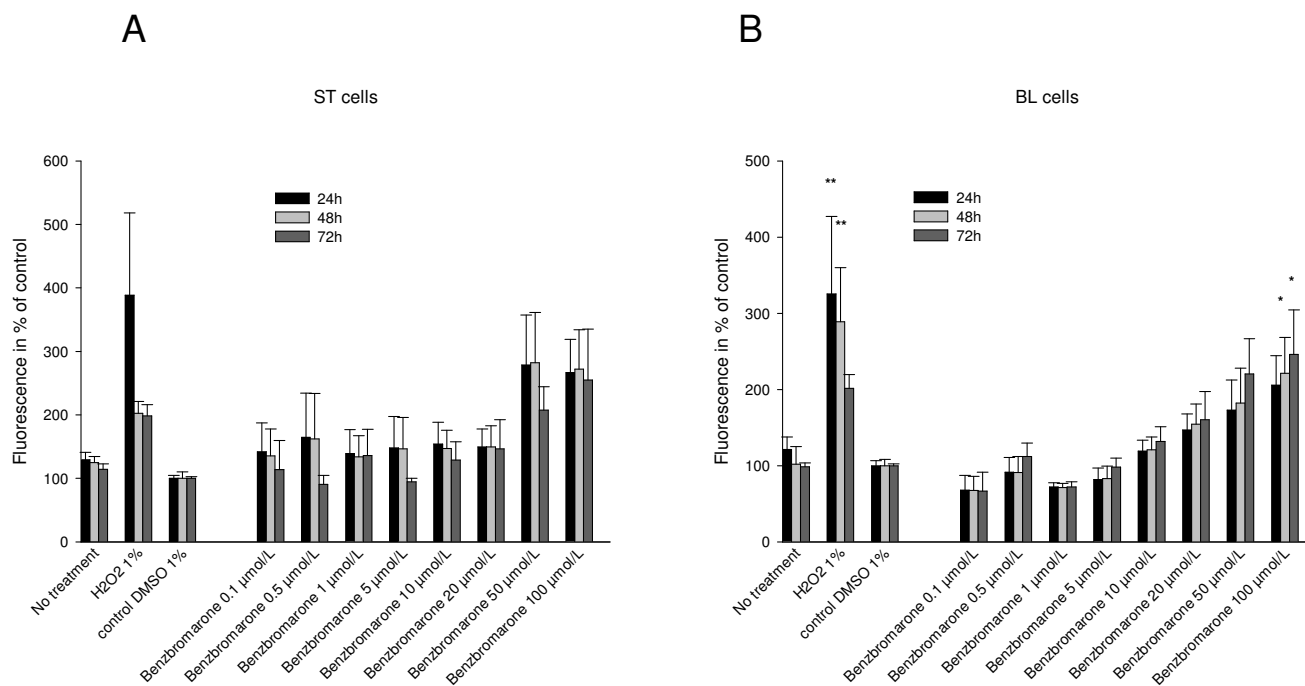
Figure 6. *ROS production in benzbromarone-treated ST and BL cells (benzbromarone treatment).* As shown in panel A, benzbromarone did not cause significant production of ROS even after 72 hours in ST cells. In BL cells, 100 µmol/L benzbromarone was significant after 48 hours. The results represent means of at least 3 independent measurements in triplicate.

7.5. Discussion

Our aim was to study the human dermal fibroblasts with mitochondrial defects in Cpt1 and VLCAD in respect for their possibly increased sensitivity towards mitochondrial toxins simvastatin and benzbromarone in comparison to "healthy" human dermal fibroblasts. Our interest was the overall toxicity of the compounds and the redox state of the cells, since both substances are mitochondrial toxins that inhibit the mitochondrial respiratory chain and therefore increase the production of reactive oxygen species in the cells [43, 157]. We found, that the administration of simvastatin and benzbromarone increased oxidative stress dose-dependently in all cell lines. Since this increase was similar in all cell lines it did not refer to an increased sensitivity of the fibroblasts suffering from the mitochondrial defect.

The reactive oxygen species formation in the simvastatin treated cells started at the concentration 25µmol/L and was rising, for all cell lines. The tendency for an increased ROS production in the benzbromarone-treated cells started at 5µmol/L and was rising, although this increase was less obvious in the control I and ST cell lines. This was before the toxicity (for all cell lines) was shown in LDH or MTT test referring to the fact that the toxicity could partly be caused by the increased radical production in the cells.

The toxic effects of simvastatin and benzbromarone in human dermal fibroblast cell lines measured with LDH and MTT assays were roughly comparable with each other referring to the fact that at least the 3 highest concentrations simvastatin and benzbromarone cause toxicity towards human dermal fibroblasts. The MTT assay seemed to be less sensitive than the LDH assay. This can be explained by the fact that the enzyme lactate dehydrogenase is actively leaking to the cytoplasm already at lower concentrations whereas the succinate dehydrogenase system can still be able to convert MTT into its spectophotometrically detectable form [171].

VLDAC and Cpt1 deficiencies are so-called inherited fatty acid oxidation (FAO) disorders. FAO is essential for the energy supply in situations that require glucose sparing, for example during major exercise or fasting. The first and rate-limiting step leading to mitochondrial β-oxidation of very long chain fatty acids with chain lengths C14-C20 is catalyzed by the VLCAD enzyme. Long-chain fatty acids are imported from the outer mitochondrial membrane into the mitochondrial matrix by the carnitine palmitoyltransferase (Cpt) system that consists of two distinguished proteins Cpt1 and Cpt2. Cpt1 in the outer mitochondrial membrane catalyzes the formation of acylcarnitine from carnitine and acyl-CoA and Cpt2 in the inner mitochondrial membrane the formation of acyl-CoA from acylcarnitine and CoA [152]. There are two tissue-specific types of Cpt1 isoforms, the so-called muscle and liver Cpt1:s [173, 174]. The liver type Cpt1 is expressed in fibroblasts [175] but not in skeletal muscle [176]. This can be the reason

why simvastatins muscle toxicity did not become apparent in dermal fibroblasts with the defect in the liver type Cpt1.

Phillips et al. [59] reported from four patients receiving statin therapy that developed myopathy without elevated creatine kinase levels. Muscle biopsies of these patients showed evidence of mitochondrial dysfunction including ragged red fibers and increased lipid stores. The histochemical studies suggested a defect in mitochondrial respiratory chain function. This assumption is only hypothetical, other suggestions include among others the effect of the cholesterol reduction in biological membranes [177-179] during statin therapy or the role of mevalonate inhibition by the statins leading to decreased synthesis of ubiquinone (coenzyme Q10) that is an antioxidant and a membrane stabilizer and is used in the electron transport chain [180]. In a study of Laaksonen et al. [181] was reported that simvastatin treatment did not lead to decreased ubiquinone concentration in comparison to placebo treated control patients as well as in another study of Blake et al. [182] about pravastatins and atorvastatins decreasing effects on ubiquinone levels after a 4-week-therapy. It is apparent that there are a lot of questions that have not yet been answered about the mechanisms behind the statin-caused myotoxicity.

Mitochondria in different cells differ in structure and function and the mitochondrial DNA (mtDNA) is very complex [1]. The unexpected toxic effects of simvastatin and benzbromaron affect muscle and liver tissue, respectively. In our study, we tried to re-establish this toxicity in dermal fibroblasts received from patient biopsies. The toxicity observed in our experiments was not higher in the fibroblasts suffering from mitochondrial defects than in control fibroblasts. Among other assumptions, this leads us to hesitate if the test system chosen for these studies was sensitive enough to re-establish the toxicity. It is possible, that fibroblasts are able to survive mitochondrial distraction by using other pathways as a source of energy, such as glycolysis.

As previously mentioned, the mitochondrial defect leading to unexpected myotoxicity or hepatotoxicity is not established. Therefore, more research has to be done to reveal the mitochondrial conditions of the patients suffering from sudden and unexpected toxic drug reactions.

8. Conclusions and Outlook

Understanding mitochondrial functions is important for the pharmacological and especially toxicological aspects in drug development. Mitochondria play an important role in cell survival and maintenance of cellular homeostasis and, at the same time, in triggering cell death [1]. Therefore, the mitochondrial involvement in the most drug adverse reactions is unevitable. A cascade of transactions leading to the apoptosis or necrosis of a cell takes place in mitochondria, affecting numerous biochemical events in the cell. A pivotal role here plays the loss of the integrity of the outer mitochondrial membrane. There are at least two ways to provoke it, depending on the cell type: First of all, the Bcl-2 family-regulated MOMP and secondly, the Ca^{2+}- and/or ROS-regulated mPT. Depending on the number of mitochondria affected, the cell concerned either survives or dies. Drugs can affect the mitochondrial mechanisms in many ways. As discussed in this thesis, the mitochondria can be impaired by several ways, e.g. by inhibition of the electron transport chain, uncoupling of the oxidative phosphorylation, affection of the mitochondrial permeability, inhibition of the fatty acid metabolism or mitochondrial DNA synthesis, or by oxidation of the mtDNA.

The main focus of this thesis considers amiodarone, an efficient antiarrhytmic agent with several side effects, possibly caused by the mechanism of mitochondrial toxicity [41, 43, 126]. Amiodarone is a representative example of a drug that can cause serious problems for a patient, beneath its valuable pharmacological effect. Many drugs have to be withdrawn form the market because of their side effects, that are discovered only after continuous use, as an example benzbromarone [183].

Chemical structure of a compound builds up the basics for the development of a new drug. Since pharmacological and toxicological forecasts can be made by comparing the chemical structures of new substances with known compounds, it is important to study the structure-effect-relationship of a new molecule. New *in silico* approaches make these forecasts easier, although there is no such thing as a model that matches the physiological reality perfectly. When studying the physiological environment of a protein, there are numerous factors to be considered, among others its stereotypical configuration. Since new drug molecules tend to be complicated in their structure it is almost impossible to avoid missing a position or a twisted ancle that already changes the relationship between the target and the substrate. New programmes are developed that match the requirements even better but the question remains if these are as confidential as needed. In this thesis, certain conclusions can be made considering amiodarone's structure-(toxic) effect-relationship. In the first study, where the investigated derivatives and amiodarone were studied more in detail, large differences in mitochondrial toxicity and inhibition of hERG channels were observed, despite similar lipophilicity profiles. This fact led us to assume, that the functional groups attached to the side chain of B2 were decisive

for the effects, not the lipophilic properties, a fact that maybe helps in the future development of antiarrhytmic drugs. In the second study considering amiodarone, it was ascertained, that the pulmonary toxicity of amiodarone is similar to the hepatic toxicity, and that the loss of the nitrogen in the side chain of amiodarone molecule decreases the affinity to the hERG channel, whereas cyclisation of the alkyl groups attached to this nitrogen renders the substances less toxic with a small drop in the affinity to the hERG channel.

The test system we chose for studying the pharmacologic effect of amiodarone and its derivatives, the inhibition of hERG channels, is associated with prolongation of the refractoriness of cardiac tissue and QT prolongation, which results in an antiarrhythmic (class III) activity [94]. However, a reduction in hERG currents due to either genetic defects or adverse drug effects can lead to hereditary or acquired long QT syndromes characterized by action potential prolongation, lengthening of the QT interval on the surface ECG, and an increased risk for "torsade de pointes" arrhythmias and sudden death [125]. This undesirable side effect of non-antiarrhythmic compounds has prompted the withdrawal of several blockbuster drugs from the market. Studies on the properties of the high-affinity drug binding site in hERG and its interaction with drug molecules have provided the basis for more refined approaches in drug design, safety pharmacology and *in silico* modelling [184]. It is important, though, to keep in mind, that the hERG current blockade is recognized not only as class III antiarrhytmic characteristics but also as a severe side effect of drugs.

The IDRs build up a very specific part of all drug adverse effects reported. The most difficult fact considering them is their unpredictability. Since the mechanisms behind these severe side effects are not completely understood, it is mostly not possible to detect them before a drug is introduced to the market. A great interest in studying this mechanism was our driving force when testing our hypothesis of an underlying mitochondrial defect behind the IDRs. Although evidence about the mitochondria involving the emergence of an IDR is already established [9], it is not an easy task to find a proper test system suitable for the studies. In our studies, there was no connection between a mitochondrial defect in VLCAD or in Cpt1 and the increased toxicity caused by benzbromarone and simvastatin in dermal fibroblasts. Therefore, we can not offer any further explanations considering this relationship but the assumptions, that our test system was not the right one. Since both simvastatin and benzbromarone did not have as intense an effect on dermal fibroblasts as on muscle or hepatic cells [43, 157], respectively, it can be supposed, that fibroblasts possess properties that help them defeat the toxicity. Unfortunately, we have to admit not bringing any further explanations considering the IDRs, then our speculations about mitochondrial defects behind these unwanted effects.

There are suggestions that IDRs are due to reactive metabolites of the drug involved. However, many drugs that form reactive metabolites have not been associated with IDRs. Drugs that cause some degree of cell stress or damage may be more likely to lead to a high incidence of IDRs. However, a screen of the effects of drugs known to be associated with an

IDR using expression genomics and proteomics may reveal a pattern of mRNA and protein expression that predict which drug will cause a high incidence of an IDR. IDRs are difficult to detect in vivo because they are just as idiosyncratic in animals as they are in humans. If the expression of certain proteins in animals treated with a drug candidate could be used as a screening method to predict a drug's potential to cause a high incidence of idiosyncratic drug reactions, it would greatly facilitate the development of safer drugs [185].

Toxicity of drugs still remains a problem to be defeated, although numerous researchers focus on finding the mechanisms behind them and the suitable test system to discover them. This thesis sheds some light in the trials of replacing amiodarone with a similarly effective but less toxic compound. Hopes are rising, that, some day, these findings lead to the development of possibly safer antiarrhytmic drugs. It could, though, not bring any further evidence in the relationship between unexpected drug adverse reations and mitochondrial abnormalities. Further studies in this field have to be conducted to reveal the cellular events leading to non-predictable toxicity of drugs.

9. References

1.   Scheffler, I.E., *A century of mitochondrial research: achievements and perspectives.* Mitochondrion, 2001. **1**(1): p. 3-31.

2.   Passarella, S., et al., *The role of mitochondrial transport in energy metabolism.* Mitochondrion, 2003. **2**(5): p. 319-43.

3.   Amacher, D.E., *Drug-associated mitochondrial toxicity and its detection.* Curr Med Chem, 2005. **12**(16): p. 1829-39.

4.   Scheffler, I.E., *Mitochondria make a come back.* Adv Drug Deliv Rev, 2001. **49**(1-2): p. 3-26.

5.   Mitchell, P., *Proton current flow in mitochondrial systems.* Nature, 1967. **214**(5095): p. 1327-8.

6.   Mitchell, P. and J. Moyle, *Chemiosmotic hypothesis of oxidative phosphorylation.* Nature, 1967. **213**(5072): p. 137-9.

7.   Silva, J.E. and R. Rabelo, *Regulation of the uncoupling protein gene expression.* Eur J Endocrinol, 1997. **136**(3): p. 251-64.

8.   Matthias, A., et al., *The bioenergetics of brown fat mitochondria from UCP1-ablated mice. Ucp1 is not involved in fatty acid-induced de-energization ("uncoupling").* J Biol Chem, 1999. **274**(40): p. 28150-60.

9.   Boelsterli, U.A. and P.L. Lim, *Mitochondrial abnormalities--a link to idiosyncratic drug hepatotoxicity?* Toxicol Appl Pharmacol, 2007. **220**(1): p. 92-107.

10.   Kroemer, G., B. Dallaporta, and M. Resche-Rigon, *The mitochondrial death/life regulator in apoptosis and necrosis.* Annu Rev Physiol, 1998. **60**: p. 619-42.

11.   Darzynkiewicz, Z., et al., *Cytometry in cell necrobiology: analysis of apoptosis and accidental cell death (necrosis).* Cytometry, 1997. **27**(1): p. 1-20.

12.   Savill, J., *Phagocyte recognition of apoptotic cells.* Biochem Soc Trans, 1996. **24**(4): p. 1065-9.

13.   Trump, B.F., et al., *The pathways of cell death: oncosis, apoptosis, and necrosis.* Toxicol Pathol, 1997. **25**(1): p. 82-8.

14.   Kroemer, G., et al., *The biochemistry of programmed cell death.* Faseb J, 1995. **9**(13): p. 1277-87.

15.   Mehendale, H.M., et al., *Novel mechanisms in chemically induced hepatotoxicity.* Faseb J, 1994. **8**(15): p. 1285-95.

16.   Zimmermann, K.C., C. Bonzon, and D.R. Green, *The machinery of programmed cell death.* Pharmacol Ther, 2001. **92**(1): p. 57-70.

17.   Zimmermann, K.C. and D.R. Green, *How cells die: apoptosis pathways.* J Allergy Clin Immunol, 2001. **108**(4 Suppl): p. S99-103.

18.   Green, D.R. and J.C. Reed, *Mitochondria and apoptosis.* Science, 1998. **281**(5381): p. 1309-12.

19.   Lelli, J.L., Jr., et al., *ATP converts necrosis to apoptosis in oxidant-injured endothelial cells.* Free Radic Biol Med, 1998. **25**(6): p. 694-702.

20.   Bandy, B. and A.J. Davison, *Mitochondrial mutations may increase oxidative stress: implications for carcinogenesis and aging?* Free Radic Biol Med, 1990. **8**(6): p. 523-39.

21.   Oliveira, P.J. and K.B. Wallace, *Depletion of adenine nucleotide translocator protein in heart mitochondria from doxorubicin-treated rats--relevance for mitochondrial dysfunction.* Toxicology, 2006. **220**(2-3): p. 160-8.

22.   Boveris, A. and B. Chance, *The mitochondrial generation of hydrogen peroxide. General properties and effect of hyperbaric oxygen.* Biochem J, 1973. **134**(3): p. 707-16.

23.   Weisiger, R.A. and I. Fridovich, *Superoxide dismutase. Organelle specificity.* J Biol Chem, 1973. **248**(10): p. 3582-92.

24.   Fromenty, B. and D. Pessayre, *Inhibition of mitochondrial beta-oxidation as a mechanism of hepatotoxicity.* Pharmacol Ther, 1995. **67**(1): p. 101-54.

25.   Green, D.R. and G. Kroemer, *The pathophysiology of mitochondrial cell death.* Science, 2004. **305**(5684): p. 626-9.

26.   Armstrong, J.S., *The role of the mitochondrial permeability transition in cell death.* Mitochondrion, 2006. **6**(5): p. 225-34.

27.   Wallace, K.B. and A.A. Starkov, *Mitochondrial targets of drug toxicity.* Annu Rev Pharmacol Toxicol, 2000. **40**: p. 353-88.

28.   Fromenty, B. and D. Pessayre, *Inhibition of mitochondrial beta-oxidation as a mechanism of hepatotoxicity.* Pharmacol Ther, 1995. **67**(1): p. 101-54.

29.   Feng, J.Y., et al., *Insights into the molecular mechanism of mitochondrial toxicity by AIDS drugs.* J Biol Chem, 2001. **276**(26): p. 23832-7.

30.   Le Bras, M., et al., *Reactive oxygen species and the mitochondrial signaling pathway of cell death.* Histol Histopathol, 2005. **20**(1): p. 205-19.

31.   Dreifuss, F.E., et al., *Valproic acid hepatic fatalities: a retrospective review.* Neurology, 1987. **37**(3): p. 379-85.

32.   Ponchaut, S. and K. Veitch, *Valproate and mitochondria.* Biochem Pharmacol, 1993. **46**(2): p. 199-204.

33.   Krahenbuhl, S., et al., *Plasma and hepatic carnitine and coenzyme A pools in a patient with fatal, valproate induced hepatotoxicity.* Gut, 1995. **37**(1): p. 140-3.

34.   Krahenbuhl, S., et al., *Mitochondrial diseases represent a risk factor for valproate-induced fulminant liver failure.* Liver, 2000. **20**(4): p. 346-8.

35.   Laub, M.C., I. Paetzke-Brunner, and G. Jaeger, *Serum carnitine during valproic acid therapy.* Epilepsia, 1986. **27**(5): p. 559-62.

36.   Vernez, L., M. Wenk, and S. Krahenbuhl, *Determination of carnitine and acylcarnitines in plasma by high-performance liquid chromatography/electrospray ionization ion trap tandem mass spectrometry.* Rapid Commun Mass Spectrom, 2004. **18**(11): p. 1233-8.

37.   Tamai, I., et al., *Molecular and functional identification of sodium ion-dependent, high affinity human carnitine transporter OCTN2.* J Biol Chem, 1998. **273**(32): p. 20378-82.

38.   Lewis, J.H., et al., *Amiodarone hepatotoxicity: prevalence and clinicopathologic correlations among 104 patients.* Hepatology, 1989. **9**(5): p. 679-85.

39.   Fromenty, B., et al., *Amiodarone inhibits the mitochondrial beta-oxidation of fatty acids and produces microvesicular steatosis of the liver in mice.* J Pharmacol Exp Ther, 1990. **255**(3): p. 1371-6.

40.   Fromenty, B., et al., *Dual effect of amiodarone on mitochondrial respiration. Initial protonophoric uncoupling effect followed by inhibition of the respiratory chain at the levels of complex I and complex II.* J Pharmacol Exp Ther, 1990. **255**(3): p. 1377-84.

41.   Spaniol, M., et al., *Toxicity of amiodarone and amiodarone analogues on isolated rat liver mitochondria.* J Hepatol, 2001. **35**(5): p. 628-36.

42.   Hautekeete, M.L., et al., *Severe hepatotoxicity related to benzarone: a report of three cases with two fatalities.* Liver, 1995. **15**(1): p. 25-9.

43.   Kaufmann, P., et al., *Mechanisms of benzarone and benzbromarone-induced hepatic toxicity.* Hepatology, 2005. **41**(4): p. 925-35.

44.   Omar, M.A. and J.P. Wilson, *FDA adverse event reports on statin-associated rhabdomyolysis.* Ann Pharmacother, 2002. **36**(2): p. 288-95. Order.

45.   Staffa, J.A., J. Chang, and L. Green, *Cerivastatin and reports of fatal rhabdomyolysis.* N Engl J Med., 2002. **346**(7): p. 539-40.

46.   Thompson, P.D., P. Clarkson, and R.H. Karas, *Statin-associated myopathy.* Jama, 2003. **289**(13): p. 1681-90.

47.   Graham, D.J., et al., *Incidence of hospitalized rhabdomyolysis in patients treated with lipid-lowering drugs.* Jama, 2004. **292**(21): p. 2585-90.

48.   Ballantyne, C.M., et al., *Risk for myopathy with statin therapy in high-risk patients.* Arch Intern Med, 2003. **163**(5): p. 553-64. Order.

49.   Rosenson, R.S., *Current overview of statin-induced myopathy.* Am J Med, 2004. **116**(6): p. 408-16.

50.   Williams, D. and J. Feely, *Pharmacokinetic-pharmacodynamic drug interactions with HMG-CoA reductase inhibitors.* Clin Pharmacokinet, 2002. **41**(5): p. 343-70.

51.   Liao, J.K., *Isoprenoids as mediators of the biological effects of statins.* J Clin Invest, 2002. **110**(3): p. 285-8.

52.   Evans, M. and A. Rees, *Effects of HMG-CoA reductase inhibitors on skeletal muscle: are all statins the same?* Drug Saf, 2002. **25**(9): p. 649-63.

53.   Flint, O.P., et al., *Inhibition of cholesterol synthesis by squalene synthase inhibitors does not induce myotoxicity in vitro.* Toxicol Appl Pharmacol, 1997. **145**(1): p. 91-8.

54.   Guijarro, C., et al., *Lipophilic statins induce apoptosis of human vascular smooth muscle cells.* Kidney Int Suppl, 1999. **71**: p. S88-91.

55.   Di Giovanni, S., et al., *Coenzyme Q10 reverses pathological phenotype and reduces apoptosis in familial CoQ10 deficiency.* Neurology., 2001. **57**(3): p. 515-8.

56.   Ogasahara, S., et al., *Muscle coenzyme Q deficiency in familial mitochondrial encephalomyopathy.* Proc Natl Acad Sci U S A., 1989. **86**(7): p. 2379-82.

57.   Giordano, N., et al., *Polymyositis associated with simvastatin.* Lancet, 1997. **349**(9065): p. 1600-1.

58.   Schalke, B.B., et al., *Pravastatin-associated inflammatory myopathy.* N Engl J Med, 1992. **327**(9): p. 649-50.

59.   Phillips, P.S., et al., *Statin-associated myopathy with normal creatine kinase levels.* Ann Intern Med, 2002. **137**(7): p. 581-5.

60.   England, J.D., et al., *Mitochondrial myopathy developing on treatment with the HMG CoA reductase inhibitors--simvastatin and pravastatin.* Aust N Z J Med, 1995. **25**(4): p. 374-5.

61.   Chariot, P., et al., *Simvastatin-induced rhabdomyolysis followed by a MELAS syndrome.* Am J Med., 1993. **94**(1): p. 109-10.

62.   Vladutiu, G.D., et al., *Genetic risk factors associated with lipid-lowering drug-induced myopathies.* Muscle Nerve, 2006. **71**: p. 1324-1330.

63.   Sirvent, P., et al., *Simvastatin induces impairment in skeletal muscle while heart is protected.* Biochem Biophys Res Commun., 2005. **338**(3): p. 1426-34. Epub 2005 Oct 26.

64.   Bogman, K., et al., *HMG-CoA reductase inhibitors and P-glycoprotein modulation.* Br J Pharmacol, 2001. **132**(6): p. 1183-92.

65.   Kaufmann, P., et al., *Mechanisms of benzarone and benzbromarone-induced hepatic toxicity.* Hepatology, 2005. **41**(4): p. 925-35.

66.   Kerner, J. and C.L. Hoppel, *Radiochemical malonyl-CoA decarboxylase assay: activity and subcellular distribution in heart and skeletal muscle.* Anal Biochem, 2002. **306**(2): p. 283-9.

67.   Palmer, J.W., B. Tandler, and C.L. Hoppel, *Biochemical properties of subsarcolemmal and interfibrillar mitochondria isolated from rat cardiac muscle.* J Biol Chem, 1977. **252**(23): p. 8731-9.

68.   Gornall, A.G., G.J. Bardawill, and M. David, *Determination of serum proteins by means of the biuret reaction.* Journal of Biological Chemistry, 1949. **177**: p. 751-66.

69.   Vassault, A., *Lactate dehydrogenase*, in *Methods of Enzymatic Analysis*, H.U. Bergmeyer, Editor. 1983, VHC: Weinheim. p. 118-125.

70.   Hoppel, C., J.P. DiMarco, and B. Tandler, *Riboflavin and rat hepatic cell structure and function. Mitochondrial oxidative metabolism in deficiency states.* J Biol Chem, 1979. **254**(10): p. 4164-70.

71.   Eastabrook, R., *Mitochondrial respiratory control and polarographic measurement of ADP:O ratios.* Methods Enzymol, 1967. **10**: p. 41-47.

72.   Blair, P.V., T. Oda, and D.E. Green, *Studies on the Electron Transfer System. Liv. Isolation of the Unit of Electron Transfer.* Biochemistry, 1963. **128**: p. 756-64.

73.   Krahenbuhl, S., et al., *Decreased activities of ubiquinol:ferricytochrome c oxidoreductase (complex III) and ferrocytochrome c:oxygen oxidoreductase (complex IV) in liver mitochondria from rats with hydroxycobalamin[c-lactam]-induced methylmalonic aciduria.* J Biol Chem, 1991. **266**(31): p. 20998-1003.

74.   Sherratt, H.S., et al., *Methods for study of normal and abnormal skeletal muscle mitochondria.* Methods Biochem Anal, 1988. **33**: p. 243-335.

75.   McGarry, J.D. and N.F. Brown, *The mitochondrial carnitine palmitoyltransferase system. From concept to molecular analysis.* Eur J Biochem, 1997. **244**(1): p. 1-14.

76.   Kiorpes, T.C., et al., *Identification of 2-tetradecylglycidyl coenzyme A as the active form of methyl 2-tetradecylglycidate (methyl palmoxirate) and its characterization as an irreversible, active site-directed inhibitor of carnitine palmitoyltransferase A in isolated rat liver mitochondria.* J Biol Chem, 1984. **259**(15): p. 9750-5.

77.   Brdiczka, D., et al., *[Compartmental dispersion of enzymes in rat liver mitochondria].* Eur J Biochem, 1968. **5**(2): p. 294-304.

78.   Haworth, R.A. and D.R. Hunter, *The Ca2+-induced membrane transition in mitochondria. II. Nature of the Ca2+ trigger site.* Arch Biochem Biophys, 1979. **195**(2): p. 460-7.

79.   Jones, S.P., et al., *Simvastatin attenuates oxidant-induced mitochondrial dysfunction in cardiac myocytes.* Circ Res, 2003. **93**(8): p. 697-9. Epub 2003 Sep 25.

80.   Ding, W.X. and C. Nam Ong, *Role of oxidative stress and mitochondrial changes in cyanobacteria-induced apoptosis and hepatotoxicity.* FEMS Microbiol Lett, 2003. **220**(1): p. 1-7.

81.   Drynan, L., P.A. Quant, and V.A. Zammit, *Flux control exerted by mitochondrial outer membrane carnitine palmitoyltransferase over beta-oxidation, ketogenesis and tricarboxylic acid cycle activity in hepatocytes isolated from rats in different metabolic states.* Biochem J, 1996. **317**(Pt 3): p. 791-5.

82.   Lemasters, J.J., et al., *Mitochondrial dysfunction in the pathogenesis of necrotic and apoptotic cell death.* J Bioenerg Biomembr, 1999. **31**(4): p. 305-19.

83.   Newmeyer, D.D. and S. Ferguson-Miller, *Mitochondria: releasing power for life and unleashing the machineries of death.* Cell, 2003. **112**(4): p. 481-90.

84.   Zamzami, N. and G. Kroemer, *Apoptosis: Mitochondrial Membrane Permeabilization - The (W)hole Story?* Curr Biol, 2003. **13**(2): p. R71-3.

85.   Nicotera, P., M. Leist, and E. Ferrando-May, *Intracellular ATP, a switch in the decision between apoptosis and necrosis.* Toxicol Lett, 1998. **102-103**: p. 139-42.

86.   Waterhouse, N.J., J.E. Ricci, and D.R. Green, *And all of a sudden it's over: mitochondrial outer-membrane permeabilization in apoptosis.* Biochimie, 2002. **84**(2-3): p. 113-21.

87.   Nishida, M., T. Nagao, and H. Kurose, *Activation of Rac1 increases c-Jun NH(2)-terminal kinase activity and DNA fragmentation in a calcium-dependent manner in rat myoblast cell line H9c2.* Biochem Biophys Res Commun, 1999. **262**(2): p. 350-4.

88.   Kaneta, S., et al., *All hydrophobic HMG-CoA reductase inhibitors induce apoptotic death in rat pulmonary vein endothelial cells.* Atherosclerosis, 2003. **170**(2): p. 237-43. Order.

89.   Kubota, T., et al., *Apoptotic injury in cultured human hepatocytes induced by HMG-CoA reductase inhibitors.* Biochem Pharmacol, 2004. **67**(12): p. 2175-86.

90.   Farmer, J.A., *Learning from the cerivastatin experience.* Lancet, 2001. **358**(9291): p. 1383-5.

91.   Lennernas, H., *Clinical pharmacokinetics of atorvastatin.* Clin Pharmacokinet, 2003. **42**(13): p. 1141-60.

92.   Neuvonen, P.J., T. Kantola, and K.T. Kivisto, *Simvastatin but not pravastatin is very susceptible to interaction with the CYP3A4 inhibitor itraconazole.* Clin Pharmacol Ther, 1998. **63**(3): p. 332-41.

93.   Ratz Bravo, A.E., et al., *Prevalence of potentially severe drug-drug interactions in ambulatory patients with dyslipidaemia receiving HMG-CoA reductase inhibitor therapy.* Drug Saf, 2005. **28**(3): p. 263-75.

94.   Singh, B.N., *Antiarrhythmic actions of amiodarone: a profile of a paradoxical agent.* Am J Cardiol, 1996. **78**(4A): p. 41-53.

95.   Singh, B.N., et al., *Amiodarone versus sotalol for atrial fibrillation.* N Engl J Med, 2005. **352**(18): p. 1861-72.

96.   Doval, H.C., et al., *Randomised trial of low-dose amiodarone in severe congestive heart failure. Grupo de Estudio de la Sobrevida en la Insuficiencia Cardiaca en Argentina (GESICA).* Lancet, 1994. **344**(8921): p. 493-8.

97.   Anonymous, *Effect of prophylactic amiodarone on mortality after acute myocardial infarction and in congestive heart failure: meta-analysis of individual data from 6500 patients in randomised trials. Amiodarone Trials Meta-Analysis Investigators.* Lancet, 1997. **350**(9089): p. 1417-24.

98.   Harjai, K.J. and A.A. Licata, *Effects of amiodarone on thyroid function.* Ann Intern Med, 1997. **126**(1): p. 63-73.

99.   Jessurun, G.A., W.G. Boersma, and H.J. Crijns, *Amiodarone-induced pulmonary toxicity. Predisposing factors, clinical symptoms and treatment.* Drug Saf, 1998. **18**(5): p. 339-44.

100.   Pollak, P.T., *Clinical organ toxicity of antiarrhythmic compounds: ocular and pulmonary manifestations.* Am J Cardiol, 1999. **84**(9A): p. 37R-45R.

101.   Morse, R.M., et al., *Amiodarone-induced liver toxicity.* Ann Intern Med, 1988. **109**(10): p. 838-40.

102.   Flanagan, R.J., et al., *Identification and measurement of desethylamiodarone in blood plasma specimens from amiodarone-treated patients.* J Pharm Pharmacol, 1982. **34**(10): p. 638-43.

103.   Ha, H.R., et al., *Identification and quantitation of novel metabolites of amiodarone in plasma of treated patients.* Eur J Pharm Sci, 2005. **24**(4): p. 271-9.

104.   Ha, H.R., et al., *Structure-effect relationships of amiodarone analogues on the inhibition of thyroxine deiodination.* Eur J Clin Pharmacol, 2000. **55**(11-12): p. 807-14.

105.   Lasselle, P.A. and S.A. Sundet, *The action of sodium on 2,2'-dichlorodiethylamine.* J Am Chem Soc, 1941. **63**: p. 2374-2376.

106.   Carlsson, B., et al., *Synthesis and preliminary characterization of a novel antiarrhythmic compound (KB130015) with an improved toxicity profile compared with amiodarone.* J Med Chem, 2002. **45**(3): p. 623-30.

107.   Braumann, T., *Determination of hydrophobic parameters by reversed-phase liquid chromatography: theory, experimental techniques, and application in studies on quantitative structure-activity relationships.* J Chromatogr., 1986. **373**(2): p. 191-225.

108.   Berry, M.N., *High-yield preparation of morphologically intact isolated parenchymal cells from rat liver.* Methods Enzymol, 1974. **32**(Part B): p. 625-32.

109.   Huang, T.H., et al., *Lactate dehydrogenase leakage of hepatocytes with AH26 and AH Plus sealer treatments.* J Endod, 2000. **26**(9): p. 509-11.

110.   Yang, N.C., et al., *A convenient one-step extraction of cellular ATP using boiling water for the luciferin-luciferase assay of ATP.* Anal Biochem, 2002. **306**(2): p. 323-27.

111.   Wang, H. and J.A. Joseph, *Quantifying cellular oxidative stress by dichlorofluorescein assay using microplate reader.* Free Radic Biol Med, 1999. **27**(5-6): p. 612-6.

112.   Estabrook, R., *Mitochondrial respiratory control and polarographic measurement of ADP:O ratios.* Methods Enzymol, 1967. **10**: p. 41-47.

113.   Freneaux, E., et al., *Inhibition of the mitochondrial oxidation of fatty acids by tetracycline in mice and in man: possible role in microvesicular steatosis induced by this antibiotic.* Hepatology, 1988. **8**(5): p. 1056-62.

114.   Spaniol, M., et al., *Development and characterization of an animal model of carnitine deficiency.* Eur J Biochem, 2001. **268**(6): p. 1876-87.

115.   Quaglino, D., et al., *Effects of metabolites and analogs of amiodarone on alveolar macrophages: structure-activity relationship.* Am J Physiol Lung Cell Mol Physiol, 2004. **287**(2): p. L438-47.

116.   Eguchi, Y., S. Shimizu, and Y. Tsujimoto, *Intracellular ATP levels determine cell death fate by apoptosis or necrosis.* Cancer Res, 1997. **57**(10): p. 1835-40.

117.   Leist, M., et al., *Intracellular adenosine triphosphate (ATP) concentration: a switch in the decision between apoptosis and necrosis.* J Exp Med, 1997. **185**(8): p. 1481-6.

118.   Lewis, J.H., et al., *Histopathologic analysis of suspected amiodarone hepatotoxicity.* Hum Pathol, 1990. **21**(1): p. 59-67.

119.   Kennedy, J.A., S.A. Unger, and J.D. Horowitz, *Inhibition of carnitine palmitoyltransferase-1 in rat heart and liver by perhexiline and amiodarone.* Biochem Pharmacol, 1996. **52**(2): p. 273-80.

120.   Fabre, G., et al., *Evidence for CYP3A-mediated N-deethylation of amiodarone in human liver microsomal fractions.* Drug Metab Dispos, 1993. **21**(6): p. 978-85.

121.   Bravo, A.E., et al., *Hepatotoxicity during rapid intravenous loading with amiodarone: Description of three cases and review of the literature.* Crit Care Med, 2005. **33**(1): p. 128-34; discussion 245-6.

122.   Pollak, P.T., A.D. Sharma, and S.G. Carruthers, *Relation of amiodarone hepatic and pulmonary toxicity to serum drug concentrations and superoxide dismutase activity.* Am J Cardiol, 1990. **65**(18): p. 1185-91.

123.   Flaharty, K.K., et al., *Hepatotoxicity associated with amiodarone therapy.* Pharmacotherapy, 1989. **9**(1): p. 39-44.

124.   Rigas, B., et al., *Amiodarone hepatotoxicity. A clinicopathologic study of five patients.* Ann Intern Med, 1986. **104**(3): p. 348-51.

125.   Hohnloser, S.H., T. Klingenheben, and B.N. Singh, *Amiodarone-associated proarrhythmic effects. A review with special reference to torsade de pointes tachycardia.* Ann Intern Med, 1994. **121**(7): p. 529-35.

126.   Waldhauser, K.M., et al., *Hepatocellular toxicity and pharmacological effect of amiodarone and amiodarone derivatives.* J Pharmacol Exp Ther, 2006. **319**(3): p. 1413-23.

127.   Mason, J.W., *Amiodarone.* N Engl J Med, 1987. **316**(8): p. 455-66.

128.   Martin, W.J., 2nd and E.C. Rosenow, 3rd, *Amiodarone pulmonary toxicity. Recognition and pathogenesis (Part 2).* Chest, 1988. **93**(6): p. 1242-8.

129.   Martin, W.J., 2nd and E.C. Rosenow, 3rd, *Amiodarone pulmonary toxicity. Recognition and pathogenesis (Part I).* Chest, 1988. **93**(5): p. 1067-75.

130.   Pitcher, W.D., *Amiodarone pulmonary toxicity.* Am J Med Sci, 1992. **303**(3): p. 206-12.

131.   Bigler, L., et al., *Synthesis and cytotoxicity properties of amiodarone analogues.* Eur J Med Chem, 2007. **42**(6): p. 861-7.

132.   Braumann, T., *Determination of hydrophobic parameters by reversed-phase liquid chromatography: theory, experimental techniques, and application in studies on quantitative structure-activity relationships.* J Chromatogr, 1986. **373**(2): p. 191-225.

133.   O'Brien, J., et al., *Investigation of the Alamar Blue (resazurin) fluorescent dye for the assessment of mammalian cell cytotoxicity.* Eur J Biochem, 2000. **267**(17): p. 5421-6.

134.   Gerber, P.R., *Charge distribution from a simple molecular orbital type calculation and non-bonding interaction terms in the force field MAB.* J Comput Aided Mol Des, 1998. **12**(1): p. 37-51.

135.   Morais-Cabral, J.H., Y. Zhou, and R. MacKinnon, *Energetic optimization of ion conduction rate by the K+ selectivity filter.* Nature, 2001. **414**(6859): p. 37-42.

136.	Bolt, M.W., et al., *Disruption of mitochondrial function and cellular ATP levels by amiodarone and N-desethylamiodarone in initiation of amiodarone-induced pulmonary cytotoxicity.* J Pharmacol Exp Ther, 2001. **298**(3): p. 1280-9.

137.	Ha, H.R., et al., *Interaction between amiodarone and lidocaine.* J Cardiovasc Pharmacol, 1996. **28**(4): p. 533-9.

138.	Card, J.W., et al., *Amiodarone-induced disruption of hamster lung and liver mitochondrial function: lack of association with thiobarbituric acid-reactive substance production.* Toxicol Lett, 1998. **98**(1-2): p. 41-50.

139.	Card, J.W., et al., *Attenuation of amiodarone-induced pulmonary fibrosis by vitamin E is associated with suppression of transforming growth factor-beta1 gene expression but not prevention of mitochondrial dysfunction.* J Pharmacol Exp Ther, 2003. **304**(1): p. 277-83.

140.	Yasuda, S.U., et al., *Amiodarone-induced lymphocyte toxicity and mitochondrial function.* J Cardiovasc Pharmacol, 1996. **28**(1): p. 94-100.

141.	Lullmann, H., R. Lullmann-Rauch, and O. Wassermann, *Drug-induced phospholipidoses. II. Tissue distribution of the amphiphilic drug chlorphentermine.* CRC Crit Rev Toxicol, 1975. **4**(2): p. 185-218.

142.	Hostetler, K.Y., J.R. Giordano, and E.J. Jellison, *In vitro inhibition of lysosomal phospholipase A1 of rat lung by amiodarone and desethylamiodarone.* Biochim Biophys Acta, 1988. **959**(3): p. 316-21.

143.	Hostetler, K.Y., et al., *Role of phospholipase A inhibition in amiodarone pulmonary toxicity in rats.* Biochim Biophys Acta, 1986. **875**(2): p. 400-5.

144.	Kaufmann, A.M. and J.P. Krise, *Lysosomal sequestration of amine-containing drugs: analysis and therapeutic implications.* J Pharm Sci, 2007. **96**(4): p. 729-46.

145.	Bolt, M.W., et al., *Effects of vitamin E on cytotoxicity of amiodarone and N-desethylamiodarone in isolated hamster lung cells.* Toxicology, 2001. **166**(3): p. 109-18.

146.	Krahenbuhl, S., et al., *Mitochondrial diseases represent a risk factor for valproate-induced fulminant liver failure.* Liver, 2000. **20**(4): p. 346-8.

147.	Uetrecht, J., *Idiosyncratic drug reactions: current understanding.* Annu Rev Pharmacol Toxicol, 2007. **47**: p. 513-39.

148.	Furberg, C.D. and B. Pitt, *Withdrawal of cerivastatin from the world market.* Curr Control Trials Cardiovasc Med, 2001. **2**(5): p. 205-207.

149.	Lasser, K.E., et al., *Timing of new black box warnings and withdrawals for prescription medications.* Jama, 2002. **287**(17): p. 2215-20.

150.	*Randomised trial of cholesterol lowering in 4444 patients with coronary heart disease: the Scandinavian Simvastatin Survival Study (4S).* Lancet, 1994. **344**(8934): p. 1383-9.

151.   Staffa, J.A., J. Chang, and L. Green, *Cerivastatin and reports of fatal rhabdomyolysis.* N Engl J Med, 2002. **346**(7): p. 539-40.

152.   Rosenson, R.S., *Current overview of statin-induced myopathy.* Am J Med, 2004. **116**(6): p. 408-16.

153.   Yan, L., et al., *Statins and myotoxicity.* Trends Pharmacol Sci, 2003. **24**(3): p. 113-4.

154.   Evans, M. and A. Rees, *The myotoxicity of statins.* Curr Opin Lipidol, 2002. **13**(4): p. 415-20.

155.   Watts, G.F., et al., *Plasma coenzyme Q (ubiquinone) concentrations in patients treated with simvastatin.* J Clin Pathol, 1993. **46**(11): p. 1055-7.

156.   Flint, O.P., et al., *Inhibition of cholesterol synthesis by squalene synthase inhibitors does not induce myotoxicity in vitro.* Toxicol Appl Pharmacol, 1997. **145**(1): p. 91-8.

157.   Kaufmann, P., et al., *Toxicity of statins on rat skeletal muscle mitochondria.* Cell Mol Life Sci, 2006. **63**(19-20): p. 2415-25.

158.   Chariot, P., et al., *Simvastatin-induced rhabdomyolysis followed by a MELAS syndrome.* Am J Med, 1993. **94**(1): p. 109-10.

159.   Giordano, N., et al., *Polymyositis associated with simvastatin.* Lancet, 1997. **349**(9065): p. 1600-1.

160.   Schalke, B.B., et al., *Pravastatin-associated inflammatory myopathy.* N Engl J Med, 1992. **327**(9): p. 649-50.

161.   Vladutiu, G.D., et al., *Genetic risk factors associated with lipid-lowering drug-induced myopathies.* Muscle Nerve, 2006. **34**(2): p. 153-62.

162.   Sirvent, P., et al., *Simvastatin induces impairment in skeletal muscle while heart is protected.* Biochem Biophys Res Commun, 2005. **338**(3): p. 1426-34.

163.   Ferber, H., U. Bader, and F. Matzkies, *The action of benzbromarone in relation to age, sex and accompanying diseases.* Adv Exp Med Biol, 1980. **122A**: p. 287-94.

164.   Kass, G.E., *Mitochondrial involvement in drug-induced hepatic injury.* Chem Biol Interact, 2006. **163**(1-2): p. 145-59.

165.   Krahenbuhl, S., *Mitochondria: important target for drug toxicity?* J Hepatol, 2001. **34**(2): p. 334-6.

166.   Ong, M.M., et al., *Nimesulide-induced hepatic mitochondrial injury in heterozygous Sod2(+/-) mice.* Free Radic Biol Med, 2006. **40**(3): p. 420-9.

167.   Bogman, K., et al., *HMG-CoA reductase inhibitors and P-glycoprotein modulation.* Br J Pharmacol, 2001. **132**(6): p. 1183-92.

168. Mosmann, T., *Rapid colorimetric assay for cellular growth and survival: application to proliferation and cytotoxicity assays.* J Immunol Methods, 1983. **65**(1-2): p. 55-63.

169. Wang, H. and J.A. Joseph, *Quantifying cellular oxidative stress by dichlorofluorescein assay using microplate reader.* Free Radic Biol Med, 1999. **27**(5-6): p. 612-6.

170. Slater, T.F., B. Sawyer, and U. Straeuli, *Studies on Succinate-Tetrazolium Reductase Systems. Iii. Points of Coupling of Four Different Tetrazolium Salts.* Biochim Biophys Acta, 1963. **77**: p. 383-93.

171. Carmichael, J., et al., *Evaluation of a tetrazolium-based semiautomated colorimetric assay: assessment of radiosensitivity.* Cancer Res, 1987. **47**(4): p. 943-6.

172. Newmeyer, D.D. and S. Ferguson-Miller, *Mitochondria: releasing power for life and unleashing the machineries of death.* Cell, 2003. **112**(4): p. 481-90.

173. Britton, C.H., et al., *Human liver mitochondrial carnitine palmitoyltransferase I: characterization of its cDNA and chromosomal localization and partial analysis of the gene.* Proc Natl Acad Sci U S A, 1995. **92**(6): p. 1984-8.

174. Yamazaki, N., et al., *Isolation and characterization of cDNA and genomic clones encoding human muscle type carnitine palmitoyltransferase I.* Biochim Biophys Acta, 1996. **1307**(2): p. 157-61.

175. Demaugre, F., et al., *Hepatic and muscular presentations of carnitine palmitoyl transferase deficiency: two distinct entities.* Pediatr Res, 1988. **24**(3): p. 308-11.

176. Tein, I., et al., *Normal muscle CPT1 and CPT2 activities in hepatic presentation patients with CPT1 deficiency in fibroblasts. Tissue specific isoforms of CPT1?* J Neurol Sci, 1989. **92**(2-3): p. 229-45.

177. Levy, Y., et al., *Reduction of plasma cholesterol by lovastatin normalizes erythrocyte membrane fluidity in patients with severe hypercholesterolaemia.* Br J Clin Pharmacol, 1992. **34**(5): p. 427-30.

178. Morita, I., et al., *Enhancement of membrane fluidity in cholesterol-poor endothelial cells pre-treated with simvastatin.* Endothelium, 1997. **5**(2): p. 107-13.

179. Lijnen, P., et al., *Influence of cholesterol lowering on plasma membrane lipids and cationic transport systems.* J Hypertens, 1994. **12**(1): p. 59-64.

180. Bliznakov, E.G., *Lipid-lowering drugs (statins), cholesterol, and coenzyme Q10. The Baycol case--a modern Pandora's box.* Biomed Pharmacother, 2002. **56**(1): p. 56-9.

181. Laaksonen, R., et al., *The effect of simvastatin treatment on natural antioxidants in low-density lipoproteins and high-energy phosphates and ubiquinone in skeletal muscle.* Am J Cardiol, 1996. **77**(10): p. 851-4.

182. Bleske, B.E., et al., *The effect of pravastatin and atorvastatin on coenzyme Q10.* Am Heart J, 2001. **142**(2): p. E2.

183. Jansen, T.L., et al., *Benzbromarone withdrawn from the European market: another case of "absence of evidence is evidence of absence"?* Clin Exp Rheumatol, 2004. **22**(5): p. 651.

184. Thomas, D., C.A. Karle, and J. Kiehn, *The cardiac hERG/IKr potassium channel as pharmacological target: structure, function, regulation, and clinical applications.* Curr Pharm Des, 2006. **12**(18): p. 2271-83.

185. Uetrecht, J., *Evaluation of which reactive metabolite, if any, is responsible for a specific idiosyncratic reaction.* Drug Metab Rev, 2006. **38**(4): p. 745-53.

10. Curriculum Vitae

Name	Katri Maria Waldhauser-Paavilainen
Date of birth	23.3.1977
Place of birth	Hyvinkää, Finland
Nationality	Finnish
Marital status	married, 1 child
Address	Lärchenstrasse 16
	CH-4142 Münchenstein
Phone	+41 (0)76 399 9868
E-mail	katri.waldhauser@gmail.com

EDUCATION

2004-2007	PhD thesis (*Phil Nat Sci*) at the Department of Clinical Pharmacology and Toxicology, University Hospital Basel, Switzerland, under guidance of Prof. Stephan Krähenbühl

Thesis title: "Mitochondrial toxicity of drugs", including following projects:

- Hepatocellular toxicity and pharmacological effect of amiodarone and amiodarone derivatives
- Mechanisms of mitochondrial toxicity of simvastatin and benzbromarone in primary dermal fibroblast cell lines
- Silencing of carnitine acylcarnitine translocase (CACT) in mouse myocyte C2 cell line
- Toxicity of statins in muscle cell lines C2 and L6

Others:

- Lectures attended e.g. in: molecular mechanisms of toxicology, clinical pharmacology, seminars on drug discovery and development.
- KLIPS: Drug Information Centre: Answering queries about drug safety
- Assistance in undergraduate courses
- TDM = Therapeutic Drug Monitoring
- WIN = Women Into Industry, a program for promoting women into pharmaceutical industry (Novartis and University of Basel)

1998-2004	University of Helsinki, Finland
	Master of Science (Pharmacy)
	Main subject pharmacology

- 01/2003-06/2003 Professional problem study for the master's thesis (advisor Prof. Ruegg, Department of Pharmacology, University of Lausanne, Switzerland)

- Topic of the master's thesis: "Investigations of Green Tea Extract and its Major Polyphenol (-)-Epicallocatechin Gallate on the Pathology of the Muscle of the mdx Mouse, a model of Duchenne Muscular Dystrophy"
- 06/2001 *Bachelor of Science (Pharmacy)*

1997-1999	University of Helsinki, Finland *Main subject* German language and literature studies *Minor subject* Journalism
1993-1997	High school of Hyvinkää, Finland
1994-1995	High school of Liestal, Switzerland

WORKING EXPERIENCE

2007-current	Kantonsspital Liestal (Community Hospital Liestal, Switzerland) • Hospital Pharmacist
09/2005-10/2006	City-Ring Apotheke, Basel (City-Ring Pharmacy, Basel) • Part-time pharmacist in customer care
09/2000- 09/2003	Yliopiston apteekki (The Pharmacy of the University, Helsinki, Finland) • Pharmacist in the customer care and in the pharmaceutical information service (phone centre) • Pharmaceutical internship
02/1999-09/2000	Helsingin Kauppatorin Apteekki (The Pharmacy on the market place, Helsinki, Finland) • Pharmaceutical internship • Technical assistance
04/1998-12/1999	Finnish Forest Industries Federation • Administrational duties • Translation Finnish-German, Finnish-English, Finnish-Swedish

PUBLICATION LIST

Waldhauser KM, Török M, Ha HR, Thomet U, Konrad D, Brecht K, Follath F, Krähenbühl S. Hepatocellular toxicity and pharmacological effect of amiodarone and amiodarone derivatives. *J Pharmacol Exp Ther* 2006; 319: 1413-1423.

Todesco L, Waldhauser K, Krähenbühl S. Mitochondrial toxicity of drugs. *Chimia 2006;60:37-39*

Kaufmann P, Török M, Zahno A, Waldhauser KM, Brecht K, Krähenbühl S. Toxicity of statins on rat skeletal muscle mitochondria. *Cell Mol Life Sci 2006; 63: 2415-2425*

Dorchies OM, Wagner S, Vuadens O, Waldhauser K, Buetler TM, Kucera P, Ruegg UT. Green tea extract and its major polyphenol (-)-epigallocatechin gallate improve muscle function in a mouse model for Duchenne muscular dystrophy. *Am J Physiol Cell Physiol* 2006; 290: 616-625.